Transmission of Temporal Information Through the Auditory Pathway Measured with Cochlear-Implant Stimulation

by

Alana E. Kirby

A dissertation submitted in partial fulfillment
of the requirements for the degree of
Doctor of Philosophy
(Neuroscience)
in The University of Michigan
2011

Doctoral Committee:

Professor Bryan E. Pfingst, Co-Chair
Professor John C. Middlebrooks, University of California, Irvine, Co-Chair
Professor Richard A. Altschuler
Professor H. Alexander Arts
Associate Professor Gina R. Poe

DEDICATION

To my parents.

ACKNOWLEDGEMENTS

This document was years in the making, and would not exist without the dedicated support and assistance I have received from my colleagues, friends, and family.

I would like to thank my advisor, John Middlebrooks, for guiding me through the process of becoming an independent researcher. From him, I learned to temper my scientific enthusiasm with rigor and skepticism. I learned that your passion for personal involvement in good science can last throughout your career. I am grateful to him for allowing me to make my own mistakes while still helping me to solve my problems. I have learned so much.

I appreciate the assistance of my thesis committee, who provided me with constructive criticism and encouragement. In particular, I'd like to thank my co-chair Bryan Pfingst for many helpful and informative conversations about our data.

The Middlebrooks Lab has been a wonderful place to work and grow. Zekiye Onsan and Chen-Chung Lee became like family to me as we made the journey from Michigan to California. Chen-Chung inspired me with his passion for music and science and in doing so kept me honest about my own efforts. Our talks together always filled me with insight and excitement. I am tremendously grateful for Zekiye's support inside and outside the lab, and respect her dedication to learning throughout her life. I treasure the time the three of us spent together. Many more lab members have helped

and supported me as well. Ian Harrington and Kevin Otto welcomed me to the lab and got me started on data analysis and experiments. Ewan MacPherson was a quiet yet funny mentor. Jim Wiler, renaissance man, taught me everything I know and I wish I'd learned more! Russ Snyder, frequent visitor and surgeon supreme, always had some interesting scientific tidbit to discuss during late nights at the lab. And of course, all the wonderful folks of the Kresge Hearing Research Institute, including: Dwayne Vaillaincourt and Chris Ellinger who constructed my research equipment and inspired me with their creativity; Jackie Blake, Abby Wilson, Gary Dootz and Dave Rodgers, for their willing assistance; Debbie Colesa and Ariane Kanicki, who taught me new techniques; and everyone at KHRI who fostered a welcoming and invigorating environment. After the move to California I have enjoyed getting to know Lauren Javier and Beth McGuire, Patricia Salgado and Justin Yao. All these people helped me, supported me, and brought out the best in me. Thank you.

I am also grateful for the support offered to me by the Medical Scientist Training Program and the Neuroscience Program at the University of Michigan. I turned to Ron Koenig to provide a calm voice of reason in the face of difficult choices. Penny Morris and Ellen Elkin, Laurie Koivupalo, and Hillka Ketola; Charma Shoemaker and Valerie Smith; Julie Winder and Rachel Flaten: all helped me to navigate treacherous administrative waters. Thank you for your patience, organization, and help.

The University of California at Irvine Medical Scientist Training Program graciously allowed me to join their ranks for the three years I was in California. Thanks to Al Goldin, Chris Varrone, and Stacie Sanchez for their help and warm welcome.

My madcap friends helped me to pass the time outside of lab. The Physics Cronies are still going strong and we're already into the next generation! Soo and Sara, occupants of the Blue Room — I couldn't ask for better friends. I didn't see enough

of the Chicagoland-Copic-Connected-Crowd, but I always felt immediately at home whenever I visited. The Motikas, Remys and Irvine board-game crowd helped me through some of the hardest moments of my life to date and I will never forget their support. My musical companions helped to keep me sane and grounded: Life Sciences Orchestra friends; choir kids; Auscultations; and MEDleys. My roommates Chelsea, Lili, Jason, Jesse, Emily, Harvest, and Jenn made my myriad homes pleasant places to be. To my oldest friends Erin and Kayt: we've changed so much, and I am so glad we are still together. Thanks to my Brothers of Mu Beta Psi for having me as your officer and your friend. I wish all the best to my MSTP and adopted UCI-MSTP-friends, who share the madness of eight+ years of schooling.

I owe so much to my family. From my earliest memories, they have encouraged my inquisitiveness, love of reading, and passion for truth. My mother instilled independence in me. She has always demonstrated calm under fire - a skill I strive to emulate. My father's idealism remains an inspiration. I remember when he received his Ph.D., and I wish he was alive to receive his copy of this dissertation. My sister shows me every day how to follow your own path. Diane demonstrated daily how to be an assertive and strong and funny woman. Nunu has more than her share of cheerfulness and grace (how does she do it?), and I am grateful to have her in my family. My Grandmothers Jane and Jean and my Aunt Frances are strong women who always asked about my progress on my experiments. I respect their determination, humor and intelligence and appreciate their love. Amma and Thaththa exude loving-kindness that I try to match. Vikasitha was funny, observant and kind and I miss his presence. I feel so lucky to have been welcomed into their family.

And last but not least, I am tremendously grateful to my partner and beloved Bodhitha Jayatilaka, for his love, support, and many, many trans-continental flights.

TABLE OF CONTENTS

LIST OF FIGURES

Figure

LIST OF TABLES

Table

ABSTRACT

Transmission of Temporal Information Through the Auditory Pathway Measured with Cochlear-Implant Stimulation

by

Alana E. Kirby

Co-Chairs: John C. Middlebrooks and Bryan E. Pfingst

Cochlear implants provide the sensation of hearing to deaf individuals through electric stimulation of the auditory nerve. Environmental sounds are band-pass filtered, and the envelope of each frequency band is used to modulate electric pulse trains that are presented through electrodes along the cochlea. Selection of cochlear-implant processing-strategy parameters influences how temporal information is transmitted to the listener. Increasing the rate of the pulsatile carrier has been hypothesized to improve temporal acuity, which is important for speech recognition. We used cochlear-implant stimulation to measure cortical coding of temporal features of the stimulus envelope. We tested the effect of pulse rates from 254-4069 pps on three measures of temporal acuity: gap detection, forward masking, and amplitude-modulation detection.

We observed that gap-detection thresholds decreased with increasing pulse rate

in awake and anesthetized animals. We measured forward masking, the suppression of a probe sound by a preceding masker, and observed two exponential components of recovery from forward masking. Based on their time constants, we attributed the rapid component to the auditory nerve and the longer component, which was stronger at lower pulse rates, to a central auditory center. We concluded that shorter gap-detection thresholds at higher pulse rates resulted from reduced forward masking. In awake animals, we observed responses to a variety of gap features. OFF-responses to the pre-gap marker contributed to gap-detection thresholds at the lowest pulse rate, in conditions for which the ON-response to the post-gap marker was suppressed.

We measured the synchrony of cortical responses to 10.6- and 21.2-Hz sinusoidal amplitude modulation on one cochlear-implant electrode in the presence of a simultaneous, interleaved stimulus on another electrode. We hypothesized that higher pulse rates and shorter inter-pulse-train delays would maximize interference between the two stimuli. There was little effect of either parameter, however, for an unmodulated pulse-train masker. When the stimuli were modulated at different frequencies, we observed cortical representations that were dominated by the sum of the stimuli. Longer interleaving delays resulted in slightly more stimulus-selective responses.

These results reveal principles of temporal processing in the auditory pathway, and may guide development and selection of future cochlear-implant processing strategies.

CHAPTER 1

Introduction and Background

Cochlear implants restore hearing to individuals with profound sensorineural deafness. These devices comprise a set of electrical contacts through which current is passed to stimulate the auditory nerve. Electrode arrays are surgically implanted into the scala tympani of the cochlea and are driven by signal processors which transform environmental sounds into electric pulses suitable for delivery to the auditory nerve. Ongoing research helps to improve these devices through development of new physical electrodes, surgical techniques, procedures for preserving or restoring cochlear neurons and their processes, signal processing strategies, and even alternative sites for electrical stimulation within the auditory system. This dissertation describes a series of experiments designed to measure the effect of a commonly modified stimulation parameter, electric pulse rate, on stimulus envelope detection in the central auditory system. The results provide insights into basic mechanisms of transmission of temporal information in the auditory pathway.

1.1 Auditory Prosthesis

1.1.1 History

The first intentional electric stimulation of the human auditory system was performed by Alessandro Volta in 1800, who applied direct current to his own ears. This

pioneering attempt was unpleasant and unsuccessful, and the concept was largely abandoned until 1957, when Djourno and Eyries (Djourno et al., 1957) performed the first surgical implantation of a device to stimulate the auditory nerve. While the patient received little benefit from the device, the seed had been planted. Over the course of the next 28 years, teams of scientists around the world worked to overcome the scientific, technical, and surgical challenges to identify appropriate numbers of electrodes, biocompatible materials, and stimulation paradigms. Notable contributions were made by: William House and colleagues in the United States; Graeme Clark et al. in Melbourne, Australia; as well as Kurt Burien, Erwin Hochmair, and Ingeborg Hochmair-Desoyer in Vienna, Austria. The steady improvements in technology and performance resulted in the approval of the Nucleus implant by Cochlear Corporation (Melbourne, Australia) by the US Food and Drug Administration in 1985. The development of new processing strategies for transforming acoustic sounds into electric stimulation markedly improved performance with the devices. The accumulated improvements led to a broadening of the patient population to include children and eventually infants. What started as the dream of a few surgeons and researchers has become a thriving industry, with the number of implanted patients approaching 220,000 worldwide and a research community investigating everything from implant design to sound processing strategies to patient satisfaction.

1.1.2 Cochlear-Implant Stimulation Strategies

Cochlear-implant stimulation strategies determine the manner in which environmental stimuli are presented to the auditory nerve through the device. The basic principle is one of place coding. In normal hearing, motion of the basilar membrane evoked by a particular frequency results in activation of the auditory nerve at a particular location. In cochlear implantees, the hair cells that transduce this motion

into electric signals in the auditory nerve are usually absent, but the tonotopic mapping of loci in the cochlea to loci in the brain remains. To direct the appropriate stimulation to each accessible cochlear place, sounds are first compressed in dynamic range through an automatic gain control mechanism to avoid overstimulation and to approximate the fast-acting compression usually performed by the intact cochlea. The compressed waveform is then fed through a bank of narrowband filters. The output of each filter is rectified and low-pass filtered with a cutoff of 200-400 Hz to extract the envelope of the stimulus. These envelopes are then used to modulate the amplitudes of fixed-rate electrical pulse trains that are presented to tonotopically appropriate cochlear-implant electrode. The sum of the activation across the cochlea coarsely reproduces the original stimulus. An example of this process is depicted in Figure 1.1.

The strategies in use by most patients today rely on pulsatile electric stimulation, as described above, to eliminate channel interactions. In continuous analog stimulation, currents are applied simultaneously to multiple electrodes, and the resultant electric fields sum directly within the cochlea. These interactions broaden the area of effective auditory nerve activation, and the sum of individually sub-threshold signals may result in perceptible auditory nerve activation. Pulsatile stimulation allows non-simultaneous stimulation of the nerve fibers and reduces these interactions. By sequentially presenting brief electric pulses to spatially-separated electrodes, each nerve population can be activated more selectively. The Continuous Interleaved Sampling (CIS) strategy was the first widely-used implementation of this strategy and resulted in immediate improvements in speech perception (Wilson et al., 1991). However, a minority of present-day cochlear-implant users still use a strategy in which the output of each narrowband filter is delivered to a tonotopically appropriate intracochlear

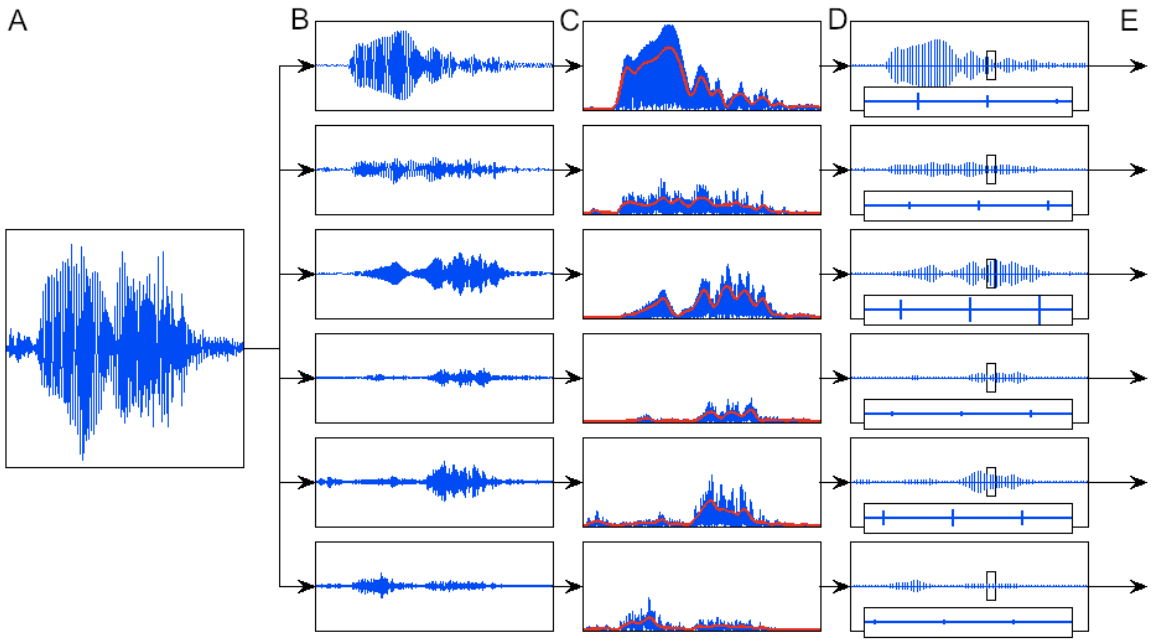

Figure 1.1: **Cochlear-implant stimulation strategy** This diagram represents the transformation from acoustic stimulus to electric stimulation. A. Sample speech waveform; B. Output of bandpass filterbank extracting six channels spanning 100-2000 Hz; C. Rectification of the resultant waveforms and the envelope, extracted with a low-pass filter, shown in red; D. Convolution with a 254-pps electric pulse train. The black box demarcates a 12-ms window which is expanded in the inset to show the amplitude-modulated, interleaved pulse trains; E. Outputs are directed to individual cochlear-implant electrodes.

electrode, resulting in continuous electric stimulation. With these strategies, the timing of peaks within the narrowband filter is preserved in the applied waveform, and these peaks elicit action potentials in the auditory nerve in a predictable fashion.

Modern-day processing strategies include several refinements which can be customized to each listener and even to different listening environments and auditory targets. One such modification involves the stimulation of a subset of the available electrodes. Given a fixed rate of overall stimulation, stimulating fewer electrodes allows more detailed sampling of their respective envelopes because the pulse rate on each channel can be higher. The Spectral Peak (SPEAK) (Skinner et al., 1996) and Advanced Combination Encoder (ACE) (Skinner et al., 2002) strategies continuously select a subset of channels corresponding to the filterbank outputs with the largest magnitude. This allows the listener to focus on the frequency channels with the highest energy, a selection which approximates the subset of most-informative channels. Also, it is often beneficial to remove some electrodes from the channel map entirely. Each patient may have some electrodes with higher thresholds and worse transmission of auditory information. Some threshold differences across electrodes are present in most cochlear implant users, but high variability in thresholds across electrodes is associated with impaired performance on speech recognition tasks (Bierer, 2007). Such cross-channel variation in threshold can arise in multiple ways. Electrode positioning during surgical implantation is critical: electrodes which travel into the scala vestibuli have poorer thresholds than those which remain within the targeted scala tympani location (Skinner et al., 2007). In addition, auditory nerve cell apoptosis may occur in the absence of stimulation, and nerve survival depends on the etiology and duration of deafness (Nadol, 1997). This can lead to "dead patches" within the cochlea, which may result in locally elevated thresholds (Shannon et al., 2002). Fi-

nally, foreign-body reactions elicited within the cochlea by the device are common (Nadol et al., 2008), and may lead to elevated thresholds at nearby electrodes.

1.1.3 Cochlear-Implant Carrier Pulse Rates

Historically, the rate of pulsatile stimulation available to cochlear implant listeners has been limited by available technology. The CIS strategy resulted in rapid gains in speech understanding in quiet and in noise using pulse rates of ∼817 pps (Wilson et al., 1991). The introduction of the SPEAK strategy, a few years after CIS, also provided patients with good speech recognition with a carrier pulse rate of 250 pps (Skinner et al., 1994). However, higher pulse rates allow more detailed sampling of the envelope of each frequency component. Skinner et al. (2002) measured patient performance and preferences with the SPEAK (250 pps), ACE (700-1800 pps) and CIS (900-1800) processing strategies and found that 60% of cochlear-implant listeners preferred the ACE strategy. The main difference between ACE and SPEAK strategies was the available pulse rate. In a study of the effect of electric pulse rate on modulation detection in human listeners (Arora et al., 2011), carrier rates from 200-900 pps were tested and listeners were most sensitive at 500 pps. There appears to be an advantage for most listeners in using pulse rates higher than 250 pps.

Theoretically, pulse rates $\geq$ 2000 pps have additional advantages. Physiological studies in animals have shown that pulse rates up to ∼1000 pps result in highly synchronous activation of auditory nerve fibers, whereas much higher pulse rates result in less synchronous firing (Zhang et al., 2007). This stochastic activity at higher pulse rates has been hypothesized to lead to auditory nerve activity that is more similar to that observed in normal hearing and thereby improve perception of cochlear-implant users (Rubinstein et al., 1999). Higher pulse rates have lead to some improvements in auditory perception. Detection thresholds decrease with increasing

pulse rate, and as a result, higher pulse rates yield an expanded dynamic range (Kreft et al., 2004). However, the effects of pulse rate on performance are inconsistent across listeners. Battmer et al. (2010) tested cochlear-implant patients with multiple pulse rates using several different experimental designs and determined that performance was best at each listener's preferred pulse rate, but that 80% of listeners preferred pulse rates from 500-1200 pps. In the Skinner et al. (1994) study, 56% of listeners who preferred the higher pulse-rate strategies (ACE and CIS) selected pulse rates of 500-900 pps, with the remainder preferring rates of 1200-2400 pps. The available data indicate that pulse rates $\geq$ 2000 pps provide a benefit to some cochlear implant listeners, but that there is no global advantage of these higher pulse rates.

Across all active channels, modern processing strategies stimulate at total rates of 14 kpps or higher. This corresponds corresponds to an interleaving delay, the length of time between pulses presented sequentially on different electrodes, of 0.07 ms or less across channels. Although pulsatile stimulation strategies reduce channel interactions compared to continuous stimulation, temporal integration of single-channel electric pulse trains contributes to decreases in detection threshold with increasing pulse rate, particularly for inter-pulse intervals shorter than 1 ms (Middlebrooks, 2004). A similar mechanism could result in cross-channel interactions between nearby electrodes at short interleaving delays. Simultaneous masking between interleaved pulsatile stimuli decreases with increasing electrode separation in human listeners (Kwon and van den Honert, 2009). Higher pulse rates require brief interleaving delays, and channel interactions resulting from temporal integration may be one reason that higher pulse rates have not been not as successful as predicted.

1.1.4 Temporal Information Available to Cochlear Implant Users

Present-day cochlear-implant processing makes use of the stimulus envelope, consisting of frequency components below 200-400 Hz, to represent the temporal dimensions of sound. In doing so, the higher-frequency components, also known as the fine structure, are discarded, including the phase information and specific timing of the peaks. For natural stimuli such as speech, fine structure cues are correlated across a range of frequencies to create harmonic structure and therefore can be important for grouping spectrally-distant components into one auditory object (Roberts et al., 2002). This is particularly relevant for the detection of speech in the presence of background distractors with similar spectrotemporal characteristics (Moore, 2008). Such tasks are quite difficult for many cochlear implant listeners, in part because of the loss of fine structure cues. In quiet conditions, however, the low-frequency envelope generally provides sufficient information to recognize speech (Shannon et al., 1995; van Tasell et al., 1987).

1.2 Temporal Acuity Across the Auditory Pathway

Temporal acuity evolves over the auditory pathway. In normal hearing, auditory nerve fiber responses reflect the output of the cochlear filter. At successive synapses, a variety of cell types extract particular stimulus features. The end result of all of this processing appears in auditory cortical sites that are able to shift their tuning over the course of seconds to extract the most relevant information for the task at hand (Lee and Middlebrooks, 2011). Several psychophysical measures of auditory temporal sensitivity have been shown in physiological measures to vary along the auditory system (Frisina, 2001). Many of the neural transformations observed result in a loss of temporal acuity when compared with the robust coding in the auditory

nerve. These transformations are still expected to operate upon the responses evoked by electric stimulation.

Temporal acuity may be measured by sensitivity to sequential stimuli. Forward masking is a phenomenon in which one stimulus (masker) suppresses the detection of a subsequent sound (probe). The shorter the interval between the masker and probe, the more suppression occurs. Forward masking tasks generally measure how intense the probe signal needs to be in order to be detectable in the presence of the masker as a function of the silent interval between them. Gap detection tasks occupy the same parameter space and measure the minimum detectable gap between two stimuli. Performance on these tasks is dependent on the frequency, duration, level, and timing of the two sounds and is easiest when the two stimuli activate the same auditory channel.

Normal-hearing listeners are sensitive to within-channel gaps of 2-5 ms. Individuals with auditory neuropathy, in whom abnormal afferent auditory nerve function has been measured, may have gap detection thresholds of 10-20 ms (Zeng et al., 2005). These patients have normal pure-tone thresholds, but disrupted temporal sensitivity and difficulty in comprehending complex acoustic stimuli such as speech in noise. On the other hand, in most cochlear-implant listeners forward masking and gap detection follow the same time course as they do in normal-hearing listeners, indicating that cochlear mechanisms are not the primary determinant of sensitivity to successive stimulation (Shannon and Otto, 1990). Indeed, physiologically-derived gap-detection thresholds measured in auditory centers from the cochlea through the thalamus have been shown to be shorter than those observed psychophysically (reviewed by Frisina (2001)).

Amplitude modulation detection is another important measure of temporal sensi-

tivity. Human listeners perceive amplitude fluctuations as shallow as 5% for modulation frequencies below about 60 Hz. Above that frequency, modulation sensitivity decreases by about 3 dB per octave, until ∼1 kHz, at which modulations evoke a percept of a steady sound, rather than rough fluctuations (Viemeister, 1979). Once again, cochlear implant listeners perform with comparable sensitivity, although some cochlear implantees have a low-pass cutoff closer to 120 Hz accompanied by a steeper decline of sensitivity (Shannon, 1992). Physiologically, the representation of amplitude modulation undergoes a particularly thorough transformation across the auditory system. Neurons in the auditory nerve are able to synchronize, or phase lock, to such amplitude modulations at rates up to ∼1kHz. Each successive level of the auditory system displays a low-pass tendency with lower and lower cutoffs, until the auditory cortex, where phase-locking is rarely seen to modulation rates above 100 Hz. Middlebrooks (2008a) showed differences among auditory-cortical lamina in regard to sensitivity to amplitude-modulated cochlear-implant stimuli: neurons in the thalamic input layers phase-locked to modulation frequencies greater than 60 Hz whereas extragranular units had lower limiting-modulation rates. Non-synchronized responses to amplitude modulations have been observed in cortex (Lu et al., 2001), where they generally encode higher modulation rates. This may be part of a central transformation from the phase-locking code to extract the modulation frequency as a feature of a particular stimulus.

1.3 Summary

Cochlear implants are devices that replace hearing in deaf individuals. The temporal information transmitted through an implant is determined both by the processing strategy and the transformations imposed by the auditory system. In this disserta-

tion, we consider the transmission of temporal information from electric stimulation to auditory cortex. Chapters 2 and 3 consider the effects of electric pulse rate on gap detection and forward masking measured in the cortex, and demonstrates that high and low pulse rates differentially activate a central component of forward suppression, resulting in shorter gap detection thresholds at higher pulse rates. Chapter 4 considers the effect of pulse rate on detection of amplitude modulation in the presence of masking stimuli. We show that the cortex responds to the summed envelope of the stimuli, even when pulse rate is low and the stimuli are interleaved with a 2-ms delay. Overall, the results suggest that there are tradeoffs in stimulus representation at each pulse rate. This research demonstrates several novel principles of central auditory processing: first, that forward suppression may be described as two processes and is differentially activated by stimuli at electric pulse rates spanning 254-4069 pps; second, that ON-, OFF- and TONIC-responses contribute to gap detection in the awake auditory cortex in a pulse-rate dependent manner; and finally, that cortical responses to simultaneous interleaved stimuli display temporal integration even at long interleaving delays, indicating that there is a central mechanism of channel interaction contributing to the perception of cochlear-implant stimulation.

CHAPTER 2

Auditory Temporal Acuity Probed with Cochlear Implant Stimulation and Cortical Recording

This work has been published in J. Neurophysiol. 2010; 103: 531-542

2.1 Introduction

Cochlear implant processors represent sound in the form of electric pulse trains to be presented to the cochlear nerve. All present-day implant processors initially analyze sound according to its frequency components using a bank of band-pass filters. The majority of processors then use the envelope of the output of each filter to modulate a constant-rate carrier pulse train, which is delivered to a cochlear electrode at the appropriate place in the cochlear frequency map. In normal hearing listeners, cues embedded in the temporal structure of the stimulus envelope contribute to speech recognition (van Tasell et al., 1987). For cochlear implant listeners, who have only limited spectral discrimination, such temporal cues are especially important. For this reason, efforts to optimize the accurate transmission of the temporal features of the acoustic envelope have the potential to improve speech reception. The carrier pulse rate influences the temporal resolution of the electrical signal presented to the auditory nerve. Higher carrier rates allow for more detailed sampling of the stimulus envelope and transmission of envelope information at higher fre-

quencies. Pulse rates also influence the basic firing characteristics of the auditory nerve. At low pulse rates, at which inter-pulse times exceed neural refractory periods, auditory nerve fibers can follow pulsatile stimulation pulse by pulse with high levels of between-fiber synchrony. As electric pulse rates increase, inter-pulse intervals shorten to less than the refractory periods of auditory fibers. In that condition, auditory-nerve responses become stochastic, exhibiting firing patterns more similar to those evoked by acoustic stimulation and, in particular, showing broadened dynamic ranges. These more-physiological, neural response patterns have been hypothesized to enhance transmission of temporal details (Rubinstein et al., 1999). Thus, any effect of increased electric pulse rate should be particularly evident in sensitivity to the stimulus envelope.

The ability of a listener to detect a gap in an ongoing sound or in an electrical pulse train is a useful measure of temporal acuity. Gap detection thresholds in cochlear implant users have been shown to be similar to those in normal hearing listeners (Shannon, 1989), suggesting that temporal acuity is limited by processing within the central auditory pathway. The effect of pulse rate on gap sensitivity in human cochlear implant listeners has been studied with mixed results (Busby and Clark, 1999; Preece and Tyler, 1989; van Wierengen and Wouters, 1999). These previous psychophysical studies of gap detection, however, tested pulse trains no higher than 1250 pulses per second (pps), which are lower than the rates that are hypothesized to foster stochastic firing of the auditory nerve.

Modulation detection is another important measure of sensitivity to the envelope-frequency content of ongoing stimuli. Sensitivity to modulation correlates with speech recognition scores in cochlear-implant users (Fu, 2002). Somewhat surprisingly, it has been shown recently that higher pulse rates result in decreased modulation sensitivity

in cochlear implant listeners (Galvin and Fu, 2005; Pfingst et al., 2007). This impaired transmission of modulation information has also been observed in the physiology of the auditory cortex (Middlebrooks, 2008b). In that study, carrier pulse rates greater than 500 pps resulted in increases in the stimulus modulation depths needed to produce cortical phase locking and resulted in reductions in the maximum modulation frequencies at which cortical phase locking was observed. These results are opposite to those predicted by the theoretical advantages of increased pulse rates.

Recordings from primary auditory cortex provide a measure of the results of brainstem processing of temporal information. We employed recordings from the primary auditory cortex of the anesthetized guinea pig to test the hypothesis that increased carrier pulse rates would result in enhanced temporal acuity for gaps in cochlear-implant pulse trains. Support for that hypothesis by early results prompted us to study the time course of recovery from forward masking as a means of exploring the mechanisms underlying the pulse-rate dependence of gap detection. The results of those studies are consistent with distinct peripheral and central mechanisms.

The present results yield new understanding of central processing of temporal information and have implications for processing strategies for auditory prosthesis.

2.2 Methods

2.2.1 Overview

Experiments were conducted at the University of Michigan with the approval of the University of Michigan Committee on the Use and Care of Animals. Single- and multi-unit activity was recorded from the primary auditory cortex of anesthetized guinea pigs using multi-site recording probes. Data were collected and stimuli were generated with Tucker-Davis Technologies System III hardware (TDT; Alachua, FL) connected to a personal computer running MATLAB (The Mathworks, Natick, MA)

and using software developed in this laboratory. Each animal was studied initially with acoustic tone stimulation, which served to guide placement of the recording probe relative to the cortical frequency representation. After suitable placement, the probe was fixed in place. In the majority of animals, cortical responses to additional acoustic stimulation were recorded. The animal was then deafened in both ears and a cochlear implant was inserted into the cochlea contralateral to the cortical recording sites. Responses to electrical cochlear stimulation were recorded for the purposes of this study. Recording sessions lasted 8-20 hours.

2.2.2 Animal Preparation and Data Acquisition

Recordings were made in the primary auditory cortex in the right hemispheres of 22 adult pigmented guinea pigs. Animals were of either sex and weighed 400-1000 g. Anesthesia was induced with an intramuscular injection containing 40 mg/kg ketamine hydrochloride and 10mg/kg xylazine hydrochloride and maintained with intramuscular ketamine hydrochloride. Body temperature was monitored with a rectal probe and maintained at or above 37° C with a heating pad.

To eliminate the possibility of unintended acoustic stimulation, the right ear was deafened by opening the bulla and ablating the cochlea. The auditory cortex was exposed on the right side. Primary auditory cortex was identified by its proximity to the pseudosylvian sulcus and by the characteristic rostrolateral to dorsomedial increase in characteristic frequencies, verified by recordings at three or more probe positions. When a cortical location within A1 with a characteristic frequency between 8 and 32 kHz had been identified, the recording probe was inserted perpendicular to the surface of the cortex. This frequency range corresponded to the tonotopic location of the cochlear implant to be placed in the basal turn of the cochlea. The exposed dural surface and silicon shank of the recording probe were covered with warmed 10%

agarose. The probe was fixed in place with methacrylate cement and dental sticky wax.

The cortical recording probe (NeuroNexus, Ann Arbor, MI) was a single thin-film silicon shank with 16 iridium-plated recording sites at 100 μm intervals. The probe was 15 μm thick and 100 μm wide, tapering to the tip. Signals from all 16 recording sites were recorded simultaneously, digitized at 24.4 kHz, low-pass filtered, re-sampled at 12.2 kHz, and stored for off-line analysis. An artifact-rejection procedure was used to eliminate electrical artifact resulting from the electrical cochlear stimulus (Middlebrooks, 2008a,b). On-line, a simple peak-picker was used to detect unit activity for experimental control. Off-line, spikes were identified using custom software that classified waveforms on the basis of the time and amplitude differences between spike peaks and troughs (Middlebrooks, 2008a). Only the off-line sorted spikes were used for quantitative analysis. We identified some well-isolated single units, but most channels provided unresolved spikes from two or more neurons. In this paper, a unit will refer to the spikes identified on a single recording channel and will include both multi-unit clusters and single units; well-isolated single units will be specifically described as such.

After acoustic stimulation, the left bulla was opened to expose the cochlea, and a small cochleostomy was drilled in the basal turn. Perilymph was wicked out and replaced with a 10% neomycin sulfate solution, which is toxic to hair cells. After 2 minutes, fluid in the basal turn of the cochlea was again replaced with 10% neomycin. A cochlear implant was inserted into the scala tympani through the cochleostomy. The cochlear implant was a six- or eight-channel banded scala tympani electrode (Cochlear Corporation), similar in design to the Nucleus 22 model designed for human use. Four to six bands could be placed within the scala tympani in our guinea-pig

preparation.

Current source density analysis (Müller-Preuss and Mitzdorf, 1984) was used to estimate the locations of recording sites relative to cortical layers. The most consistent feature was a short-latency sink which we have found previously in histological reconstructions to correspond to the transition from layer III to IV (Middlebrooks, 2008a). That landmark provided a depth reference that could be compared across animals (as in Figs. 2.4 and 2.8).

2.2.3 Stimuli

Acoustic and electric stimuli were created by Tucker Davis System III hardware controlled by a personal computer with custom software written in MATLAB. The data required to compute an individual measurement, such as a detection threshold, gap detection threshold, or forward masking recovery function, were collected in a single block of trials, and several measurements were obtained from each block. For example, gap detection stimuli were varied over presentation level and gap duration to obtain gap detection thresholds for each of the presentation levels. Each configuration of stimulus parameters was presented 20 times, and within each iteration the stimuli were interleaved randomly. To avoid systematic effects of the duration of anesthesia, the order of testing of various parameters was varied among experiments.

Acoustic stimuli consisted of tones and broadband noise bursts presented from a loudspeaker located about 15 cm from the left ear; tone and noise levels were calibrated, and noise spectra were flattened, using a precision microphone positioned at the approximate position of the ear in the absence of the animal. Tonal stimuli were used to characterize the location of the recording probe in the cortex on the basis of characteristic frequencies of neurons. The depth of the probe relative to cortical lamina was estimated from current source density analysis of 200-300 presentations

of 4 ms broadband noise bursts. Gap detection thresholds for broadband noise were obtained in normal-hearing conditions in 15 of the 22 animals. Pre-gap markers lasted 200 ms, post-gap markers lasted 120 ms, and both were presented at the same sound level. Gap duration and stimulus intensity were varied parametrically. Intensity levels were set to 20 and 40 dB above the detection threshold of the pre-gap marker.

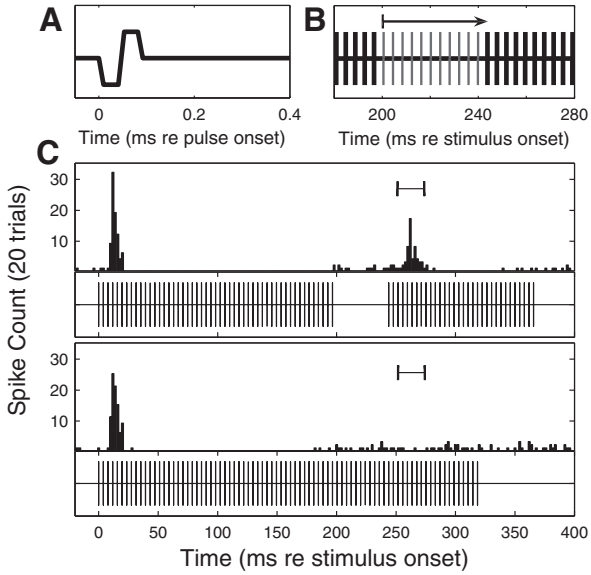

Figure 2.1: **Gap detection stimuli and cortical responses.** A: Electric pulse shape. B: Gaps presented in electric pulse trains in this study were integer multiples of the carrier period; in this case, ∼4 ms for 254 pps. C: PSTH of responses of a well-isolated single unit to a gap detection stimulus with a 43 ms gap (upper) and with no gap (lower). Underneath each PSTH is a diagram of the eliciting stimulus. The interval for comparison of spike count between gap and no-gap conditions is indicated on both histograms.

Cochlear implant stimulation was presented to all animals in this study. Electrical stimuli were generated by a custom eight-channel optically isolated current source, which was controlled by a TDT RX8 digital-to-analog convertor. A monopolar electrode configuration was used in which a single intracochlear electrode was active and a wire in a neck muscle was the return. Thresholds were estimated for each cochlear-implant electrode, and the electrode with the lowest threshold (always one of the

three most apical electrodes) was selected for subsequent stimulation. Figure 2.1A depicts the pulse shape. The phase duration was 41 μs, the interphase interval was 0 ms, and the leading phase was cathodic. The pulse rates tested were 254, 1017, and 4069 pps.

Electric gap detection stimuli consisted of pulse trains in which gaps were formed by deleting one or more pulses. Durations of pre- and post-gap markers were 196.6 and 121.9 ms, respectively, which corresponded to integer multiples of the pulse period. As shown in Fig. 2.1B, gap duration was defined relative to the first missed pulse, meaning that a gap of 0 ms was an uninterrupted pulse train. The minimum possible non-zero gap (corresponding to one missed pulse) was 3.93, 0.983, or 0.246 ms for pulse rates of 254, 1017, and 4069 pps respectively. Uninterrupted pulse trains also were tested as the 0-ms control stimuli. The longest gap routinely tested was 64 ms. Gap detection stimuli were presented at several current levels, most often 2, 4, and 6 dB above detection threshold. During gap-detection trials, pulse rates and pre- and post-gap marker durations were fixed but stimulus intensity and gap duration varied. Each block of trials yielded one gap detection threshold per stimulus intensity.

Forward masking was measured in 10 animals to shed light on mechanisms contributing to the pulse-rate dependence of gap thresholds that was observed. Forward-masking stimuli were similar in form to gap detection stimuli in that they also consisted of a pre-gap stimulus (masker), a silent gap (delay), and a post-gap stimulus (probe), but differed in two important ways. First, the probe stimulus was varied in intensity independent of the level of the masker in order to determine the probe threshold at each time delay. Second, the probe stimulus was shortened to measure the recovery from masking more precisely at one point in time. Masker duration was 196.6 ms and probe duration was 3.9 ms; that probe duration corresponded to 2

pulses at the 254-pps rate and 17 pulses at the 4069-pps rate; our previous work in this animal model has shown that cortical thresholds are dominated by the first ∼1 ms of electrical pulse trains (Middlebrooks, 2004). Eight to eighteen delays were presented, extending from 0 ms to 64 ms from masker offset. Masker levels were 0-6 dB above un-masked detection threshold. Masker and probe durations were fixed in each block of trials, but masker intensity, probe intensity and delay varied parametrically. A recovery-from-masking curve was generated for each masker intensity presented in the stimulus block. In addition, a threshold was measured for the 3.9-ms unmasked probe stimulus.

2.2.4 Data Analysis

Detection thresholds based on neural spike counts were measured using signal detection procedures (Green and Swets, 1966; Macmillan and Creelman, 2005); the specific procedures are described in (Middlebrooks and Snyder, 2007). Briefly, receiver-operating characteristic (ROC) curves were formed from the trial-by-trial distributions of spike counts in probe trials and background trials; the characteristics of the probe and background trials in various conditions are defined in the following paragraph. The area under the ROC curve gave the percent correct detection, which was expressed as a detection index (d').

In unmasked detection trials, the probe was the pulse train to be detected, and the background was no stimulus. Spikes were counted in the 7-30-ms interval after probe onset or in an equivalent interval during the background. In gap-detection trials, probe trials contained a gap in the pulse train and background trials had an uninterrupted pulse train (Fig. 2.1C). Spikes were counted in the 7-30-ms interval after the onset of the post-gap pulse train or in an equal interval in the background. In forward-masking trials, the probe was a pulse train of varying level presented

at a particular time after masker offset, and the background was the masker with no probe. Spikes were counted in the 7-20 ms interval after probe onset or in an equivalent post-masker interval in the absence of the probe. In all conditions, plots of d' versus probe level or versus gap duration were interpolated to find thresholds at $d'= 1$. In the case of gap detection, whereas all gaps presented were integer multiples of the carrier pulse period, interpolated gap detection thresholds could fall anywhere between the minimum and maximum gaps tested.

Recovery from masking was tracked by measurement of probe detection thresholds at successive delays after masker offset. At a delay of 0 ms, the probe stimulus had to be elevated above the level of the masker to elicit a significant response. Probe thresholds were expressed in units of current in μA. A single-exponential function was fit to current shifts relative to the unmasked threshold. The function had the form:

$$\Theta_m - \Theta_0 = Ce^{-t/\tau} + C_0, \tag{2.1}$$

where Θ_m is the masked threshold of the probe stimulus, Θ_0 is the unmasked threshold, τ is the time constant of recovery from forward masking, and C and C_0 are constants. Next, a dual-exponential function was fit to the same data:

$$\Theta_m - \Theta_0 = C_1e^{-t/\tau_1} + C_2e^{-t/\tau_2}, \tag{2.2}$$

where Θ_m is the masked threshold of the probe stimulus, Θ_0 is the unmasked threshold, τ_1 and τ_2 are the time constants of recovery from forward masking, and C_1 and C_2 are constants, referred to as the magnitudes of the exponential recovery processes. All fitted parameters were constrained to be positive. The fitting algorithm was a separable non-linear least squares curve fit using the Levenberg-Marquardt process (Nielsen 2000).

The data were fit in several ways. Originally, each forward masking condition for each unit was fit with the single-exponential function. Afterward, the dual-exponential function was applied to the data with different constraints. First, each forward masking condition for each unit was fit with the dual-exponential function. Then, the fitting functions for each unit were constrained across stimulus pulse rate so that a single set of time constants τ_1 and τ_2 were obtained for each animal, while C_1 and C_2 varied freely. In this procedure, the parameter that was minimized was the combined sum of squared errors ($CSSE$), defined as:

$$CSSE = \sum_{n} \sum_{p} \sum_{l} SSE^{n}_{p,l'} \tag{2.3}$$

where $SSE^{n}_{p,l'}$ was the sum of squared errors between the data and the fitted curve for the unit n, at the pulse rate p, and current level l, for all pulse rates and current levels presented. With each iteration of the curve fitting algorithm, the C_1 and C_2 parameters for each curve-fit shifted independently of one another to minimize the $CSSE$, while the τ_1 and τ_2 parameters shifted together so that they were always common to all fitted curves. The curve fit for an individual recovery function was selected for further analysis if it met the criteria: $R^2 > 0.7$; and long time constant $\tau_1 < 1000$ ms. The latter criterion excluded one animal from the analysis.

To measure growth of masking, we calculated median probe threshold shifts elicited by varying masker levels presented to each animal. Median values were calculated across all units for which a detection threshold was obtained. Linear regressions were then computed for each growth-of-masking function. All linear regressions were significantly different from a horizontal line through the mean, and 95% confidence intervals for each linear fit were computed.

Levels of gap-detection stimuli and forward maskers were set relative to thresholds for detection of unmasked stimuli. Such detection thresholds varied across cortical

depth. Thus, the intensity of a given stimulus could be computed either by comparison with the threshold of each individual channel, resulting in 16 individual levels, or by comparison with one detection threshold chosen to represent the probe penetration, such as the mean or the minimum detection threshold. We performed all analyses with both methods, which yielded similar results. The results presented in this paper were all plotted using the first method, with each unit assigned its own detection threshold. Units for which the detection threshold was above the maximum level presented were not considered in the analysis.

2.3 Results

2.3.1 Neural Responses to Gap Stimuli

Qualitatively similar response patterns were recorded in response to noise bursts and to electrical pulse trains at various pulse rates. We presented long, uninterrupted pulse trains for the 0 ms gap condition, shown in Fig. 2.1C and in the lowest row of Fig. 2.2. These control responses were typical in that there was a robust response to the stimulus onset, a period of suppression typically lasting 50 to 200 ms, and often a weak, temporally irregular tonic response beginning after the period of suppression. These response characteristics were similar across all electric pulse rates. The period of suppression and the tonic response typically were more temporally diffuse in acoustic-stimulation conditions than in electric-stimulation conditions, possibly because the broadband acoustic noise contained greater envelope structure than was present in the unmodulated electrical pulse trains.

Introduction of a gap of sufficient duration resulted in an onset response to the post-gap noise burst or pulse train, as seen in the upper blocks of rasters in Fig. 2.2. In addition, these onset responses to the post-gap stimulus were succeeded by a similar period of suppression and tonic response at all but the shortest detectable

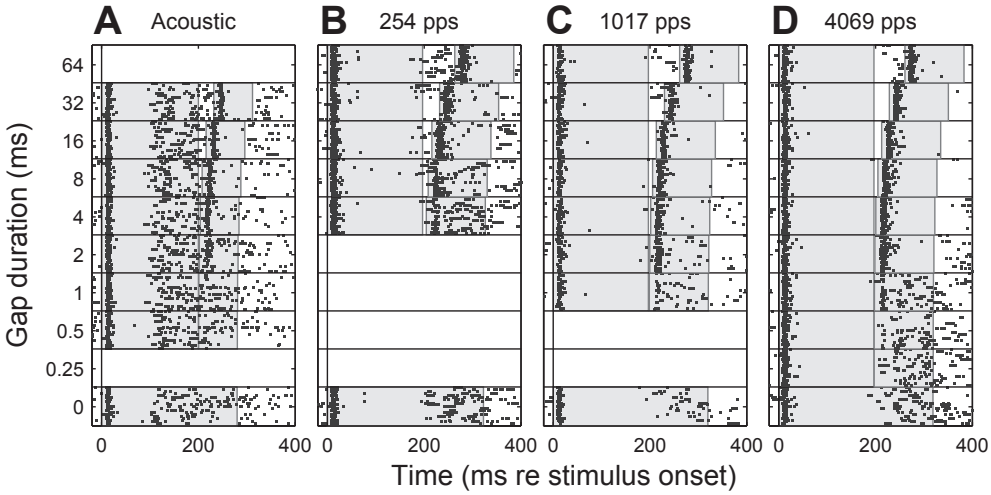

Figure 2.2: **Raster plot of multi-unit ensemble response to gap detection stimuli.** Each row corresponds to one trial and each dot is one spike. Trials are ordered by gap duration. Twenty trials were presented for each gap condition. Blank areas are placeholders for gap durations that were not presented for a given stimulus condition. The shaded grey areas represent the durations of the pre- and post-gap markers. Gap thresholds in this example were 3.50 ms for acoustic and 3.93, 1.08, and 0.75 ms for 254, 1017, and 4069 pps respectively.

gaps. As described in the METHODS, gap thresholds were computed using an ROC procedure that compared spike counts within restricted time windows in gap and no-gap conditions. In the illustrated example, gap detection thresholds were: 3.50 ms for acoustic; 3.93 ms for 254 pps; 1.08 ms for 1017 pps; and 0.75 ms for 4069 pps. This unit exhibited gap thresholds among the shortest 10% among the unit sample.

The example in Fig. 2.2 is typical of our data set in that gap detection thresholds tended to be shorter for higher-pulse-rate stimuli than at lower rates. That tendency was significant across the population of 336 units ($p < 0.001$, Kruskal-Wallis test; non-parametric one-way ANOVA). We calculated the cumulative distribution function (CDF) for each pulse rate, shown in Fig. 3. The median gap detection thresholds, equivalent to the CDF at $p = 0.5$, were well-separated: 16.7 ms for 254 pps, 2.7 ms for 1017 pps, and 1.3 ms for 4069 pps.

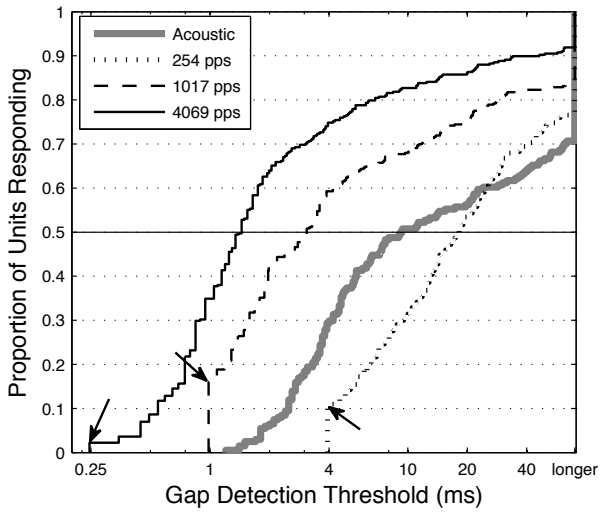

Figure 2.3: **Cumulative distribution of gap detection thresholds.** The graph represents the proportion of the population of units of each pulse rate with gap detection thresholds shorter than the given duration. Arrows indicate the proportion of units responding to one missed pulse for each pulse rate. These distribution functions were limited to gap thresholds obtained at 4-6 dB above detection threshold and channels located in -800 to +400 μm cortical depth.

The minimum non-zero gap duration that could be tested was determined by the duration of one missed pulse, which varied among pulse rates from 3.93 ms at 254 pps to 0.248 ms at 4069 pps. It was a concern that the gap detection thresholds might vary by pulse rate simply due to this trend. In Fig. 2.3, the proportions of units responding to one missed pulse are indicated with arrows. At every pulse rate, far fewer than 50% of units responded with an onset burst following only one missed pulse. For that reason, median values of gap detection thresholds were not influenced by minimum tested gap durations that varied among pulse rates. Nevertheless, we compared the d' statistic for a 3.93 ms gap at each pulse rate for the data depicted in Fig. 2.3, and found that there was a significant difference in the median d' across the population: 0.32 for 254 pps, 1.32 for 1 kpps, and 1.71 for 4 kpps ($p < 0.0001$, Kruskal-Wallis). Within individual units, the d' measured at any particular gap duration tended to increase with increasing stimulus pulse rate. Acoustic gap detection thresholds did not have an experimentally-imposed minimum, but the minimum gap detection threshold observed was greater than 1 ms.

As many as 20% of units failed to respond to the post-gap marker after the longest gap that was tested, 64 ms. The proportion of units that failed to respond after the longest gaps increased with decreasing pulse rates ($p < 0.05$, Mann-Whitney rank sum test).

2.3.2 Laminar Dependence of Gap Detection Thresholds

We assessed the degree to which intra-cortical mechanisms contribute to gap detection thresholds. We reasoned that systematic differences in gap thresholds among cortical laminae would be indicative of intra-cortical processing, whereas a lack of such differences would suggest that gap thresholds are determined primarily by subcortical processes. As described in the METHODS, we used current source density

analysis to estimate the depths of recording sites relative to the transition between layers III and IV. Median gap detection thresholds and intra-quartile ranges were calculated for each relative cortical depth (Fig. 2.4). Gap thresholds tended to be large at the deepest and shallowest depths. We speculate that this was due to the generally poor responses in those laminae observed in anesthetized conditions. Aside from the deepest and shallowest depths, however, there was no significant dependence of gap detection threshold on relative cortical depth across broad ranges of cortical depth. Solid black bars in Fig. 2.4 represent the relative cortical depths from -800 to $+700$ μm across which there was no significant dependence of gap threshold on cortical depth for any tested pulse rate ($p = 0.12$, Kruskal-Wallis, depths grouped with 300 μm resolution).

2.3.3 Gap Thresholds Depend on Stimulus Level

In human listeners, gap detection thresholds decrease with increasing stimulus intensity in both acoustic and electric conditions. In the present physiological study, stimulus levels were fixed relative to detection levels, and detection levels varied with pulse rate. For that reason, the pulse rates were presented at varying levels in the same animal. We tested whether differences in stimulus levels could have accounted for the observed dependence of gap thresholds on pulse rates. Fig. 2.5 shows the distributions of gap thresholds as a function of stimulus level for the three tested pulse rates.

Gap detection thresholds decreased substantially with increasing stimulus level for both acoustic stimulation and electric stimulation at all pulse rates. Gap sensitivity near detection threshold was poor at all pulse rates, with many units failing to respond to the longest gap tested. Improvements in gap detection thresholds started to level off at stimulus levels higher than 4 dB above threshold for electric stimulation. The

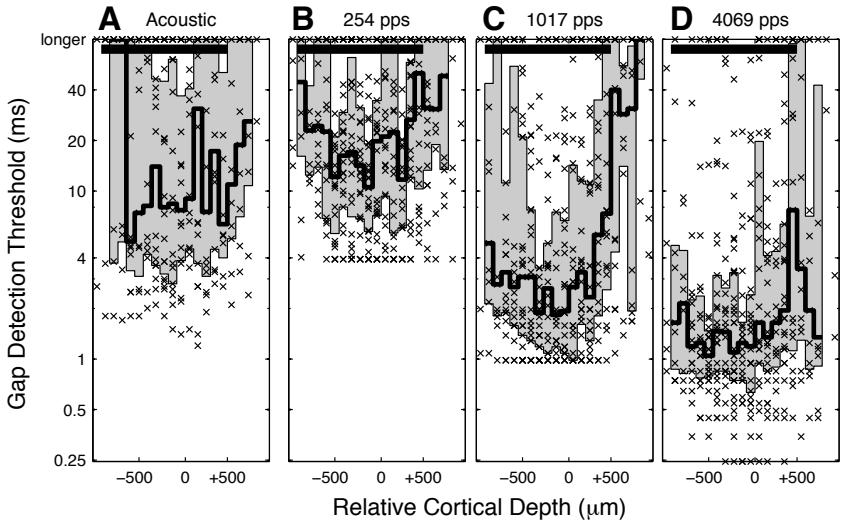

Figure 2.4: **Gap detection thresholds across cortical depth.** Cortical depth is measured relative to the Layer III/IV boundary, identified by the cortical depth exhibiting the earliest current sink. Symbols depict the individual gap detection thresholds. The shaded area represents the intraquartile range, computed in 100 μm increments of depth. The shallowest and deepest locations were merged so that distributions contained at least 10 gap-detection thresholds. The solid black bar at the top of the graph represents the cortical depths over which there was no significant difference between gap detection thresholds with cortical depth for any pulse rate. ($p \leq .12$, Kruskal-Wallis, data grouped in 300 μm increments of cortical depth) The gap detection thresholds were obtained at 4-6 dB above detection threshold for electric stimulation and 30-45 dB above detection threshold for acoustic stimulation.

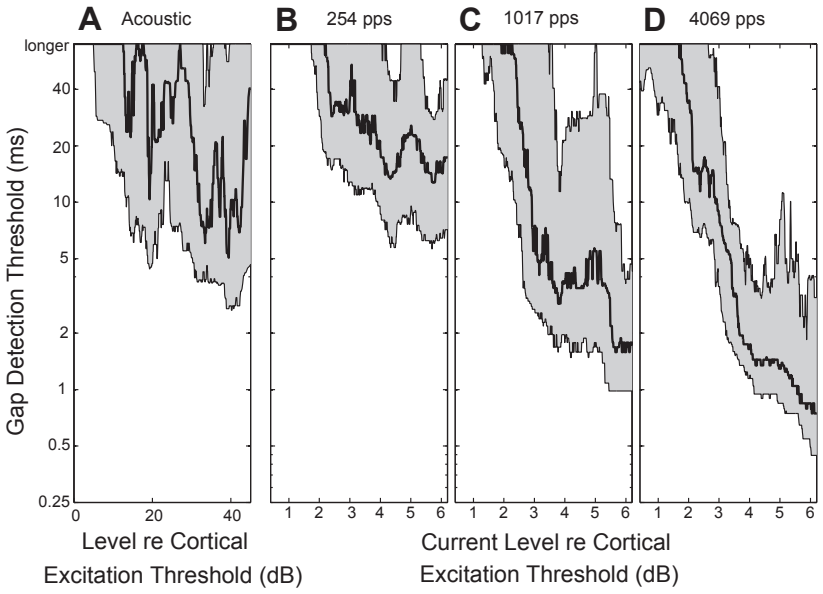

Figure 2.5: **Gap detection thresholds by level.** This graph shows distributions of gap detection thresholds for all units for which a detection threshold was obtained. Distributions were computed within a moving window that encompassed 10% of the sample. The shaded area is the intraquartile range, and the black line is the median gap detection threshold. Thresholds were limited to those obtained from -800 to $+600$ μm cortical depth.

pulse-rate dependence of gap thresholds was most evident at these higher stimulus levels. In order to consider gap detection thresholds from a near-asymptotic portion of the dynamic range, Figs. 2.3 and 2.4 plotted only thresholds obtained at 4-6 dB above detection threshold for cochlear implant stimulation and 30-45 dB above detection threshold for acoustic stimulation. We note that the highest levels tested relative to detection threshold were higher in absolute (μA) terms for the 254-pps pulse rate than for the 4069-pps rate because temporal integration at the highest rate resulted in lower detection thresholds. Thus, gap detection thresholds were dependent on stimulus levels relative to threshold rather than on absolute stimulus levels.

2.3.4 Forward Masking Recovery Depends on Pulse Rate

One possible explanation for the increased temporal acuity (i.e., decreased gap-detection thresholds) associated with higher pulse rates is that the recovery from forward masking might be faster when pulse rates are higher. We tested that hypothesis by measuring masked thresholds across a range of masker-probe delays, fitting recovery-from-masking curves, and then computing recovery functions (as described in the METHODS). The first function fit to the data, Eq. 2.1, was a single exponential curve with a constant term representing residual masking. The curve fits demonstrated a significant interaction of pulse rate and exponential time constant ($p < 0.001$). The median time constants [τ in Eq. 2.1] were: 18.9 ms at 254 pps, 10.7 ms at 1017 pps, and 9.1 ms at 4069 pps. These curve fits are not displayed.

The single exponential produced a reasonable fit to the data, but it was difficult to construct a plausible physiological mechanism that would explain a dependence of τ [Eq. 2.1] on pulse rate. For that reason, a dual-exponential function, given by Eq. 2.2, was fit to the data; an example for one unit is shown in Fig. 2.6. These curves comprised long and short recovery functions, and a pair of time constants was

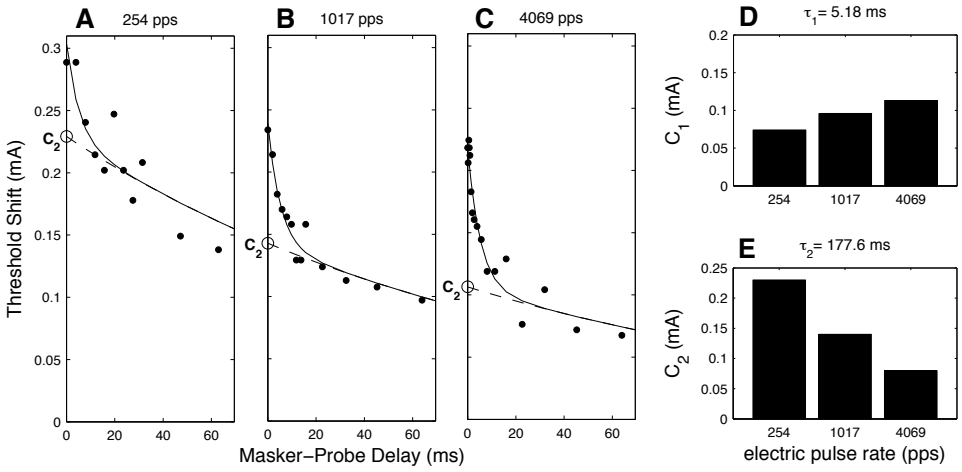

Figure 2.6: **Recovery from forward masking for one unit.** A,B,C. Threshold shifts at 11-18 time points after masker offset are plotted for each pulse rate condition, along with the constrained curve fits. The maskers were presented at 4.3, 4, and 3.8 dB above this unit's threshold for 254, 1017, and 4069 pps respectively. The magnitude of the longer exponential component (C_2) is indicated on the y-axis. D. The magnitude of the rapid ($\tau_1 = 5.18$ ms) and E. longer ($\tau_2 = 177.6$ ms) exponential terms for the curve-fits by pulse rate.

computed for each animal [τ_1 and τ_2 in Eq. 2.2] as described in the METHODS. For a single pair of time constants to describe all forward masking conditions, these time constants should be independent of stimulus level, pulse rate, and cortical depth. To verify these assumptions, we also fit a dual exponential curve to each recovery-from-masking dataset independently. When each stimulus condition was fit with a different pair of time constants (not shown), these time constants did not differ across stimulus level ($p = 0.12$, ANOVA), pulse rate ($p = 0.08$, ANOVA), or cortical depth ($p = 0.5$, ANOVA). The two time constants obtained for each animal are displayed in Fig. 2.7A. The magnitude of the contribution of the long exponential recovery process [C_2 in Eq. 2.2] was significantly smaller at higher pulse rates ($p < 0.001$, Kruskal-Wallis) (Fig. 2.7C), whereas the magnitude of the short exponential recovery [C_1 in Eq. 2.2] was not ($p = 0.083$, Kruskal-Wallis) (Fig. 2.7B). When combined, these terms describe a more rapid recovery process at higher pulse rate conditions. Faster

recovery should lead to a shorter gap detection threshold, as the lagging stimulus would elicit a response at a shorter gap.

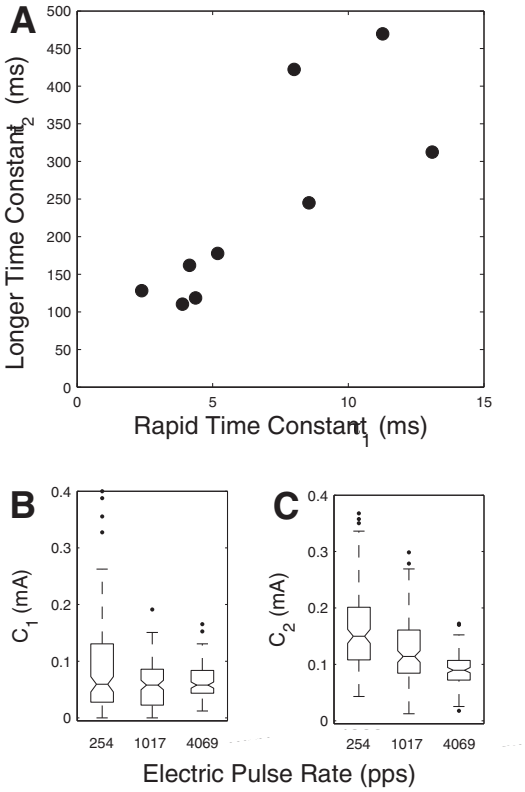

Figure 2.7: **Summary of forward masking curve fits.** A. Time constants obtained for each animal that met goodness-of-fit criteria. B. Magnitude of rapid time constant component (C_1) at each pulse rate across all units meeting the goodness-of-fit criteria. C. Magnitude of longer time constant component (C_2) at each pulse rate across all units meeting the goodness-of-fit criteria.

2.3.5 Growth of Masking is Linear

The non-linear dependence of gap detection thresholds on stimulus level might arise solely from the exponential dependence of masking on time after stimulus offset, or it might reflect an additional nonlinearity in the growth of masking. We measured the linearity and magnitude of the growth of masking for a series of time points after masker offset, summarized in Fig. 2.8. Within-animal growth-of-masking functions were uninformative because only two masker levels were presented to most animals.

However, it is notable that growth-of-masking functions compiled across animals were linear. Growth of masking slopes were near 1 at masker offset and were significantly shallower at 64 ms after masker offset for all pulse rates. Thus, the decrease in gap detection thresholds at higher stimulus levels is consistent with the fact that the masking provided at one stimulus level is insufficient to mask a probe presented at the same stimulus level.

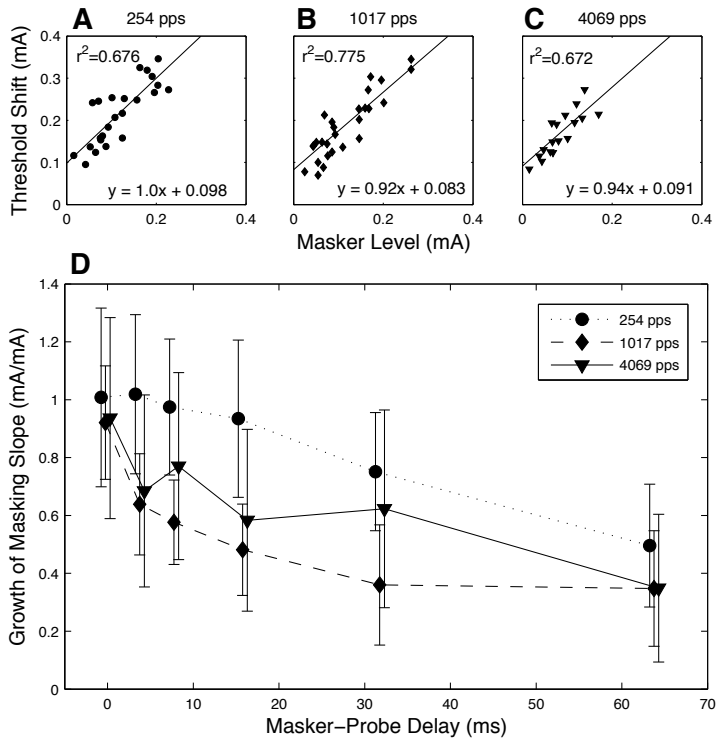

Figure 2.8: **Growth of masking.** The increase in forward masking with masker level is linear at all time points after masker offset, and the slope decreases over time. A, B, C. Growth of masking at 0 ms after masker offset. Each data point represents the median values of masker level and probe threshold shift across all units recorded in one animal. Each animal contributed at least two data points. D. Growth of masking slopes at various masker-probe delays. Error bars represent 95% confidence intervals of the least-squares linear regression.

2.3.6 Laminar Dependence of Forward Masking

Figure 2.9 demonstrates another important similarity to gap detection thresholds: the magnitude and time course of forward masking did not vary significantly with

cortical depth. This suggests that the forward masking and subsequent recovery processes described in our equation reflected sub-cortical processing.

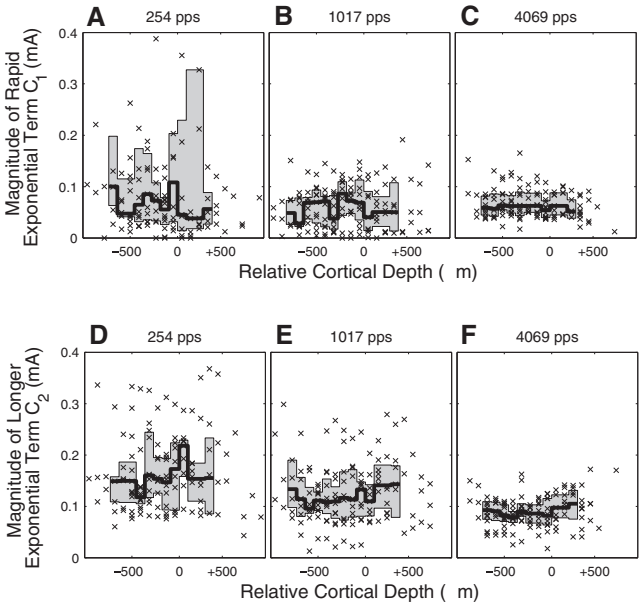

Figure 2.9: **Forward masking across cortical depth.** Each symbol represents one term from a dual-exponential curve fit to at least four forward masking time points. The shaded area represents the intraquartile range of the population, and the black line represents the median magnitude. Cortical depth is measured relative to the Layer III/IV boundary as in Fig. 2.4. There is no significant difference in masking over cortical laminae. Forward masking recovery constants are based on data for all masker levels. A, B, C: Magnitude of rapid exponential component (C_1) D, E, F: Magnitude of longer exponential component (C_2).

2.3.7 Forward Masking Model Predicts Gap Detection Thresholds

To test the hypothesis that forward masking and gap detection reflect the same underlying auditory processes, we used our forward masking curve fits to create a model of gap detection. In a subpopulation of 76 units, both gap detection and forward masking data were available with identical masker levels. Of these units, 38 yielded a gap detection threshold that exceeded 64 ms for one or two stimulus conditions, primarily at low stimulus levels and pulse rates. These conditions were excluded, since the exact durations of the gap thresholds were not measured. We

then took the forward masking curve fit and the gap detection threshold for each of the remaining stimulus conditions for each unit and computed the expected shift in detection threshold at the duration of the first detectable gap, using the recovery-from-masking equation. In Fig. 2.10, we compared these computed thresholds to the actual post-gap probe stimulus in the gap detection that evoked the minimum detectable gap and computed linear regressions. The 95% confidence intervals included a slope of 1 and intercept of 0 for every pulse rate, indicating that our gap detection and forward masking results are in good agreement. Note that these data points are drawn from responses to the entire range of current levels. This result supports both our model of forward masking and our hypothesis that gap detection and forward masking are supported by similar temporal processes.

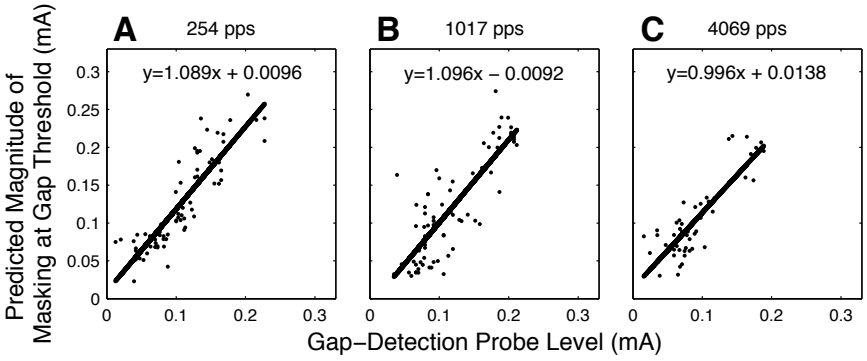

Figure 2.10: **Forward masking curve-fit predictions for gap detection results.** The magnitude of the forward-masked threshold shift for one unit was calculated at the masker-probe delay corresponding to the gap-detection threshold for that unit and compared to the actual post-gap marker level that elicited the detection of the gap. For all pulse rates, 95% confidence interval ranges of the linear regression included the equality equation.

2.4 Discussion

The principal finding of this study is that gap detection thresholds decrease substantially with increasing pulse rate. We begin the discussion by comparing this

result with previous psychophysical and physiological studies. Second, we consider the pulse-rate dependence of gap threshold in the context of an exponential recovery model of forward masking. We then discuss the effect of stimulus level on gap detection thresholds. Finally, we conclude with the observation that gap detection represents a temporal process distinct from modulation detection.

2.4.1 Comparison with Human Psychophysics

The present physiological results indicate that gap detection thresholds measured in the auditory cortex are substantially shorter at higher pulse rates. A decrease in perceptual gap detection threshold with high pulse rate has been observed in human cochlear implant users although, as is often the case in these studies, the range of performance across subjects is broad. Preece and Tyler (1989) tested detection of gaps in 63-4000 Hz electric sinusoids by cochlear implant listeners. After matching loudness across carrier rates, they observed that gap thresholds decreased with increasing stimulus frequency at current levels near detection threshold, although there was no difference in gap detection thresholds between carrier frequencies at higher current levels. van Wierengen and Wouters (1999) compared gap detection at 400 and 1250 pps and found that gap detection thresholds were shorter at the higher pulse rate for three out of four subjects. The fourth subject showed no difference in gap sensitivity. Grose and Buss (2007) did not explicitly compare gap detection thresholds across pulse rate, but obtained thresholds of 1 ms or less in several listeners at a pulse rate of 3 kpps. This accords with the current observation of gap detection thresholds under 1 ms at 4069 pps and is shorter than the typical 2-5 ms psychophysical gap detection thresholds obtained at lower pulse rates (Shannon, 1989). Studies that tested stimulation rates only up to 1000 pps have shown little or no correlation between pulse rate and gap detection threshold. Busby and Clark (1999) found no

consistent pattern of sensitivity across pulse rates in the range 200-1000 pps. Similarly, Chatterjee et al. (1998) also observed no significant difference in two of three listeners across pulse rates from 125-1000 pps.

2.4.2 Comparison with Physiological Studies of Gap Detection

Studies of auditory-evoked cortical potentials in human subjects demonstrate that the temporal acuity of the auditory cortex is comparable to behavioral gap detection thresholds in normal hearing listeners. Gaps in broadband noise elicited middle-latency responses associated with primary auditory cortex at gap durations similar to the behavioral thresholds measured in the same listeners (Lister et al., 2007). In a study of mismatch negativity (Heinrich et al., 2004) using gaps in tones, dipole source modeling suggested that the gaps were represented in or near the primary auditory cortex.

Previous electrophysiological studies focused on neural mechanisms in the auditory cortex for the detection of gaps in noise. Eggermont (2000) described the responses of cat primary auditory cortex under anesthesia to gaps with varying leading burst durations. For broadband noise stimuli similar in temporal structure to those tested in the current study, gap detection thresholds were 5-10 ms. Wang et al. (2006) measured local field potentials obtained in the primary auditory cortices of normal-hearing, awake guinea pigs and observed gap detections thresholds of 4-6 ms with broadband noise bursts. These thresholds are equal to or in some cases longer than psychophysical thresholds, and are consistent with the acoustic gap detection thresholds obtained in this study.

2.4.3 Neural Basis of Gap Detection Dependence on Pulse Rate

Gap detection thresholds can be elucidated by examination of the time course of cortical sensitivity after the offset of the pre-gap stimulus. We obtained forward masking results that were in agreement with our gap detection findings. Higher pulse rates evoked shorter-lasting forward masking, and this difference was more pronounced at longer masker-probe delays. Forward masking and gap detection likely result from the same neural mechanisms, as these stimuli share a common temporal structure and have been shown to give consistent results in human psychophysical studies (Plomp, 1964). This hypothesis is supported by the constancy of temporal acuity across cortical laminae that we observed in both gap detection and forward masking. The forward masking data therefore provide a framework in which to understand gap detection.

In order to quantify the influence of pulse rate on recovery from masking, we fit two curves to the forward masking data obtained in this study. The first was a single exponential similar to that used in Nelson and Donaldson's (2002) examination of electric pulse train forward masking in human listeners. Using this approach on the data in the present study, we obtained time constants of recovery that were significantly shorter at higher electric pulse rates. This result implied that the pulse rate of a forward masker influenced the speed of recovery following the cessation of the masker, which is difficult to explain with a physiologically plausible model. For that reason, we considered models incorporating more than a single component.

We hypothesized that the forward masking observed in cochlear implant stimulation has both peripheral and central components that could be reflected in a dual-exponential model. Such a dual-exponential model was used by Chatterjee (1999) to fit psychophysical recovery-from-masking curves in human cochlear implantees: she

obtained one rapid (2-5 ms) and one longer (50-200 ms) time constant. The rapid exponential component likely reflected adaptation within the auditory nerve. Zhang et al. (2007) described responses to electric pulse trains in the cochlear nerve of the cat. They measured a rapid time constant of adaptation with a median value of 8 ms, which did not differ significantly between 250, 1000, and 5000 pps pulse trains. They attributed this time constant to refractory effects in the auditory nerve, which should also contribute to forward masking. The longer time constant observed by Chatterjee (1999) is more difficult to attribute to any one physiological source. In that study, the longer time constant was quite variable between subjects. Support for a forward masking mechanism central to the auditory nerve is provided by Shannon and Otto's (1990) observation that the time course of recovery from pulse train forward masking is similar in listeners with cochlear implants and auditory brainstem implants. Nelson et al. (2009) measured forward masking in the inferior colliculi of awake marmosets. In a sub-population of neurons, forward-masked thresholds were similar to those measured psychophysically in normal-hearing subjects (such as Oxenham and Plack (2000)), reflecting a central contribution to forward masking that was most consistent with an adaptive or inhibitory mechanism. The 100-500 ms time constant in the current study also may reflect the sum of several processes central to the auditory brainstem.

Using this dual exponential function and allowing the time constants to vary freely, we obtained results similar to those in Chatterjee's study in 9 out of 10 animals. These time constants did not differ systematically with pulse rate, stimulus level, or cortical depth, supporting our hypothesis that the underlying neural mechanism remains the same at any pulse rate or stimulus level. To obtain the best measurement of each time course, we linked the curve fits together so that a single pair of time constants

was obtained for each animal. The rapid time constants fell in the range of 3-13 ms, with a median of $\tau_1 = 5.18$ ms; the longer time constant was 100-500 ms with a median of $\tau_2 = 177$ ms. The results of this model were mutually consistent with our gap detection results, in that the forward masking results could predict the threshold shift at the gap detection threshold in a subset of units for which both stimuli were presented at the same current levels. The predicted threshold shift correlated strongly with the level of the post-gap marker above threshold.

The time course of recovery from forward masking explains the dependence of gap detection on electric pulse rate. Neither the time constant nor the magnitude of the rapid recovery-from-masking process, likely located in the periphery, differed with increasing pulse rate. In contrast, the longer recovery process, putatively reflecting more central contributions, contributed a greater magnitude of masking in response to a lower-rate pulse train. Higher pulse rates evoked less central masking, leading to significantly lower masked thresholds less than 10 ms after masker offset. Therefore, shorter gap detection thresholds occurred at high pulse rates because the masked detection threshold dropped below the level of the post-gap marker relatively quickly after masker offset.

Results in human cochlear-implant users are consistent with the notion of distinct peripheral and central mechanisms. Brown et al. (1996) compared ECAP recovery and psychophysical forward masking with the same stimuli. Whereas ECAP recovery followed a time course similar to that described by the rapid time constant in the current study, psychophysical recovery from masking frequently followed a longer time course, indicating an additional contribution to forward masking central to the auditory nerve. This study also demonstrated selective activation of this central component. Within each individual listener, stimulating one cochlear-implant chan-

nel might yield a rapid recovery similar to that measured with ECAP, while other channels elicited a longer time course of recovery.

In the auditory nerve, the amount of adaptation to a stimulus several hundred milliseconds in duration increases with increasing pulse rate (Zhang et al., 2007). A low-rate pulse train evokes an auditory nerve response that maintains its spike rate throughout the duration of a long pulse train, providing constant input to central processing centers for hundreds of milliseconds. A high-rate pulse train, on the other hand, elicits more spikes at the onset of the stimulus, but produces a less sustained response. During a masker stimulus of sufficient length, ascending input to higher processing centers decreases at higher pulse rates, leading to a more rapid time course of recovery. This leads in turn to shorter gap detection thresholds.

Our previous work in this animal model has demonstrated decreases in thresholds for activation of the auditory cortex as carrier pulse rates are increased beyond $\sim$1 kpps (Middlebrooks, 2004). That effect was interpreted to reflect temporal integration of electrical pulses at the level of the auditory nerve. Although that form of temporal integration resulted in an overall increase in sensitivity to the onsets of masker pulse trains and probe stimuli, there was no indication that temporal integration produced any net increase in the sustained effects of masker pulse trains - indeed, the available evidence cited above indicates that high pulse rates result in increases in adaptation in auditory-nerve response patterns.

There are two plausible mechanisms for the decrease in the magnitude of a central component of forward masking with increasing pulse rate. One is that the magnitude of the masking provided by the stimulus is proportional to the number of spikes evoked in the auditory nerve near the end of the masker duration. At high pulse rates, the central component of masking would decline in proportion to the adaptation in the

auditory nerve. Another possibility is that the central mechanism of forward masking is activated by ascending input only above a certain threshold of spike rate. At high pulse rates, the auditory nerve spike rate may fall below this threshold during the masking pulse train. In this case, the activation of the central component of masking would end prior to the offset of the stimulus. The data do not distinguish between these explanations.

2.4.4 Effect of Level on Gap Detection and Forward Masking

At each pulse rate that we tested, gap thresholds decreased with increasing current levels. It is difficult to compare absolute stimulus levels between physiological and psychophysical results because of the lack of a measure of perceptual loudness in physiological studies. Nevertheless, human studies generally agree with our results, showing decreasing gap detection thresholds with increasing stimulus level (Preece and Tyler, 1989; Shannon, 1989). To explain this finding, we examined growth of forward masking with stimulus level. The slope of the growth-of-masking functions increased with decreasing masker-probe delay. As gap durations shorten, the growth of response to the post-gap stimulus should exceed the growth of masking only at higher stimulus levels.

We observed that growth of masking with current level was linear for electric stimulation at all time points after masker offset. These cortical results are consistent with other reports of linear growth of masking in the auditory nerve (Brown et al., 1996) as well as in human perception of cochlear implant stimulation (Nelson and Donaldson, 2001, 2002). Oxenham and Plack (2000) demonstrated with acoustic stimulation in normal hearing listeners that the nonlinearities evident in the growth of masking with masker level, duration, and frequency were the result of peripheral nonlinearities at the basilar membrane, and that forward masking in normal hearing

could be separated into a nonlinearity at the periphery followed by a linear response more centrally. We infer that measurements of forward masking evoked by cochlear implant stimuli provide a direct measure of the forward masking processes central to the inner hair cell synapse, which is absent in deaf subjects.

2.4.5 Comparison with Modulation Detection

Sensitivity to amplitude modulation of electric pulse trains is an alternative measure of temporal acuity that may be compared to gap detection. Prior comparisons of the sensitivity of cortical responses to acoustic gap-related amplitude-modulated stimuli have indicated that coding of these features may differ. Phillips and Hall (1990) showed that the precision of the first spike latency in auditory cortex of anesthetized cats is similar to that found peripherally in the auditory nerve, whereas phase-locking to ongoing modulated stimuli is low-pass filtered from the periphery to the cortex. Sinex and Chen (2000) demonstrated that there is no consistent relationship in the responses of neurons in the central nucleus of the inferior colliculus between sinusoidally modulated tones and artificial consonant-vowel pairs that vary in voice onset time. Recent electrophysiological studies of cortical modulation detection from our laboratory produced results that differed in several ways from the present gap-detection results (Middlebrooks, 2008a). First, modulation sensitivity in that study decreased with increasing electric pulse rate. This is the opposite of the effect of pulse rate on gap detection threshold. Second, the cortex was more sensitive to shallow modulation depths at lower stimulus levels, in contrast with the longer gap detection thresholds observed at low current levels. Finally, modulation detection in anesthetized guinea pig cortex showed a significant dependence of limiting modulation frequency on cortical depth. Compared to thalamic afferent layers, extragranular layers showed phase-locking at lower limiting modulation frequencies

and showed longer group delays. Those observations suggest the presence of an intra-cortical low-pass filtering mechanism. In contrast, our present results indicate that gap detection thresholds are not significantly different over a 1.5 mm depth of the cortex that spans most of the layers in primary auditory cortex, including the input layers. These observations suggest that within-channel gap detection thresholds are determined by sub-cortical mechanisms. The central auditory processing for gaps and modulation detection is distinct.

2.4.6 Conclusions

We observed enhanced temporal acuity in primary auditory cortex with increasing electric pulse rate. Gap detection thresholds were shorter and recovery from forward masking was more rapid with higher pulse rates. Gap detection thresholds shortened with increased stimulus level. Given the enhanced temporal acuity at high pulse rates observed in the present cortical study, the failure of higher pulse rates to enhance speech reception is puzzling. One possible explanation is that temporal acuity finer than normal hearing, such as we have seen in our gap detection thresholds at 4069 pps, could actually produce confusion of common speech cues. For example, voice onset times are similar in duration to across-channel gap detection thresholds in normal hearing listeners (Phillips et al., 1997). Perhaps temporal hyper-acuity would disrupt discrimination of voiced and unvoiced stop consonants. Another possibility is that cochlear implant performance is limited by sensitivity to amplitude modulation of electric pulse trains. Sensitivity to amplitude modulated signals has been shown to be important in speech recognition in both normal hearing listeners responding to acoustic stimuli (Elliot and Theunissen, 2009) and in cochlear implant listeners (Fu, 2002). This form of temporal processing is actually less sensitive at higher pulse rates.

We note that amplitude modulated pulse trains may produce less adaptation in the auditory nerve than unmodulated pulse trains, even at high pulse rates. For that reason, the difference in adaptation to a long pulse train between low and high pulse rates might be less during typical use of a cochlear implant, compared to our physiological testing conditions.

When designing processor strategies it will be important to keep in mind that the central auditory system may interpret ascending cochlear stimulation differently at different pulse rates. Central contributions to forward masking and gap detection thresholds decrease with increasing pulse rate. The dependence of neural responses on carrier pulse rate occurs not only at the level of the processor and nerve but also higher in the auditory system.

CHAPTER 3

Unanesthetized Auditory Cortex Exhibits Multiple Codes for Gaps in Cochlear-Implant Pulse Trains

This work is under revision with J. Assoc. Res. Otolaryngol.

3.1 Introduction

Cochlear implants restore hearing by stimulating the auditory nerve with amplitude-modulated electric pulse trains. In animal studies, pulse rates slower than ∼1000 pps elicit highly synchronous auditory-nerve firing (Zhang et al., 2007). Much higher rates have been hypothesized to decrease neural synchrony, thereby better approximating the responses of the auditory nerve to sounds (Rubinstein et al., 1999). Some human listeners prefer high pulse rates (Battmer et al., 2010), but differences in speech recognition performance generally are small across pulse rates ranging from 400 to 4800 pps (Holden et al., 2002; Loizou et al., 2000; Plant et al., 2007; Shannon et al., 2011; Verschuur, 2005).

Gap detection is a measure of temporal acuity in normal hearing. Listeners attempt to detect a silent gap lying between leading and trailing stimuli that activate the same (within-channel) or different (across-channel) peripheral channels. Normal-hearing listeners can detect within-channel gaps as brief as 2-5 ms. Cochlear-implant listeners can detect gaps of similar duration in electrical pulse trains (Shannon,

1989). That gap thresholds are similar between normal-hearing listeners and cochlear-implant users, in whom cochlear mechanotransduction is absent, suggests that gap detection thresholds are determined largely by central auditory mechanisms. Elevated gap-detection thresholds are symptomatic of poor speech recognition, at least in cases of auditory neuropathy (Zeng et al., 2005), although available studies of cochlear-implant listeners have not yet shown a correlation of gap acuity with speech recognition (Busby and Clark, 1999).

Several studies have demonstrated parallels between perceptual gap-detection thresholds and those measured in the cortex. In a study in humans, gap-detection thresholds for leading markers of 5, 20 and 50 ms measured with magnetoencephalography were within 1 ms of those measured psychophysically (Rupp et al., 2004). In awake animals, 74% of cortical neurons in cat (Liu et al., 2010) and 25% in macaque (Recanzone et al., 2011) encoded gap duration with sufficient sensitivity to account for behavioral performance in those species.

We reported previously the responses of auditory cortex neurons in anesthetized guinea pigs to cochlear-implant pulse trains (Kirby and Middlebrooks, 2010). The onset of a leading pulse train consistently elicited a burst of spikes and, following a gap of sufficient duration, the trailing pulse train elicited a second burst of spikes. A period of suppression lasting $\sim$100 ms after the onset response blocked detection of gaps presented in that period. We suspected that the highly stereotyped patterns of responses in that study were largely due to the use of anesthesia.

The present study was conducted in awake, non-behaving guinea pigs. We observed a variety of features of cortical responses that could signal the presence of a gap, and those responses varied with stimulus pulse rate, current level, and short-versus-long leading pulse-train duration. We confirmed our previous observation

from anesthetized conditions that temporal acuity increased with increasing electrical pulse rate. We further tested the hypothesis that differences across pulse rate were attributable to auditory nerve adaptation by comparing gap-detection thresholds for gaps lying early and late in the pulse-train stimulus. Finally, we tested the hypothesis that, as with human psychophysical measures, cortical gap-detection thresholds decrease with increasing stimulus level.

This study provides a basis for understanding the ways in which pulse rate shapes the coding of cochlear-implant stimulus envelopes. The effects of carrier pulse rate persist beyond the periphery as auditory nerve fiber responses are transformed by the central auditory system.

3.2 Methods

3.2.1 Overview

Extracellular spike activity was recorded from the primary auditory cortex (area A1) of awake, non-behaving guinea pigs using chronic multi-electrode recording probes. Each animal underwent a surgical procedure to implant a recording probe, with placement guided by cortical frequency tuning to acoustic tones. After suitable placement, the probe was fixed in place. The animal was then deafened and a cochlear implant was inserted into the cochlea contralateral to the cortical recording sites. Recording sessions lasted 1-2 hours and took place 3-8 days after the surgical procedure. All experiments were performed with the approval of the University of California at Irvine Institutional Animal Care and Use Committee.

3.2.2 Animal Preparation

Recordings were made in the primary auditory cortex in the right hemispheres of 6 adult albino guinea pigs. Animals were of either sex and weighed 340-490 g at the

time of surgery. The implantation procedure was performed under sterile conditions.

To eliminate the possibility of unintended acoustic stimulation, the right ear was deafened by infusion of 10% neomycin sulfate into the scala tympani (Middlebrooks, 2004). The auditory cortex was then exposed on the right side. Primary auditory cortex was identified by its proximity to the pseudosylvian sulcus and by the characteristic rostrolateral to dorsomedial increase in characteristic frequencies, verified by recordings at three or more probe positions. When a cortical location within A1 with a characteristic frequency between 8 and 32 kHz had been identified, the recording probe was inserted perpendicular to the surface of the cortex. This frequency range corresponded approximately to the tonotopic location of the cochlear implant to be placed in the basal turn of the cochlea. The exposed dural surface and silicon shank of the recording probe were covered with a calcium alginate gel (Nunamaker et al., 2007). The flexible ribbon cable connecting the probe and connector was encased in silicone elastomer (World Precision Instruments, Sarasota, FL). The connector was fixed to the skull with methacrylate cement. A screw was placed in the skull near the craniotomy to serve as a recording reference.

The left bulla was opened to expose the cochlea. A cochleostomy was drilled in the basal turn of the scala tympani, and the ear was deafened with neomycin. A cochlear implant was inserted through the cochleostomy into the scala tympani. The cochlear implant was an eight-electrode banded array (Cochlear Corporation), identical in dimensions to the distal 8 electrodes of the clinical Nucleus 22. Only five bands could be placed within the scala tympani in our guinea-pig preparation. The implant was sealed in place with biocompatible carboxylate cement (3M ESPE, St. Paul, MN). A platinum-iridium wire was placed into a neck muscle to serve as a monopolar return contact. All connectors were encased in methacrylate cement. The

skin was closed around the two (stimulating and recording) percutaneous connectors. The animal was allowed to recover with supportive care.

3.2.3 Awake Recording and Data Acquisition

Stimulus generation and data acquisition employed System III hardware from Tucker-Davis Technologies (TDT; Alachaua, FL) coupled to a personal computer running MATLAB (The Mathworks, Natick, MA) and using software developed in this laboratory. Pulsatile electric stimuli were generated by a custom eight-channel optically-isolated current source controlled by the TDT hardware.

Recording sessions took place 3-8 days after surgery. Data presented from each animal were taken during one or two consecutive 1- to 2.5-hr recording sessions, with 2.5 to 6 hours elapsing between the first and last recordings. The order of stimulus presentation was different in each animal. Prior to recording, the recording electrodes were "rejuvenated" by passing 2.0 VDC through each recording site for 4 s to improve the signal-to-noise ratio (Johnson et al., 2004). Animals were lightly restrained with a Guinea Pig Snuggle (Lomir Biomedical, l'Ile Perrot, Quebec). Their heads were free, and they were monitored during the recording session to ensure that they did not sleep, struggle or show signs of distress.

The cortical recording probe (NeuroNexus, Ann Arbor, MI) was a single silicon-substrate shank with 16 iridium-plated recording sites at 100 μm intervals. The probe was 15 μm thick and 100 μm wide, tapering to the tip; a monolithic silicon-substrate ribbon cable carried the signals to the skull-mounted connector. Signals from all 16 recording sites were recorded simultaneously, digitized at 24.4 kHz, low-pass filtered, re-sampled at 12.2 kHz, and stored for off-line analysis.

One of two artifact-rejection procedures was used to eliminate electrical artifact resulting from the electrical cochlear stimulus. For 254-pps stimuli, a sample-and-

hold procedure was implemented such that the recorded neural signal was clamped at the onset of the electrical pulse, and recording resumed shortly after the pulse. In some cases in which voltage drift occurred between the onset and offset of the hold period, we interpolated the sampled voltage values between hold onset and onset. For 1017- and 4069-pps stimuli, artifact was removed with a comb filter tuned to the stimulus pulse rate. The comb filters eliminated artifact elicited by all but the first and last pulses of each stimulus, which were easily excluded from further analysis.

On-line, a simple peak-picker was used to monitor unit activity for experimental control. Off-line, spikes were identified using custom software that classified waveforms on the basis of the time and amplitude differences between spike peaks and troughs. Only the off-line sorted spikes were used for quantitative analysis. Most channels provided unresolved spikes from two or more neurons. In this paper, a unit refers to the aggregate of spikes identified on a single recording channel.

Current-source-density analysis (Müller-Preuss and Mitzdorf, 1984) was used to estimate the locations of recording sites relative to cortical layers. The most consistent feature was a short-latency sink which we have found previously in histological reconstructions to correspond to the transition from layer III to IV (Middlebrooks, 2008a). That landmark provided a depth reference that could be compared across animals.

3.2.4 Stimuli

The data required to compute an individual detection threshold or gap-detection threshold were collected in a single block of trials, and several measurements were obtained from each block. For example, gap-detection stimuli were varied over presentation level and gap duration to obtain gap-detection thresholds for each of the presentation levels. Each configuration of stimulus parameters was repeated 20 (4

animals) or 40 (2 animals) times, and within each repetition the stimuli were interleaved randomly. Trials in which movement artifact was present in any recording trace, usually as a result of the animal chewing, were eliminated offline. At least 85% of trials were usable in 95% of conditions; the minimum was 13 trials in one condition. The order of testing of various parameters was varied among experiments.

Cochlear-implant stimuli were presented in a monopolar electrode configuration in which a single intracochlear electrode was active and a wire in a neck muscle was the return. Thresholds for activation of the auditory cortex were estimated for each cochlear-implant electrode and for each electrical pulse rate, and the electrode with the lowest threshold (always one of the two most apical electrodes) was selected for subsequent stimulation. Biphasic stimulus pulses were 41 μs per phase in duration with no interphase gap and with cathodic leading phase. The pulse rates tested were 254, 1017, and 4069 pps.

Electric gap-detection stimuli consisted of pairs of electric pulse trains ("markers") with identical pulse rate and current level separated by a pulse-free gap that varied in duration. All pulse-train durations and gaps were integer multiples of 0.246 ms, which is the period of the 4069-pps pulse rate. The duration of the leading marker was 23.6 or 196.6 ms. Gap duration was defined relative to the first missed pulse, such that that a gap of "0 ms" corresponded to an uninterrupted pulse train. Gaps that were shorter than the pulse period of the 254- or 1017-pps pulse rates were achieved by delaying the entire trailing pulse train. Seven to fifteen gap durations were presented in the ranges 0.492-256 ms for 254 pps and 0.246-256 ms for 1017 and 4069 pps pulse trains. Three sample stimuli are shown in the bottom of each panel of Figure 3.1. Gap detection stimuli were presented at three current levels, most often 2, 4, and 6 dB above the most common threshold among the 16 recording sites.

During blocks of gap-detection trials, pulse rates and leading- and trailing- marker durations were fixed, but stimulus intensity and gap duration varied from trial to trial. Each block of trials yielded one gap detection threshold per stimulus level.

3.2.5 Data analysis

Current-level detection thresholds based on neural spike counts were computed offline using signal detection procedures (Green and Swets, 1966; Macmillan and Creelman, 2005); the specific procedures are described by Middlebrooks and Snyder (2007). Briefly, receiver-operating-characteristic (ROC) curves were formed from the distribution of spike counts in trials that contained a stimulus and in trials that contained no stimulus. The area under the ROC curve gave the proportion of correct detections, which was expressed as a detection index (d'). Plots of d' versus stimulus level were interpolated to find thresholds at $d' = 1$. This procedure was followed for stimuli presented at each pulse rate. Detection thresholds were obtained for pulse trains 196.6 ms in duration, the same as the leading pulse train in the late-gap condition. The windows for spike rate analysis were selected to include the phasic ON response to the pulse train, as this response was elicited by the lowest current levels. Detection thresholds decreased systematically with increasing pulse rate. Across all units, median detection thresholds were -14.0, -14.4, and -16.9 dB re 1 mA for 254, 1017 and 4069 pps respectively.

Three estimates of gap-detection threshold were computed for each unit and each stimulus condition based on ROC analysis of spike count distributions within each of 3 time windows. Those windows corresponded to the onset of the trailing pulse train (the Trail-ON window), the offset of the leading pulse train (the Lead-OFF window), and a period of suppression of the tonic response between the two other windows (the TONIC window). In each case, trial-by-trial spike counts within a particular

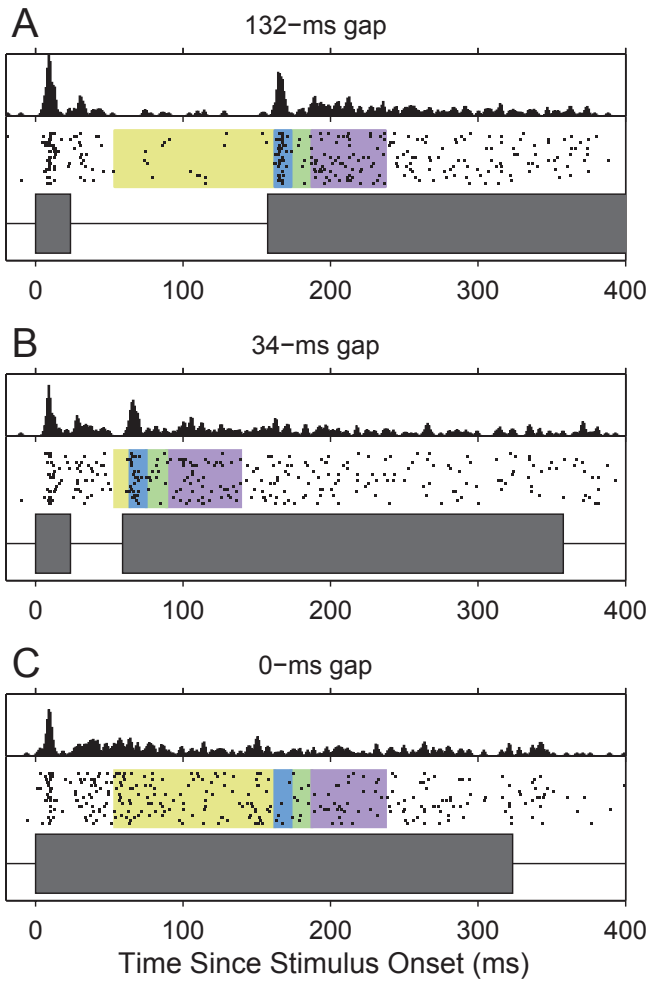

Figure 3.1: **Gap-detection stimuli, cortical responses and analysis.** At the bottom of each panel is a diagram of the 1017-pps pulse train. Above is a raster plot, where each dot represents a spike and each row a stimulus presentation. The shaded areas represent analysis windows for the spike-count ROC analysis. Gold shading: TONIC window; blue shading: short-latency ON window; green shading: post-ON suppression window; purple shading: long-latency ON window. At top, the summed PSTHs of these responses. A. An early gap 132 ms in duration. B. A 34-ms gap. C. An uninterrupted pulse train, or 0-ms gap, shown with the analysis windows for the 132-ms gap.

time window were compared between responses to stimuli that did or did not contain a gap — the time window was adjusted to accommodate each gap duration. For each gap duration, a ROC curve was formed from the distributions of spike counts in gap and no-gap conditions, and d' was computed from the area under the ROC curve. An alternative to comparing absolute spike counts between gap and no-gap stimulus conditions would have been to compare spike rates across various portions of the response to a single stimulus. Spike rates varied throughout the duration of any stimulus, however, regardless of the presence or absence of a gap. For that reason, it would have been necessary to compute spike-rate increments (or decrements) at particular post-stimulus-onset times relative to some measure of baseline spike rate and, then, to compare the magnitudes of the increments or decrements between stimulus conditions. That procedure might have provided a form of normalization across varying overall spike rates. Nevertheless, in a trial-by-trial analysis of fairly sparse spike patterns, the need to estimate the baseline in addition to estimating the response to the gap in a particular time window would have introduced an additional source of trial-by-trial variance in the measure of response magnitude.

The d' values were then linearly interpolated between tested gap durations. The shortest interpolated duration at which $d' = 1$ (for onset and offset responses) or $d' = -1$ (for post-onset suppression and tonic responses) was taken as the gap detection threshold. Responses visible in the aggregate data, such as the Trail-ON response to 0.5-ms gap in Figure 2C, sometimes occurred during individual trials of gap durations shorter than the calculated gap-detection threshold. Those responses represent trial-by-trial variance that did not meet the $d' = 1$ criterion in the ROC analysis of all the trials. Whereas all gaps presented were integer multiples of the 4069-pps carrier pulse period, interpolated gap-detection thresholds could fall anywhere between the

minimum and maximum gaps tested.

Selection of time windows was crucial to the performance of the spike count measure because the spike patterns elicited by the gap stimuli varied from unit to unit as well as with stimulus level. Figure 3.1 illustrates the analysis windows chosen for one unit. Phasic ON responses were elicited by the onset of the leading marker and, in the presence of gaps of sufficient duration, about 5-30 ms after the onset of the trailing marker. For some units, such as the one in Figure 3.1, this short-latency ON response to the onset of the trailing marker was followed by a period of suppression, which was followed by a late-ON response. Thus, for some units, the spikes elicited by the onset of a trailing marker could be counted in up to three non-overlapping time windows. Figure 3.1 shows, for one unit, a short-latency ON window (5-16 ms, shaded in blue), a post-onset suppression window (16-30 ms, shaded in green), and a long-latency ON window (30-80 ms, shaded in purple), all measured relative to the onset of the trailing marker. For each unit, the gap detection threshold was computed for each of these windows and the shortest of these gaps was chosen as the Trail-ON gap detection threshold. OFF responses, as seen in Figure 3.2 and Figure 3.3, generally had a longer latency, with most OFF responses occurring 10-30 ms (outlined in red in Figure 3.2A) after the offset of the leading and/or trailing marker. Longer OFF-response latencies, 30-120 ms, were observed in 3% of units for stimuli at any pulse rate, and some OFF responses exhibited longer durations, with >100 ms of enhanced firing rate. The same OFF response window was used for all gap durations within a particular unit and stimulus level. The gap detection threshold computed for this window was the Lead-OFF gap detection threshold. TONIC responses, evident in Fig. 3.1, were the third type of response characterized with this spike count measure. This analysis window (shaded in yellow) generally fell between

the end of the offset window and the beginning of the short-latency onset window and measured the reduction in tonic firing that sometimes was observed during a gap in the stimulus. In the unit in Fig. 3.1, the tonic firing is derived from the long-latency onset response to the leading pulse train. This analysis provided the TONIC gap detection threshold. These three measures (Trail-ON, Lead-OFF, and TONIC gap thresholds) were based on spike timing only and might have included spikes from multiple neurons.

The latency and duration of each time window for the measurement of Trail-ON and Lead-OFF responses were selected manually under visual guidance, but selection was informed by characteristics of responses throughout the entire duration of the stimuli to avoid overfitting. Windows were restricted to time ranges that were appropriate for responses elicited by all epochs of the stimulus, even those that were not informative about gaps. For instance, the onset of the leading marker evoked an ON response, which helped to verify the Trail-ON time-window selection. This decreased the likelihood of inadvertently selecting time windows to capture isolated fluctuations in firing rate. In some units, however, response timing varied with gap duration, such as the long-latency Trail-ON responses for 8-25 ms gaps in Fig. 3.2B, and analysis windows were chosen to accommodate these responses. Each window was at least 10 ms in duration to avoid overfitting.

For sufficiently short gaps, Lead-OFF and Trail-ON response windows overlapped. In this case, spike latencies and rates were used to assign a particular response to the appropriate category. For instance, in Fig. 3.2A, the response to the 8-ms gap was consistent either with a Lead-OFF or Trail-ON response. However, the unambiguous response to a 16-ms gap contained a Lead-OFF response and no Trail-ON response. Therefore, the significant response to the 8-ms gap was attributed to an OFF response

and the ON-derived gap detection threshold was selected at the next upward $d' = 1$ transition in the interpolated gap-d' curve, 26 ms. In contrast, Figure 3.2B displays a response to gaps shorter than 2 ms that is most consistent with the spike count and latency of an ON response. Although the response to an 8-ms gap could once again be considered ambiguous, the response to a 12-ms gap clearly shows a superposition of Lead-OFF (shorter-latency) and Trail-ON (longer-latency) responses — in other words, more spikes were elicited for the longer duration gap. Therefore, the Lead-OFF gap detection threshold in such cases was derived by interpolating the shortest gap at which the ambiguous response differed in spike count and latency from the ON response. In this case, the gap-detection threshold fell between 8-12 ms. Responses consistent with Lead-OFF spike rate and latency were never seen following a Trail-ON response, so this procedure generally resulted in a gap-detection threshold determined by the difference between the latencies of Lead-OFF and Trail-ON responses. Finally, in Figure 3.2C there is no significant OFF response at the longest, unambiguous gap durations, so no OFF-derived gap detection threshold was obtained even though spikes fell within the offset analysis window. This procedure was followed for each unit in the sample.

3.3 Results

3.3.1 Responses to Pulse Trains Containing Gaps

Neurons in cortical area A1 responded to cochlear-implant electrical pulse trains with phasic bursts of spikes associated with onsets and offsets of pulse trains and with sustained firing throughout the duration of the pulse train. The first example is shown in Figure 3.1, which shows the spikes elicited at one recording site for two early-gap stimuli and one control no-gap stimulus. In response to a continuous pulse train (Fig. 3.1C), this unit produced a burst of spikes 5-16 ms after the stimulus onset,

followed by a 15-ms pause, followed by sustained firing that gradually decreased over the course of the stimulus. In Figs. 3.1A and B, the ON response was observed after the onset of the leading pulse train and after the onset of pulse trains trailing the gaps. In this example, an ON response to the trailing stimulus was sufficient to reveal the presence of a gap.

Cortical response patterns differed according to the temporal position of the gap within the pulse train, the pulse rate, and the gap duration. Figure 3.2 represents the responses recorded on a single site for the late-gap condition and pulse rates of 254 pps (Fig. 3.2A), 1017 pps (Fig. 3.2B), and 4069 pps (Fig. 3.2C). At the lowest pulse rate and longest gap duration (Fig. 3.2A, 63-ms gap), both the leading and trailing pulse trains elicited an ON response with 5-20 ms latency, an OFF response with a 10-30 ms latency, and a weak TONIC response sustained for the duration of the pulse train. ON responses to the leading pulse train were present at all pulse rates and for all gap durations, whereas ON responses to the trailing pulse train were present only for gap durations of sufficient length. In contrast, OFF responses were evoked by the leading pulse train only for the lower pulse rates and the longest gap durations. The relative strength and sensitivity of ON and OFF responses elicited by gaps varied with pulse rate. At 254 pps, OFF responses to the leading pulse train were evident down to gap durations as short as 4 ms, whereas ON bursts to the trailing pulse train were evident only for gaps 24 ms and longer. At 1017 pps, however, it was the ON response to the trailing pulse train that persisted to the shortest gaps (as demonstrated by the latency of the spikes, measured relative to the onset of the trailing pulse train), whereas the response to the offset of the leading pulse train was evident only for gaps of 12 ms or longer. At the highest pulse rate (Fig. 3.2C), there was no response to offset of the leading pulse train, but the unit

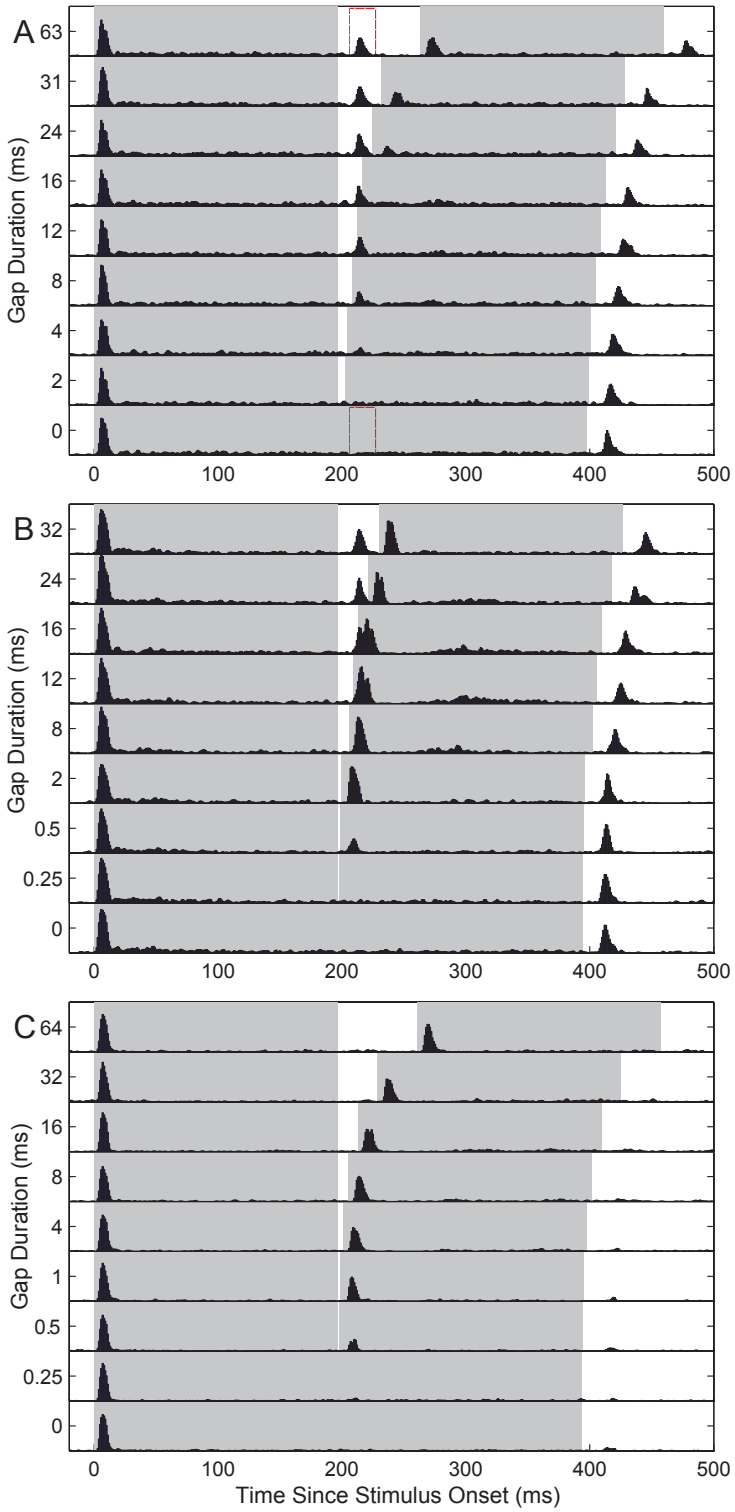

Figure 3.2: **Multi-unit ensemble response to late-gap detection stimuli.** Peri-stimulus time histogram of one unit's responses to late-gap detection stimuli presented at 6dB re stimulus threshold. Shaded areas represent the durations of leading and trailing markers. The height of each row corresponds to an instantaneous spike rate of 1000 spikes/s. A. 254-pps carrier rate with best gap detection threshold of 5.0 ms. The red outline demarcates the OFF response window. B. 1017-pps carrier rate with best gap detection threshold of 0.43 ms. C. 4069-pps carrier rate with best gap detection threshold of 0.6 ms.

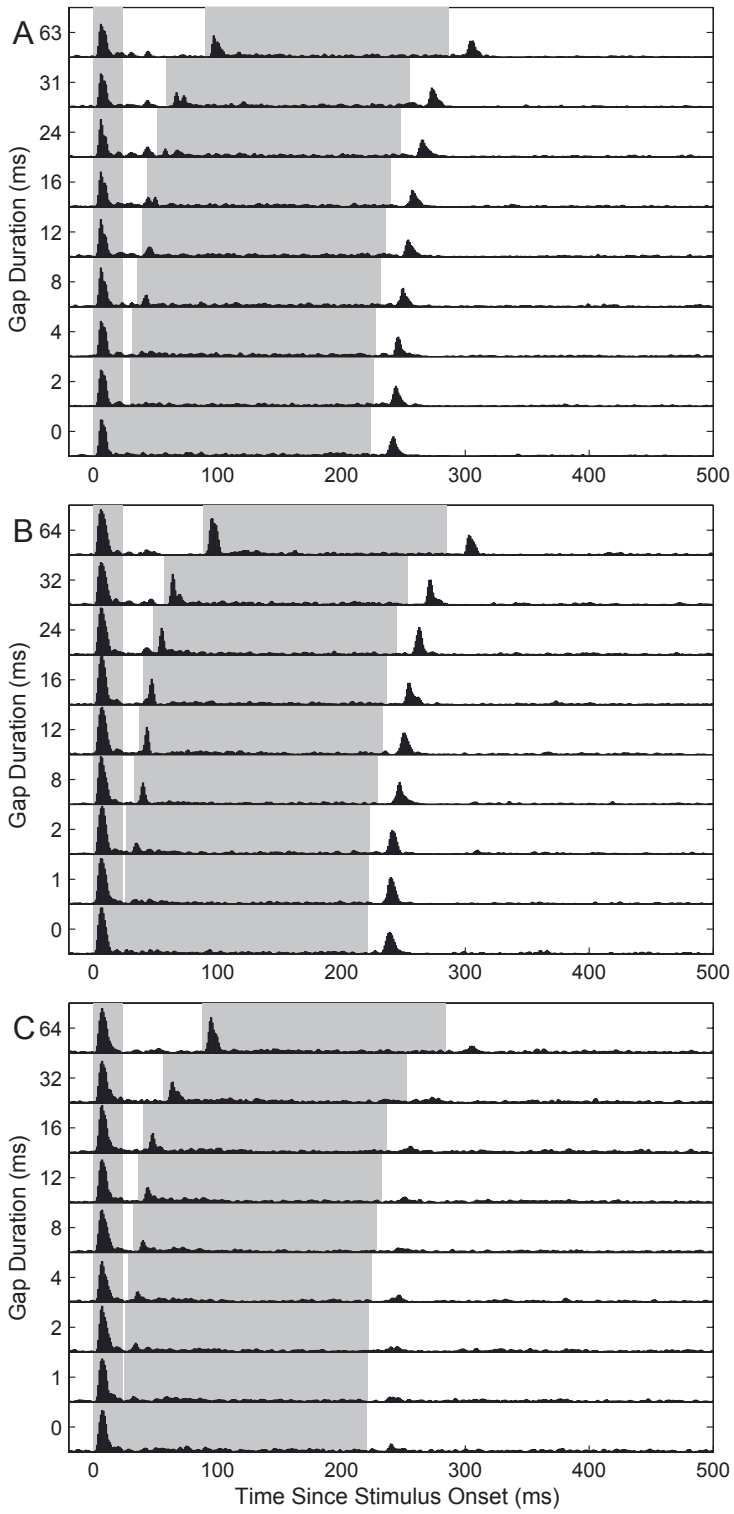

Figure 3.3: **Multi-unit ensemble response to early-gap detection stimuli.** Peri-stimulus time histogram of one units responses to early-gap detection stimuli presented at 6 dB re stimulus threshold. Shaded areas represent the durations of leading and trailing pulse trains. The height of each row corresponds to an instantaneous spike rate of 1000 spikes/s. A. 254-pps carrier rate with best gap detection threshold of 6.6 ms B. 1017-pps carrier rate with best gap detection threshold of 4.0 ms C. 4069-pps carrier rate with best gap detection threshold of 3.4 ms.

responded reliably to the onsets of the pulse trains trailing the gaps.

ON and OFF responses were not simply superimposed, but showed nonlinear interactions. For instance, in the 254- and 1017-pps examples in Fig. 3.2, gap durations in the range of 8 to 24 ms resulted in an OFF response to the leading marker that collided with the ON response to the trailing marker, resulting in the appearance of a long-latency response to the trailing marker; that pattern was not seen in the 4069-pps condition, in which there was no leading-marker OFF response. The appearance of a long-latency response after collision of OFF and ON responses was seen in several units in each of multiple animals, and could be a rebound from inhibition enhanced by the coincidence of those responses. Figure 3.3 shows responses of the same unit in conditions of a shorter leading pulse train. In these early-gap conditions, there was little to no response to the offset of the leading pulse train. In contrast to the 254-pps long-lead case, ON responses were most informative about gap duration.

3.3.2 Gap Detection Thresholds vary with Carrier Pulse Rate and Gap Position

As described in Methods, the presence of gaps could be detected by the presence of responses to the offset of the leading pulse train (the Lead-OFF response), the onset of the trailing pulse train (the Trail-ON response), and/or a decrease in tonic activity during the silent gap (the TONIC response). Each of these features was observed for one or more units in each of six animals. We also observed suppression of spontaneous activity in response to electric stimulation in several units, but since these responses were evoked reliably in only two animals, we did not include an analysis in the current study. The apparent paucity of suppressive responses may be due to the difficulty of detecting such responses in the context of low spontaneous rate. To better understand the contributions of specific spike-train features to the overall pattern discrimination, we performed an ROC analysis of spike count within time windows chosen to be

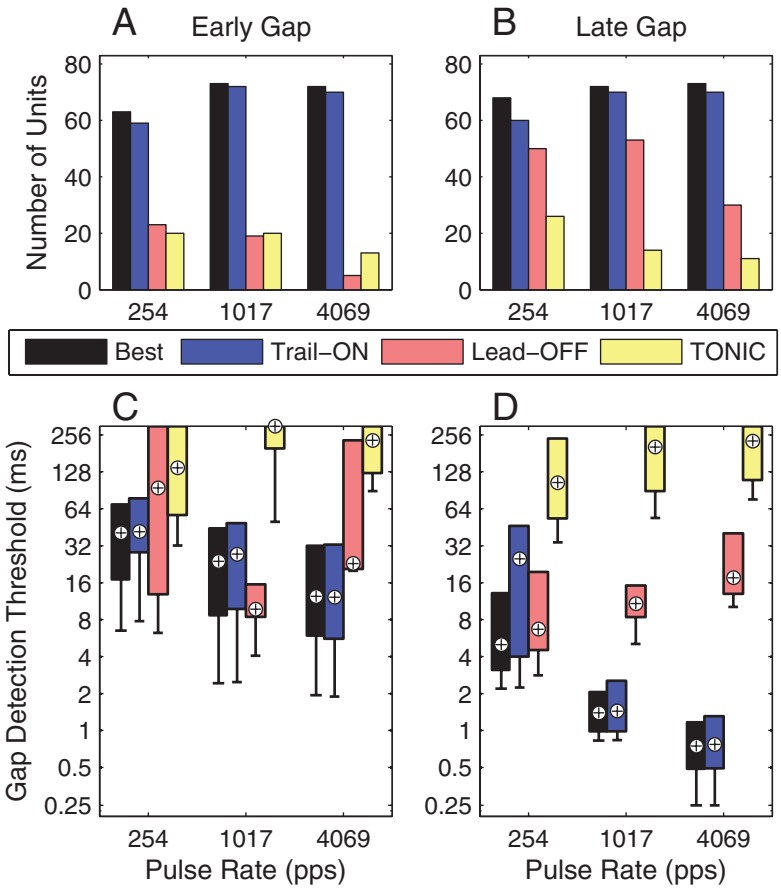

Figure 3.4: **Population summary of gap-detection thresholds.** The upper panels represent the numbers of units for which a gap detection threshold was obtained at any of the levels presented, for each analysis method and for the best gap detection threshold for each unit. The lower panels show the distributions of gap detection thresholds for each analysis, elicited by stimuli presented at least 4.5 dB above detection threshold. Filled bars represent the intraquartile range, circles represent the median gap detection thresholds, and tails indicate the 5^{th} percentile. A, C. Early-gap stimuli. B, D. Late-gap stimuli.

selective for each feature. The most frequently observed feature was a response to the onset of the trailing pulse train consisting of a constellation of as many as three components: a temporally compact short-latency burst of spikes, a brief period of suppression, and a longer-latency elevation of spike rate. For most units, that Trail-ON response was present at the lowest current levels, at which no other stimulus-related feature could be detected. The latency of the initial burst tended to decrease with increasing stimulus level, reaching a median first-spike latency of 9.9 ms for stimuli at least 4.5 dB above threshold. All three components (short-latency ON, suppression, and long-latency ON) contributed to gap encoding. For instance, the long-latency response could signal the presence of a gap in conditions in which the short-latency ON response was not apparent. We computed the gap thresholds for each of the 3 components of the response to the trailing burst and reported the shortest as the Trail-ON threshold.

Responses to the offset of the leading pulse train (referred to as Lead-OFF) typically appeared at higher stimulus current levels than did Trail-ON responses, with a mean difference in thresholds of 3.7 dB for the 200-ms leading pulse train ($p < 0.0001$, Students t-test). The median first-spike latency for Lead-OFF bursts, 19.9 ms, did not change systematically with level, and was longer than for ON responses for stimuli at least 4.5 dB above threshold ($p < 0.0001$, Kruskal-Wallis). OFF responses were preferentially evoked by longer stimulus durations, which can be seen in Figure 3.3A: the OFF response to the offset of the 225-ms uninterrupted pulse train in the 0-ms gap condition is more robust than the response to the offset of the 25-ms leading pulse train. Lead-OFF responses were more prevalent at lower pulse rates.

TONIC responses consisted of sustained firing throughout the duration of the stimulus. For some 25% of units, the presence of a gap in the stimulus could be

detected by a significant decrease in tonic firing during the gap compared to the spike rate at a corresponding time in the standard no-gap stimulus. Decreases in tonic firing associated with gaps were susceptible to interference from OFF responses occurring within the gap.

The effect of pulse rate and gap placement on gap-detection thresholds is summarized in Figure 3.4. The overall ("Best"; black bars) gap-detection threshold for each unit was selected to be the shortest gap detection threshold derived from the Trail-ON, Lead-OFF, and TONIC response features. The number of units that displayed sensitivity to gaps for one or more gap durations did not appear to vary systematically across stimulus conditions (Figs. 3.4A and B). Nevertheless, gap-detection thresholds varied significantly across both pulse rate and gap position. The distributions of gap thresholds given by specific features (Figs. 3.4C and D)) reflect in each case only the units for which the particular feature was present; for instance, the distribution of Lead-OFF thresholds is based on the subset of units that showed a Lead-OFF response. For early gaps, median Best gap-detection thresholds were 38, 26 and 12 ms for 254, 1017, and 4069 pps; for late gaps, median gap detection thresholds were 5.3, 1.4 and 0.77 ms respectively. Late gaps evoked significantly shorter gap-detection thresholds than did early gaps ($p < 0.001$, Kruskal-Wallis; all pulse rates). In normal hearing human listeners, gap detection thresholds do not vary as much between early and late gaps of comparable durations (Phillips et al., 1998). In the present study, restriction of the analysis to the most-sensitive 10% of units brought the difference between early- and late-gap thresholds down to only a few milliseconds, bringing the cortical data more in line with human psychophysical results.

The contribution of the various features of spike patterns to overall gap sensitivity varied with pulse rate and gap position. Fig. 3.4C and D summarize gap-detection

thresholds obtained for each response type for gaps in pulse trains presented at least 4.5 dB above threshold to ensure that all three response features were represented. Statistical comparisons were made between groups using Kruskal-Wallis non-parametric analysis of variance. Across all units, gap thresholds obtained from Trail-ON responses were the most prevalent and were not significantly different from the Best gap detection thresholds for any stimulus condition ($p = 0.05$, 254-pps late gap; $p > 0.40$, all other pulse rate and gap position combinations). Trail-ON gap-detection thresholds were longer for early-gap stimuli than late-gap ($p < 0.01$, 254 pps; $p < 0.001$, 1017 and 4069 pps). Lead-OFF responses to late gaps contributed to Best gap encoding at 254 pps, but Lead-OFF-derived gap thresholds were significantly higher than Best thresholds at higher pulse rates ($p = 0.26$, 254 pps; $p < 0.0001$, 1017 and 4069 pps, late gap). In the 254-pps late-gap condition alone, if a Lead-OFF response was present it tended to give a shorter gap threshold than that given by the Trail-ON responses ($p < 0.05$). For early gaps, Lead-OFF-derived gap-detection thresholds were not significantly different from the Best thresholds ($p > 0.12$, all pulse rates), but were present in relatively few recordings. Lead-OFF gap detection thresholds were longer for early-gap stimuli than for late-gap at 254 pps ($p < 0.001$), but there was no effect of gap position at higher pulse rates ($p = 0.76$, 1017 pps; $p = 0.19$, 4069 pps). TONIC responses encoded both early and late gaps, but these gap detection thresholds were significantly less sensitive for all conditions ($p < 0.001$). In addition, there was no significant effect of gap position on TONIC-derived gap-detection thresholds. In summary, Trail-ON responses were particularly important for gap sensitivity at high pulse rates and for early gaps, whereas Lead-OFF responses were most important at 254 pps for late gaps. Each of these effects of gap position, stimulus pulse rate, and response feature were observed in all six

animals.

Intracortical processing has been known to play a role in shaping sensitivity to temporal features in auditory stimul (Eggermont, 1999a; Middlebrooks, 2008a). To test for a possible contribution of cortical columnar circuits to gap sensitivity, we aligned the data based on cortical depth relative to the input layers. Overall gap-detection thresholds did not vary significantly with cortical depth ($p > 0.05$, Kruskal-Wallis for all stimuli; analysis limited to data presented at least 4.5 dB above threshold; data were grouped in 300-μm bins across cortical depth). We also compared the prevalence of each response type across cortical depth, and found no significant localization of these response types. We infer that gap detection in a non-behaving awake animal is largely inherited from sub-cortical auditory centers.

3.3.3 Gap Detection Thresholds Depend on Stimulus Level

The results in Fig. 3.4 showed a general decrease in gap-detection thresholds associated with increasing pulse rate. Studies in human listeners, however, show that gap-detection thresholds also decrease with increasing levels within a listeners dynamic range (Garadat and Pfingst, 2011) and that detection thresholds decrease at higher pulse rates (Kreft et al., 2004). For those reasons, there was a concern that our demonstration of a pulse-rate dependence of gap thresholds might have been confounded with a dependence on levels. In order to address that concern, we measured gap-detection thresholds at multiple current levels. For each pulse rate in each animal, we tested three current levels relative to the modal detection threshold estimated on-line among jointly-recorded units. Off-line, we computed the detection threshold for each unit (as described in Methods) and expressed the three current levels relative to that unit's threshold at that pulse rate. That procedure resulted in a continuum of levels tested relative to the thresholds in the unit sample. Moving

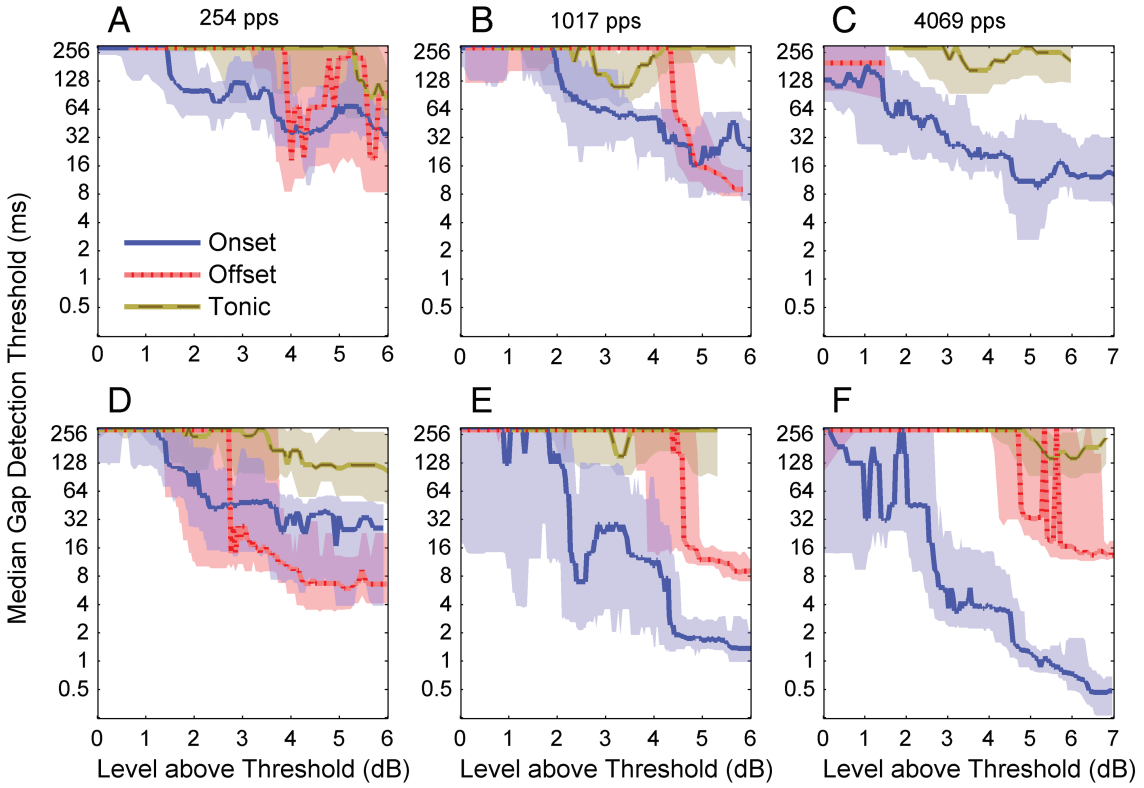

Figure 3.5: **Gap detection thresholds by level.** Each panel represents the distributions of gap detection threshold with level for each analysis type. Levels were calculated relative to the detection threshold for each unit. The shaded area denotes the intraquartile range and the line represents the median. Distributions were computed with averages taken across a moving window that encompassed 12.5% of the sample in each point, or a minimum of 13 points for small sample sizes. The upper panels (A,B,C) represent early gaps and the lower panels (C,D,E) represent late gaps.

averages of the gap detection thresholds obtained across these relative stimulus levels are plotted in Figure 3.5. In each condition, sensitivity to gaps was poor for stimuli near threshold, and improved over the levels presented. Gap-detection thresholds depended on stimulus level within the dynamic range for each stimulus condition. The dynamic range of gap detection appeared to be larger for 4069 pps than 254 pps, which is consistent with reports of wider dynamic ranges at high pulse rates (Kreft et al., 2004). Gap-detection thresholds decreased with increasing pulse rate in all six animals.

In human listeners, loudness matching reduces differences in gap detection thresholds across cochlear-implant stimulation channels (Garadat and Pfingst, 2011). However, the mechanisms for encoding loudness in neural data are not well established. We examined the dependence of gap detection thresholds on stimulus level to determine if there was a way to transform the resulting functions such that the difference in gap detection thresholds across pulse rate was minimized. Such a transformation could be considered a conservative estimate of loudness matching. However, it does not appear possible to transform the data in such a way. Detection thresholds generally were higher at lower pulse rates, so that the low-rate data were obtained at higher absolute current levels. For that reason, the differences in gap thresholds among pulse rates are even larger when expressed at absolute current levels than when expressed relative to detection thresholds (as in Fig. 3.5). Furthermore, although detection thresholds and response growth were similar for early- and late-gap stimuli within each pulse rate, more sensitive responses were observed for late gaps at high stimulus levels. Therefore we expect that the dependence of gap-detection thresholds on pulse rate and gap position should withstand the equalizing effects of loudness matching in a psychophysical task. These observations of the sensitivity

of gap thresholds demonstrate that, overall, differences in gap-detection thresholds across pulse rate and gap position are not simply due to level effects.

3.3.4 Interactions between Onset and Offset Responses to Gaps

The relative importance of Trail-ON and Lead-OFF responses for encoding gaps in electric pulse trains varied with electric pulse rate. That is, in response to a 254-pps stimulus, the Lead-OFF response often produced a shorter gap threshold than did the Trail-ON response, and the opposite was observed at 1017- and 4069-pps pulse rates. We tested that rate-dependent switch in dominant feature across the range of stimulus levels. At 254-pps, only the Trail-ON response contributed a gap threshold at the lowest current levels, but as soon as levels increased to the point at which Lead-OFF responses were evident, the Lead-OFF revealed shorter gaps than could be detected with Trail-ON responses (Fig. 3.5D). At higher pulse rates, the Lead-OFF feature was absent at low stimulus levels, and for stimuli >4.5 dB above threshold, the Trail-ON feature generally yielded shorter gap thresholds, as shown in Figure 3.4. Thus, the Trail-ON feature was dominant at all stimulus levels for higher pulse rates.

We observed interactions between Lead-OFF and Trail-ON responses that seemed to indicate the presence of forward suppression by cortical neurons in which the leading response would suppress the lagging response. This appeared to happen for the 254-pps stimulus in Fig. 3.2A: the Trail-ON response is suppressed at times when it would occur less than 20 ms after the Lead-OFF response. If the cortical Lead-OFF response suppressed the Trail-ON response, however, similar suppression presumably would have occurred across all pulse rates. Contrary to that presumption, the Trail-ON response to the 1017-pps stimulus in Fig 3.2B was not suppressed by the Lead-OFF response. In addition, Figure 3.2B demonstrated superimposed ON and OFF

responses for gap durations at which the two responses were nearly simultaneous and demonstrated an absence of Lead-OFF responses for shorter gaps. Forward suppression is characterized by increasing amounts of suppression with decreasing interval, but in this case, the OFF response disappeared as the ON-OFF interval increased. This finding occurred throughout the population whenever the Trail-ON response preceded the Lead-OFF response window. Finally, Lead-OFF responses with long response latencies were blocked by Trail-ON responses to the gap. Although it is possible that forward suppression could last 100 ms, we routinely observed Trail-ON gap detection thresholds of much less than 75 ms, indicating that successive ON responses were not subject to inhibition in this fashion. For these reasons, the data do not support intracortical or thalamocortical forward suppression as the primary interaction between ON and OFF responses.

In a previous study in anesthetized guinea pigs with stimuli similar to the late-gap condition (Kirby and Middlebrooks, 2010), no responses were observed to the offset of the leading marker, and yet the gap sensitivity of onset responses was very similar to Trail-ON gap-detection thresholds in the present study. In the previous study, we found evidence for a centrally-generated forward suppression that was stronger at lower pulse rates, possibly because lower pulse rates produced less adaptation in auditory-nerve input to central sites (Zhang et al., 2007). Shorter leading pulse trains provide less time for adaptation to occur, and this difference should be greater at higher pulse rates. To test this hypothesis, we compared Trail-ON gap-detection thresholds between early- and late- gap conditions in a subset of 32 units to which these stimulus pairs were presented consecutively. Trail-ON-derived gap-detection thresholds were significantly longer for early gaps than late gaps for 1017-pps ($p < 0.01$, Wilcoxon sign-rank; 32 units) and 4069 pps ($p < 0.01$) but not for 254-pps

($p = 0.82$) stimuli. The log-ratio of the early-gap to the late-gap detection threshold was larger (i.e., longer gap-detection thresholds at early gaps) for 4069 than 254 pps ($p < 0.0001$, ANOVA) or 1017 pps ($p < 0.05$), but there was no significant difference in the distributions obtained at 254 and 1017 pps ($p = 0.22$). These results are consistent with increased adaptation in the auditory nerve at 4069 pps leading to less forward suppression of ON-responses and thus more sensitive gap-detection thresholds.

Lead-OFF responses were clearly dependent on gap duration and, by extension, on the onset of the trailing pulse train. In the present study, there were no examples of a Lead-OFF response occurring after a Trail-ON response. Therefore, at high pulse rates, the OFF-derived gap detection thresholds depended on the latency of the Lead-OFF response and the threshold of the Trail-ON response. Although the current data cannot tell us the level of the auditory pathway site at which responses to stimulus offset are generated, it appears that a preceding Trail-ON response has the ability to block the Lead-OFF response. Thus, the shortest Lead-OFF gap-detection thresholds may be a byproduct of the forward suppression of Trail-ON responses.

3.4 Discussion

Recordings from the auditory cortex of the unanesthetized guinea pig demonstrated a diversity of features of spike patterns that could code temporal features of cochlear stimuli. The relative strengths of ON, OFF, and TONIC responses varied with stimulus conditions, including stimulus level, duration of the leading pulse train and, most conspicuously, the rates of electrical pulse trains. We begin our discussion by relating the present results to previous psychophysical and electrophysiological studies, including a discussion of sensitivity to electric pulse rates and to early and

late gaps. We conclude with implications for cochlear implant listeners.

3.4.1 Relation to Psychophysical Studies

Gap-detection studies in cochlear-implant users have measured only thresholds for late-gap stimuli (i.e., leading pulse train $\geq$50 ms). At pulse rates $\leq$1000 pps, gap-detection thresholds were 1-5 ms for postlingually deafened subjects (Chatterjee et al., 1998; Shannon, 1989) and 1-50 ms for prelingually deafened subjects, but there was no consistent relationship of gap thresholds with pulse rate. van Wierengen and Wouters (1999) observed gap-detection thresholds of 2-8 ms at 400 pps and 1-4 ms at 1250 pps, shorter at the higher pulse rate for three out of four listeners. In a test of very high pulse rates (3000 pps), two users had gap-detection thresholds of 1 ms or less (Grose and Buss, 2007). Garadat et al. (2010) concluded that there was no consistent relationship between gap-detection thresholds and pulse rate of 250-, 1000-, and 4000-pps across subjects. Nevertheless, they showed that gap-detection thresholds were longer at the lowest pulse rate for five of six subjects: 5-15 ms for 4000-pps and 15-75+ for 250-pps stimuli at the lowest current levels tested; and 1-5 ms for 4000-pps and 4-12 ms for 250-pps stimuli at the highest current levels. For gap-detection thresholds acquired in the middle of the dynamic range, where the greatest inter-subject variability in gap-detection thresholds arose, 250-pps stimuli were generally perceived as louder than 4000-pps stimuli, a confounding factor. Overall, human psychophysical results display a trend of decreasing gap-detection threshold with increasing pulse rate, but the effect of pulse rate is not as pronounced as in the present physiological study. Further studies that control for loudness may show a stronger effect of pulse rate on gap-detection threshold.

Early gaps have not been tested in cochlear-implant listeners, but studies in normal-hearing listeners show little effect of gap position on gap-detection threshold.

Phillips et al. (1998) found a small (1-2 ms) but significant elevation of within-channel gap-detection thresholds for early gaps in experienced listeners; that difference can be as high as 8 ms in inexperienced listeners (Snell and Hu, 1999). The most sensitive 10 % of units in the current study had gap-detection thresholds of 2-8 ms across pulse rates for a 25-ms leading marker, indicating that the required sensitivity is available even in a passively-hearing, naïve guinea pig.

3.4.2 Comparison with Physiological Studies

The current study is the first measurement of within-channel early-gap thresholds in awake animals. In a study in anesthetized cats Eggermont (2000) thresholds for early gaps (i.e., 20-ms leading marker) were highly elevated compared to late-gap physiological thresholds and to early-gap psychophysical thresholds (Phillips et al., 1998; Snell and Hu, 1999). The elevated early-gap thresholds observed under anesthesia likely are a result of the ∼50-200-ms period of suppression that typically follows the ON responses of cortical neurons in anesthetized conditions (Eggermont, 2000; Kirby and Middlebrooks, 2010). The elevated early-gap thresholds were not seen in the present study in the absence of anesthesia.

Several studies have suggested that the presence of a gap in a stimulus could be signaled by a depression in ongoing neural activity. In the auditory nerve, for instance, gap-evoked fluctuations in sustained responses are particularly important for detection of the shortest gaps (Zhang et al., 1990). In addition, psychophysical studies of forward masking suggest that persistence of a response to a leading stimulus may contribute to masking of a subsequent probe (Plack and Oxenham, 1998). Tonic responses are the most likely mediator of such an effect. This type of persistence was observed in a small proportion of neurons in the inferior colliculus of awake marmosets (Nelson et al., 2009) and in primary auditory cortex of guinea pigs (Alves-Pinto et al.,

2010), but did not represent the limits of sensitivity to probes in either study. An effect similar to persistence was seen in the current study, as the sustained firing of TONIC responses continued for as long as 30 ms past stimulus offset, extending into the gap. Such persistent activity reduced the difference in firing rate between gap and no-gap conditions and limited TONIC-derived gap-detection thresholds to gaps longer than the duration of the persistent activity. Nevertheless, persistence and/or suppression of sustained activity had only a minor influence on detection of gaps in the present study. ON and OFF responses were more informative within the same responses and provided gap sensitivity more consistent with psychophysical data. The limits of physiological gap detection are not determined by the persistence of stimulus representation in the primary auditory cortex.

The current study confirms and extends our previous work in anesthetized guinea pigs (Kirby and Middlebrooks, 2010). Gap-detection thresholds obtained from Trail-ON responses were similar between ketamine-anesthetized and awake guinea pigs. However, only in awake animals did the Lead-OFF gap-detection thresholds result in more sensitive gap-detection thresholds for the 254-pps condition. Cortical OFF responses have been observed in spike activity of neurons in anesthetized cat (Eggermont, 1999b) and in local field potentials in awake chinchilla (Guo and Burkard, 2002) for leading markers 200 and 50 ms in duration respectively, but only for gaps longer than 40 ms in duration. The most sensitive responses to gaps in noise bursts in these studies were always elicited by ON responses to trailing bursts. The Lead-OFF-dominant gap-detection thresholds observed in the current study indicate that stimulation at 254 pps may produce temporal cues in the cortex unlike those elicited by acoustic stimulation.

3.4.3 Implications for Cochlear Implant Users

The present results illustrate some features of cortical responses that could signal specific temporal elements of speech. Inasmuch as the prevalence of those cortical responses depends on electrical pulse rate, level, and duration of steady-state pulse trains (i.e., leading markers), those same stimulus parameters are likely to influence speech recognition. As an example, cross-channel gap detection thresholds for a 10-ms broadband noise leading marker and a 300-ms narrowband noise trailing marker were correlated with sensitivity to voice onset time in a synthesized ba-pa continuum in normal-hearing listeners (Elangovan and Stuart, 2008), suggesting that performance in such a task is important for categorization of voiced and voiceless consonants. Lead-OFF responses such as those observed in the present study may be especially important in across-channel gap detection because cortical ON- and OFF- responses often are tuned to different frequencies in normal hearing (Qin et al., 2007), which could result in overlapping Lead-OFF and Trail-ON responses. In another study, gap duration discrimination performance within a synthesized-formant stimulus was correlated with performance on consonant and word discrimination tasks for cochlear-implant listeners (Sagi et al., 2010). TONIC and Lead-OFF responses, which encode the duration of the leading marker, may provide a more relevant cue than the onset-onset interval.

We have shown that cortical responses to gaps vary qualitatively with carrier pulse rate. Higher pulse rates evoke more sensitive ON responses to gaps, and responses to the highest rate tested showed little representation of stimulus features other than pulse-train onsets. Low pulse rates, on the other hand, display robust coding of features throughout the duration of the stimulus, but do not drive ON responses to trailing markers at such short gap durations as those seen for higher pulse rates.

Zhang et al. (2007) showed that the auditory nerve entrained to 250-pps pulse trains with little adaptation over the course of a 300-ms stimulus, whereas auditory nerve fibers showed significantly more spike-rate adaptation at 5000 pps. Based on the current results, a lack of adaptation over the course of a low pulse-rate stimulus may result in enhanced representation of duration cues and enhanced forward suppression of subsequent stimuli in the central auditory system, whereas the sensitivity to successive stimulus onset shown for high-rate pulse trains comes at the cost of a degraded representation of the rest of the stimulus. We conclude that intermediate pulse rates, such as 1017 pps, produce responses to gaps that are most similar to those seen in acoustic stimulation.

There is some evidence for the existence of a "sweet spot" in cochlear-implant pulse rate. Amplitude modulation detection is impaired in human listeners at high pulse rates (2000 or 4000 pps), compared to low pulse rates (200 or 250 pps) (Galvin and Fu, 2005; Pfingst et al., 2007); a similar result is found in auditory cortex of anesthetized guinea pigs (Middlebrooks, 2008a). Arora et al. (2011) tested modulation detection threshold for carrier rates from 200-900 pps, and listeners were most sensitive for a carrier rate of 500 pps. A number of studies have measured the effect of pulse rate on speech performance, with mixed results. Recently, Battmer et al. (2010) performed a multi-stage, multi-center study and determined that performance was best at each listeners preferred pulse rate, but 80% of listeners preferred pulse rates from 500-1200 pps. The present results may help to explain why intermediate pulse rates are the most appropriate choice for many cochlear-implant listeners.

CHAPTER 4

Summation and Segregation in Transmission of Amplitude-Modulated Cochlear-Implant Pulse Trains to Auditory Cortex.

4.1 Introduction

Cochlear implants restore hearing through electrical stimulation of the auditory nerve. Unlike normal hearing listeners, for whom information is conveyed continuously along the basilar membrane, cochlear implant listeners receive auditory input through a finite number of electrodes which are highly susceptible to between-channel interactions. These interactions are reduced through the use of interleaved pulsatile stimulation, which reduces channel interaction mediated by current summation. Nevertheless, implant users typically receive no more than about 8 independent channels of information despite the use of pulsatile stimulation strategies (Fishman et al., 1997).

Our lab has previously shown that interleaved electric pulses delivered within $\sim$1 ms to different electrodes can result in detection threshold shifts in primary auditory cortex, to the extent of rendering the combination of two sub-thresholds pulse trains detectable (Middlebrooks, 2004). Kwon and van den Honert (2009) observed similar interactions between interleaved pulse trains in human subjects, and two out of four subjects showed evidence for temporal integration longer than 1 ms. Interactions

are maximized by high pulse rates, short interleaving delays, and close electrode spacing, indicating that successive pulses interact within an overlapping population of auditory nerve cells, despite temporal and spatial separation. The interleaving delays in use in modern processing strategies are generally much shorter than 1 ms.

Outside of the laboratory, cochlear implant stimulation consists of interleaved amplitude-modulated pulse trains. Each electrode receives a pulse train that has been modulated with the extracted envelope of a tonotopically-appropriate frequency band, but the observed interactions between pulse trains likely reduce separability between these channels. Cochlear-implant listeners, who often have excellent speech perception in quiet, are susceptible to interference from background noise (Firszt et al., 2004), which may be due to an insufficient number of spectral channels to fully transmit phoneme-recognition cues (Xu and Pfingst, 2007). In particular, fluctuating backgrounds such as competing talkers can severely impair comprehension (Stickney et al., 2004). An amplitude-modulated stimulus would be expected to elicit more interaction with neighboring pulse trains at peak current levels; in addition, the spread of this interleaved interaction would increase at these higher levels. The result might be a continually varying amount of interaction between pulse trains, depending on the amplitude of each pulse train.

We measured the interactions in modulation detection elicited by two cochlear-implant pulse trains. We presented interleaved pulse trains with sinusoidally amplitude-modulated envelopes to two cochlear-implant channels separated by 1.5 mm. We measured modulation detection thresholds in the presence of unmodulated maskers and in the presence of competing modulated pulse trains based on the patterns of response elicited by these stimulus combinations. We also varied the pulse rate and interleaving delays of the stimuli in order to better understand the source of these

interactions in the auditory system. For high pulse rates and short interleaving delays (82 and 123 μs), temporal integration is likely to lead to direct cochlear summation. On the other hand, longer interleaving delays available at lower pulse rates (492 and 1966 μs) are unlikely to sum in the auditory nerve, so any interactions observed would be attributable to central mechanisms.

4.2 Methods

4.2.1 Overview

Data were collected from the auditory cortices of anesthetized guinea pigs in response to electric pulse trains presented in the contralateral cochlea. Data were collected and stimuli were generated with Tucker-Davis Technologies (TDT) System III hardware (Alachua, FL) connected to a personal computer running MATLAB (The Mathworks, Natick, MA) and using software developed in this laboratory. Animals were anesthetized and a recording probe was placed in the right primary auditory cortex. Placement of the probe was guided by responses to acoustic tones. The recording electrodes were sealed in place, the animal was deafened bilaterally and a stimulating electrode array was inserted into the scala tympani of the left ear. Cortical responses to amplitude-modulated electric pulse trains were studied.

4.2.2 Animal Preparation

Recordings were made in the primary auditory cortex in the right hemispheres of 20 adult albino guinea pigs. Animals were of either sex and weighed 340-490 g. Animals were premedicated with atropine sulfate (0.1 mg/kg) and were anesthetized with a mixture of ketamine (60 mg/kg) and xylazine (15 mg/kg), administered intramuscularly. Additional doses of ketamine and xylazine were given throughout the experiment to maintain an areflexive state. Animal preparation typically lasted 2 h,

followed by 10-12 h of data collection. The animals right cochlea was ablated with a carbide burr to eliminate auditory responses to the animals breathing sounds and other acoustic input. The auditory cortex was then exposed on the right side. Primary auditory cortex was identified by its proximity to the pseudosylvian sulcus and by the characteristic rostrolateral to dorsomedial increase in characteristic frequencies, verified by recordings at three or more probe positions. When a cortical location within A1 with a characteristic frequency between 8 and 32 kHz had been identified, the recording probe was inserted perpendicular to the surface of the cortex. In two animals, a second recording probe was placed obliquely into cortex to sample complementary frequencies. A silver ball was placed within the craniotomy rostral to A1 to serve as a recording reference. The probe was then fixed in place. The left bulla was opened to expose the cochlea. A cochleostomy was drilled in the basal turn, and the ear was deafened with a direct infusion of neomycin into the scala tympani (Middlebrooks, 2004). A cochlear implant was inserted through the cochleostomy into the scala tympani. The cochlear implant was an eight-electrode banded array (Cochlear Corporation), identical in dimensions to the distal 8 electrodes of the clinical Nucleus 22. Five bands could be placed within the scala tympani in our guinea-pig preparation. A platinum-iridium wire was placed into a neck muscle to serve as a monopolar return contact.

4.2.3 Electric Stimulus Generation and Cortical Recording

Cochlear electrical stimuli were generated by a custom eight-channel optically-isolated current source that was capacitatively coupled to the electrodes with an output time constant of 3 ms. The current source was controlled by a multi-channel 16-bit D/A converter (TDT model RX8). Stimuli were presented in a monopolar configuration. The active electrode was a single intrascalar electrode, and the return

electrode was a wire inserted in a neck muscle. Typically, the most apical electrodes had the lowest current thresholds for cortical activation, so that one of the two most apical electrodes was used as an active electrode. Interleaved competing stimuli were presented through the electrode located 1.5 mm further basal.

Each stimulus comprised cathodic-first, biphasic pulses with a 21-μs phase duration and a 21-μs interphase gap, as shown in Figure 4.1A. Sinusoidally amplitude-modulated stimuli were generated with a modulation function of:

$$1 + m \sin(2\pi f_m t) \tag{4.1}$$

where m was the modulation index, ranging from 0 to 1, and f_m the modulation frequency in Hz. The starting modulation phase was always 0 rad. The modulation depths were typically expressed in decibels, $20 \log(m)$. Apical stimuli were presented interleaved with basal stimuli, with pulses on the basal channel presented at a fixed delay after the pulses on the apical channel. This interleaving delay was varied as an experimental parameter. Typical interleaving delays for a 1017-pps masker are shown in the lower rows of Figure 4.1A.

Recording probes (NeuroNexus, Ann Arbor, MI) comprised sixteen iridium-oxide electrodes spaced at 100 μm intervals on a silicon-substrate shank. Signals from all 16 recording sites were recorded simultaneously, digitized at 24.4 kHz, low-pass filtered, re-sampled at 12.2 kHz, and stored for off-line analysis. An artifact-rejection procedure was used to eliminate artifact resulting from the electrical cochlear stimulus (Middlebrooks, 2008a,b). On-line, a simple peak-picker was used to monitor unit activity for experimental control. Off-line, spikes were identified using custom software that classified waveforms on the basis of the time and amplitude differences between spike peaks and troughs. Only the off-line sorted spikes were used for quantitative analysis.

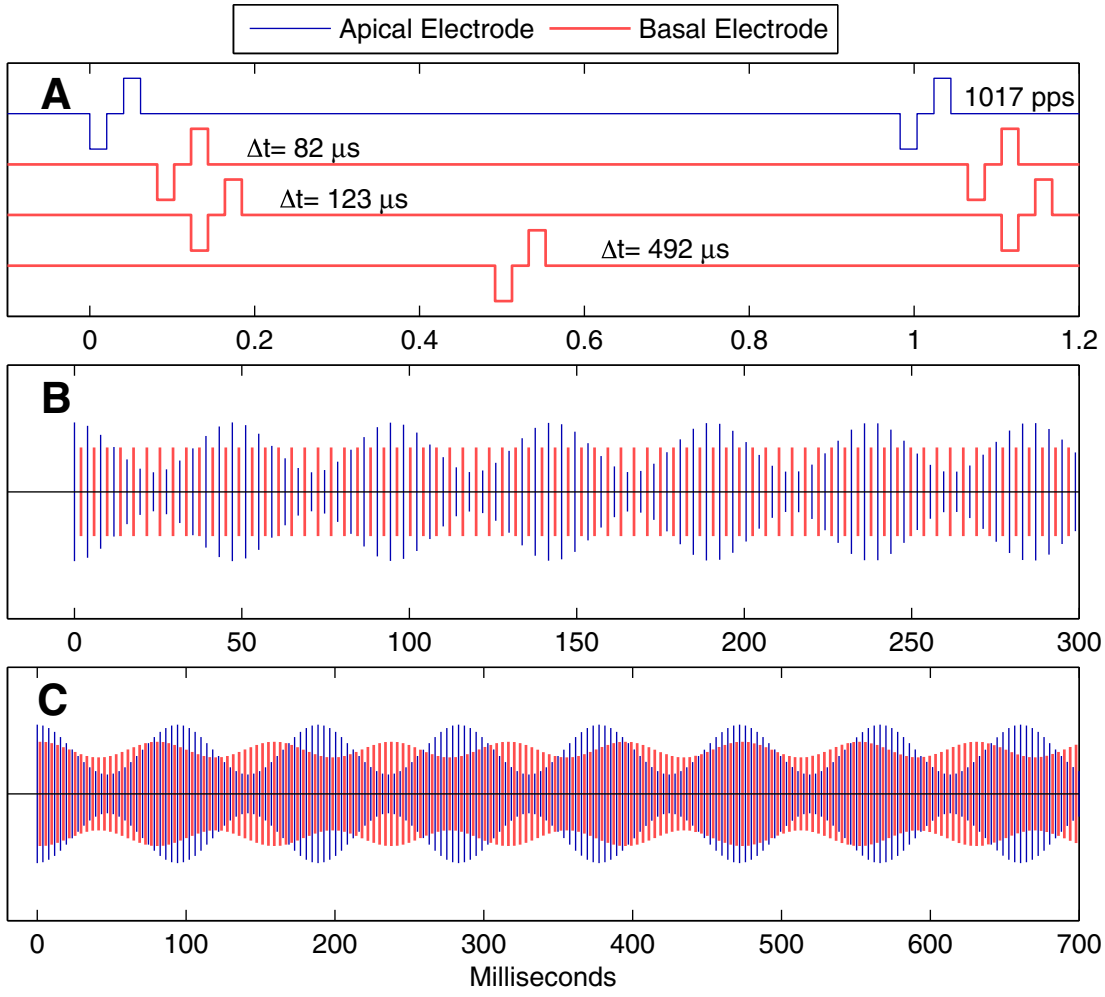

Figure 4.1: **Diagrams of Experimental Stimuli.** A. Electric pulse waveform of a 1017-pps stimulus. The top blue line is the stimulus delivered to the apical electrode. The lower red lines represent possible stimuli for different interleaving delays. B. Sample stimulus from Experiment 1. The first 300 ms of a 600-ms 254-pps pulse train presented to the apical electrode (blue), modulated at 10.6Hz with -5 dB modulation depth and masked with an unmodulated pulse train presented to the basal electrode (red) presented at a 1966-μs interleaving delay. C. Sample stimulus from Experiment 2. The first 700 ms of a stimulus consisting of two 254-pps pulse trains, one modulated at 10.6 Hz and -5 dB depth and presented to the apical electrode (blue) and the other at 12.72 Hz and -15 dB modulation depth presented to the basal electrode (red), and interleaved with a 1966-μs delay.

4.2.4 Experiment 1: Masking by Unmodulated Pulse Trains

In the first experiment, we examined the degree to which unmodulated pulse trains on one electrode impaired detection of modulation in a pulse train presented on a second electrode. The modulated signal was tested at three pulse rates, two modulation frequencies, and two or three interleaving delays. We obtained data from 169 multi-unit clusters and 11 well-isolated single units from recordings in 14 animals. Due to the low number of single units, all analyses were performed on multi-unit clusters. The first 300 ms of a sample stimulus for Experiment 1 is shown in Figure 4.1B. The signal was a 600-ms amplitude-modulated pulse train presented at a current level 4 dB above detection threshold. Pulse trains were modulated with a frequency of either 10.6 or 21.2 Hz and modulation depths ranging from -35 dB (2% modulation) to -5 dB (56% modulation). The masker was identical in duration and was presented at 5-6 current levels, ranging from -4 dB to +6 dB relative to masker-channel threshold. Signal and masker were presented at the same pulse rate, either 254, 1017, or 4069 pps. The interleaving delay between the two was minimal (82 μs), intermediate (123 μs) or maximal (1/2 the pulse period). At 4069 pps, only two conditions were presented because the intermediate condition equaled the maximal condition.

Modulation-detection thresholds were obtained for each unit at each pulse rate, interleaving delay, and masker level. Modulation detection was quantified by the vector strength, which measured the synchronization between stimulus and response. As in previous work (Middlebrooks, 2008a), the portion of the response immediately following the stimulus onset response was omitted from analysis to avoid the erroneous appearance of phase locking due to the typical robust cortical response to stimulus onset. The final 283 ms (three or six periods of the modulation frequency) of the

stimulus was used to calculate the vector strength. Each spike elicited by a particular stimulus was represented as a unit vector with an angle corresponding to the modulator phase at which it occurred. The vector sum was taken over all spikes elicited within the response window, and the magnitude of the resultant vector formed the vector strength. Spikes elicited preferentially at a particular phase therefore resulted in vector strengths close to one, while non-phase-locked responses cancelled out and the vector strength was near zero. The modulation-detection threshold was determined using a signal-detection theory analysis for each pulse-rate, interleaving-delay and masker-level combination using. To avoid overly sparse spike responses, vector strength was calculated for bootstrapped averages of four trials. This procedure was repeated to create 40 measurements of vector strength for each modulation depth. The distribution of vector strength for each modulation depth was compared to that obtained for the shallowest modulation depth (usually unmodulated) and the d' index was calculated. The modulation-detection threshold was chosen to be the depth at which the interpolated modulation depth-d' curve exceeded 1. These masked modulation thresholds were then compared across conditions.

4.2.5 Experiment 2: Multiple Modulators

In the second experiment, two competing modulated pulse trains were presented at the signal and masker electrodes. Since either stimulus could be considered the signal in this experiment, we refer to Stimulus A and Stimulus B. Stimulus A was always: presented on the more apical electrode, modulated by the lower-frequency modulator, and leading in time. We obtained 139 multi-unit clusters and 4 well-isolated single units from recordings in 10 animals. Both stimuli were 1100-ms amplitude-modulated pulse trains presented 4 dB above threshold, at eight modulation depths ranging from -35 to -5 dB in 5-dB steps, plus the unmodulated case. Thus, for each pulse rate

and interleaving delay, 64 combinations of Stimulus-A and Stimulus-B modulation depths were obtained. The first 700 ms of a sample stimulus are shown in Figure 1C. The modulation frequency pairs were either 10.6/12.72 Hz or 18.2/21.2 Hz, and were presented at a carrier rate of 254, 1017, or 4069 pps with either maximal or minimal interleaving delay.

The presence of two different modulation frequencies meant that vector strength was no longer an appropriate measure of phase locking. That is, the period histogram based on modulation frequency A would be contaminated by additional phase locking to modulation frequency B, and vice versa. Instead, we calculated the Fourier transform of the peri-stimulus time histogram (PSTH) of the spike response to determine the strength of response at each frequency component. Each peak magnitude was normalized by the DC component of the Fourier Transform, to eliminate variation with spike rate. The average PSTH over all 20 trials was calculated (7.6-ms bins). The first 400 ms containing the onset were discarded, and a Hamming windowing function was applied to the resulting histogram to reduce sidelobes in the frequency domain and optimize separation between responses to A and B modulation frequencies.

To quantify the response-interactions between Stimuli A and B, we performed singular value decomposition (SVD) on the 8x8 matrices of A- and B- Fourier peak magnitudes (M_{FP}). This technique requires the factorization of the matrix $M = A\Sigma B^*$ such that Σ is a diagonal matrix containing eigenvalues. SVD is often used in Spectro-Temporal Receptive Field analysis, in which the receptive field of a cell is decomposed into a spectral response function and a temporal response function. Applying SVD to a Fourier Peak matrix allows us to extract two response functions for either Fourier peak, each varying with the modulation depth of either Stimulus

A or Stimulus B. In this case, a useful way of considering this process is that:

$$M_{FP} = \sum_{i=1}^{8} \lambda_i (a_i \times b_i) \tag{4.2}$$

In other words, the matrix of Fourier peak values can be broken down into a sum of linear approximations through SVD. Each element in the sum is the cross-product of two 8-element vectors a_i and b_i, corresponding to the dimensions of Modulation Depth of the two stimuli, and magnitude of each component is weighted by the scalar term λ_i.

The SVD allowed us to examine interactions between A and B modulation in two ways. First of all, the separability of the matrix MFP could be estimated as the fraction of the power captured by the largest component of the sum:

$$S = \lambda_1^2 / \sum_{i=1}^{8} \lambda_i^2 \tag{4.3}$$

A low separability fraction would indicate that interactions between the two stimuli could not be captured simply by the product of two vectors, but require further corrections to approximate the response. Second, the first resultant vectors from SVD can be considered the contributions of Stimulus A and Stimulus B to the magnitude of the Fourier Peaks for each condition and can be used to measure the interactions between competing stimuli as well as the growth of each frequency component across modulation depth.

4.3 Results

4.3.1 Experiment 1

Neurons in cortical area A1 of anesthetized guinea pigs responded to amplitude-modulated pulse trains with a phasic onset response and a period of suppression lasting 50-120 ms, followed by phase-locked fluctuations in tonic firing rate, the

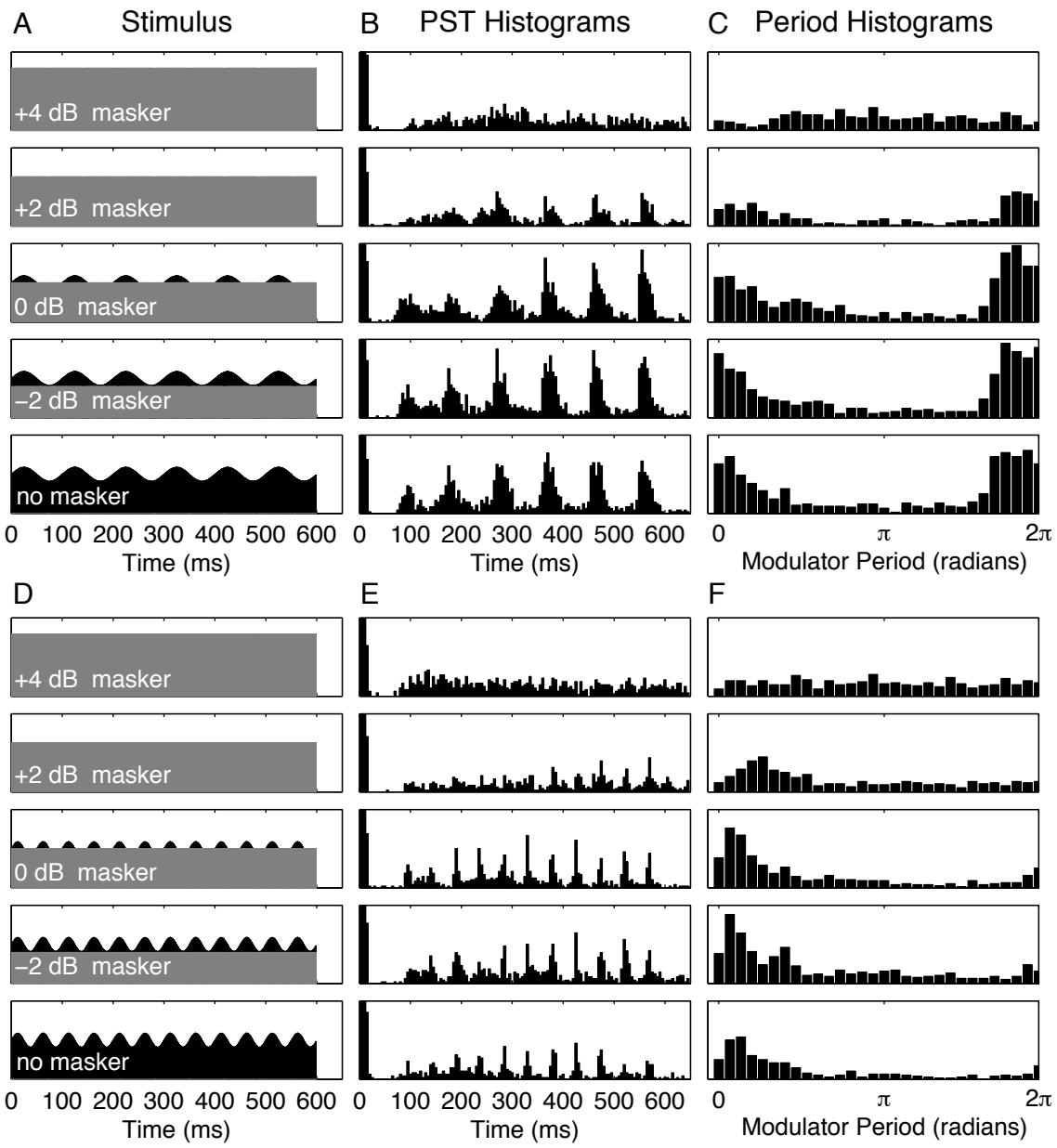

Figure 4.2: **Cortical responses to masked modulated pulse trains.** Responses to 10.6-Hz (A-C) and 21.2-Hz (D-F) modulation at modulation depths of -20 dB. A, D. Diagram of stimulus. The black waveform indicates the signal, presented to the apical electrode. The grey waveform represents the unmodulated masker, presented to the basal electrode. B, E. PSTH of responses to each signal and masker combination. C, F. Period histograms in which the spike count is plotted according to the relative phase of the stimulus. Note that the modulator period is different between frequencies.

magnitude of which depended on the modulation depth. An example of responses recorded at a single cortical site is shown in Figure 4.2. In the absence of a masker, this 18%-modulated (-20 dB) stimulus evoked a periodic response at both 10.6 Hz and at 21.2 Hz (Fig. 4.2B and E). The details of the phase-locked activity are clearer in the period histograms, in which spike rate is plotted as a function of the phase of the modulated signal (Fig. 4.2C and F). As the masker level on the basal electrode increased, the phase locking was reduced and the overall spike rate decreased. A masker presented 4 dB above the signal abolished phase-locking to the signal.

We tested the hypothesis that higher pulse rates would lead to greater masking of the amplitude modulation of the signal. Modulation detection thresholds were calculated in the presence of each pulse-train masker by determining the minimum modulation depth at which significant phase-locking was observed. We made pairwise comparisons between modulation-detection thresholds obtained at different pulse rates, restricting our analysis to units that showed significant phase-locking to unmasked stimuli presented at both pulse rates. Table 4.1 summarizes these comparisons (Wicoxon sign-rank test) for all pairs of pulse rates at interleaving delays of either 82-μs or 123-μs across the most commonly-presented masker levels.

Three general trends were present in these data. First, in the absence of a masker modulation-detection thresholds for both 10.6-and 21.2-Hz modulators were more sensitive for 254-pps than for 1017- or 4069-pps carriers, consistent with previous work (Middlebrooks, 2008b). This enhanced modulation sensitivity for 254-pps pulse train was abolished for maskers presented 2 dB above the current level of the signal, because many units were not phase-locked to either stimulus. Second, at intermediate masker levels, the difference in modulation sensitivity between high and low pulse rates was greater than in the no-masker condition, particularly for 21.2 Hz modulation. This

		10.6 Hz						21.2 Hz					
Delay	Masker:	none	-4 dB	-2 dB	0 dB	+2 dB	+4 dB	none	-4 dB	-2 dB	0 dB	+2 dB	+4 dB
82 μs	254 vs. 4096	<0.0005 (254)	<0.001 (254)	<0.0005 (254)	<0.05 (254)	0.14	0.63	<0.05 (254)	<0.005 (254)	<0.0001 (254)	0.51	0.06	0.94
82 μs	1017 vs. 4069	0.20	0.15	0.11	0.64	0.33	0.77	0.52	0.93	0.50	0.12	0.10	<0.05 (4096)
82 μs	254 vs. 1017	<0.005 (254)	<0.005 (254)	<0.05 (254)	0.19	<0.05 (254)	0.58	0.19	<0.05 (254)	<0.05 (254)	0.22	0.87	0.15
123 μs	254 vs. 4096	<0.0001 (254)	<0.005 (254)	<0.05 (254)	<0.05 (254)	0.29	<0.0001 (4096)	<0.0005 (254)	<0.05 (254)	0.13	0.20	<0.05 (4096)	<0.0001 (4096)
123 μs	1017 vs. 4096	0.06	0.26	0.69	0.91	0.34	0.14	0.83	<0.05 (1017)	0.15	<0.05 (4096)	<0.05 (4096)	0.08
123 μs	254 vs. 1017	0.18	<0.05 (254)	0.06	0.39	0.35	<0.05 (1017)	<0.005 (254)	<0.005 (254)	<0.05 (254)	0.45	0.80	0.14

Table 4.1: **Comparison across carrier pulse rate.** Each field represents a pairwise comparison (Wilcoxon sign-rank test) between modulation-detection thresholds presented at two different carrier rates. Masker levels are defined relative to signal level. Analysis restricted to units that showed significant phase-locking to both stimuli.

occurred even when there was no difference in modulation sensitivity between pulse rates in the unmasked condition (254- vs. 1017-pps, 123 μs, 10.6 Hz; 254- vs. 1017-pps, 82 μs, 21.2 Hz). Finally, at the highest masker levels there were several instances of greater modulation sensitivity for the higher-rate pulse train (254- vs 1017-pps,123 μs; 254- vs. 4069-pps, 123 μs; 1017- vs. 4069- pps, 82 μs, 10.6 Hz). These arose from a population of units for which phase-locking to the lower pulse-rate was abolished and phase-locking to the higher pulse rate was not.

Units receiving input from cochlear sites in closer proximity to the active electrode might have an advantage in encoding fluctuations in amplitude modulation. The characteristic frequencies of the units obtained in the current study varied from 8 to 32 kHz, whereas we estimate that the cochlear stimulating electrode typically was located at the 16 kHz-place or even more basal. That estimate is based on the variant on the Greenwood function obtained in albino guinea by Tsuji and Liberman (1997), $\%d = 66.438.2 \log(F)$ and an estimate of a 20 mm basilar membrane. That means that many of our recordings were from neurons receiving input from cochlear sites located apical to the stimulating-electrode site. Monopolar electric stimulation produced quite broad cochlear excitation and resulting broad cortical activation. For that reason, all cortical neurons with CFs between 8 and 32 kHz were activated with fairly uniform electrical thresholds. Nevertheless, comparison of cortical units with CFs above or below the frequency corresponding to the electrical cochlear stimulation site yielded interesting differences in modulation sensitivity.

We compared modulation detection thresholds in a subset of cortical units with CFs above or below 16 kHz. Masked modulation thresholds for populations of units distinguished by CF are shown in Fig. 4.3 (modulation frequency 10.6 Hz) and Figure 4.4 (21.2 Hz). In lower-CF neurons, unmasked differences between 254-pps pulse

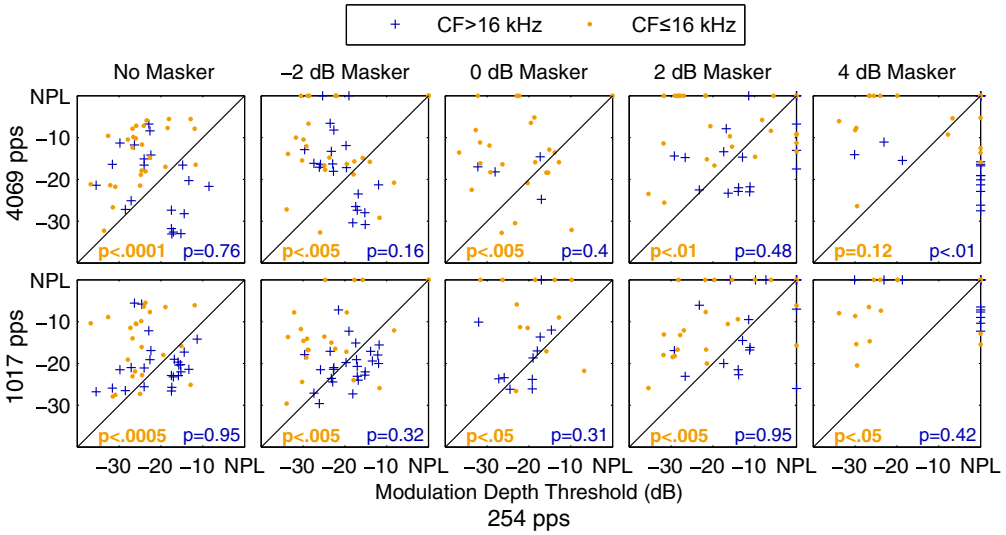

Figure 4.3: **Masked Modulation Detection Thresholds, 10.6 Hz.** Units with CF>16 kHZ are plotted in blue; units with CF≤16 kHz are plotted in orange. Each point represents a pairwise comparison of the modulation-detection thresholds elicited at one cortical recording site by 10.6-Hz modulated stimuli presented at two different pulse rates, for an interleaving delay of 82 μs. Masker level is defined relative to signal level and increases across the columns from left to right. The top row contains comparisons between 254- and 4069- pps, and the bottom row comparisons between 254- and 1017-pps. Significance levels (Wilcoxon sign-rank test) are shown in the bottom of each panel for each CF-group

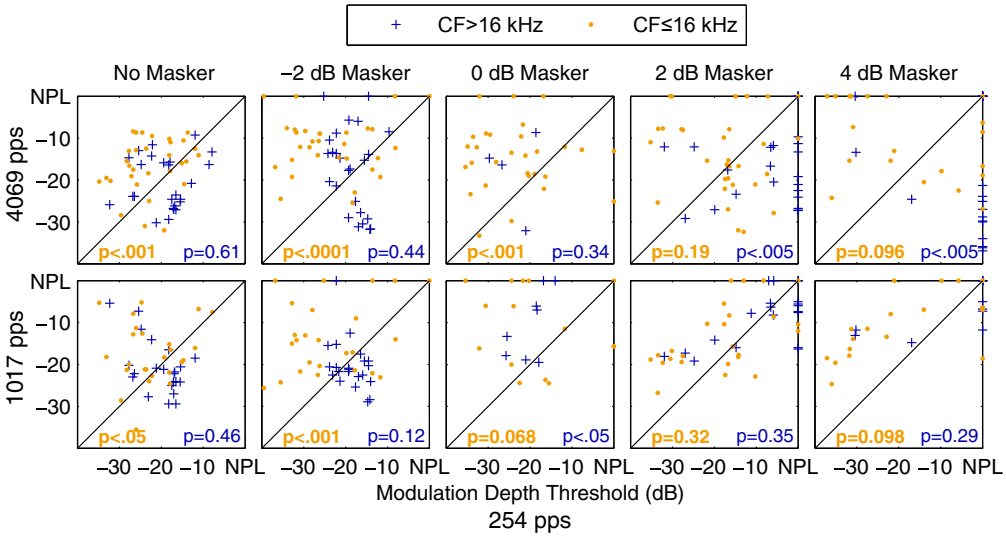

Figure 4.4: **Masked Modulation Detection Thresholds, 21.7 Hz.** Similar to Figure 3, for 21.2-Hz modulation.

trains and higher rates were particularly pronounced and were observed even in the presence of high-level maskers. On the other hand, higher-CF units did not show a significant difference between pulse rates in the unmasked condition and, primarily at the 21.7-Hz modulation frequency, showed enhanced modulation sensitivity at higher pulse rates in conditions of high masker levels. These data indicate that masking grows more quickly for lower pulse rates than higher pulse rates. It is possible that this is an effect of the lower current levels used at higher pulse rates. However, the same pattern of results was observed even when the pairwise comparisons were performed with maskers sorted by absolute current level. Another possibility is that, since lower pulse rates have compressed dynamic ranges compared to higher pulse rates in the same unit or individual, a high-level masker in a low pulse-rate condition results in more effective masking. Unfortunately, since we did not measure the upper limit of sensitivity to electric stimulation, we were unable make comparisons within masker levels segregated by percentage of the dynamic range.

In previous studies (Middlebrooks, 2004), shorter interleaving delays resulted in greater interactions between sub-threshold unmodulated pulse trains than did delays >1 ms. In addition, short interleaving delays (82, 123 μs) fall within the temporal integration window for current pulses in the cochlea. Therefore, we tested the hypothesis that shorter interleaving delays led to greater masking. Table 4.2 contains a summary of pairwise comparisons between interleaving delays within each pulse rate. Contrary to our expectations, there were few significant differences in modulation sensitivity across interleaving delay within the same pulse rate. There were isolated differences in the behavior of individual units but no clear pattern. Restricting the frequency range, regrouping maskers according to absolute current level, or grouping the data by cortical depth did not reveal any underlying effects of interleaving delay

		10.6 Hz						21.2 Hz					
Pulse Rate	Masker:	none	-4 dB	-2 dB	0 dB	+2 dB	+4 dB	none	-4 dB	-2 dB	0 dB	+2 dB	+4 dB
254 pps	82 vs. 1966	0.95	0.57	0.80	0.40	0.61	0.08	0.72	0.67	0.47	0.50	0.39	0.32
254 pps	82 vs. 123	0.39	0.50	0.56	0.30	0.10	<0.001 (123)	0.13	0.42	0.85	0.22	0.13	<0.0005 (123)
254 pps	123 vs. 1966	0.24	0.98	0.38	<0.005 (1966)	0.64	0.06	0.33	0.57	0.24	0.06	0.83	<0.005 (1966)
1017 pps	82 vs. 492	0.70	0.41	0.70	0.63	0.99	0.14	0.21	0.93	0.72	0.38	0.40	0.41
1017 pps	82 vs. 123	0.73	0.99	0.54	0.73	0.90	0.14	0.42	0.66	0.37	0.37	0.20	0.15
1017 pps	123 vs. 492	0.93	0.63	0.48	0.38	0.95	0.41	0.74	0.43	0.88	0.84	0.65	0.43
4069 pps	82 vs. 123	0.22	0.07	0.17	0.94	0.65	0.56	0.22	0.06	0.08	0.78	0.55	0.14

Table 4.2: **Comparison across interleaving delay.** Each field represents a pairwise comparison (Wilcoxon sign-rank test) between modulation-detection thresholds presented at two interleaving delays. Masker levels are defined relative to signal level. Analysis restricted to units that showed significant phase-locking to both stimuli.

on modulation masking.

4.3.2 Experiment 2

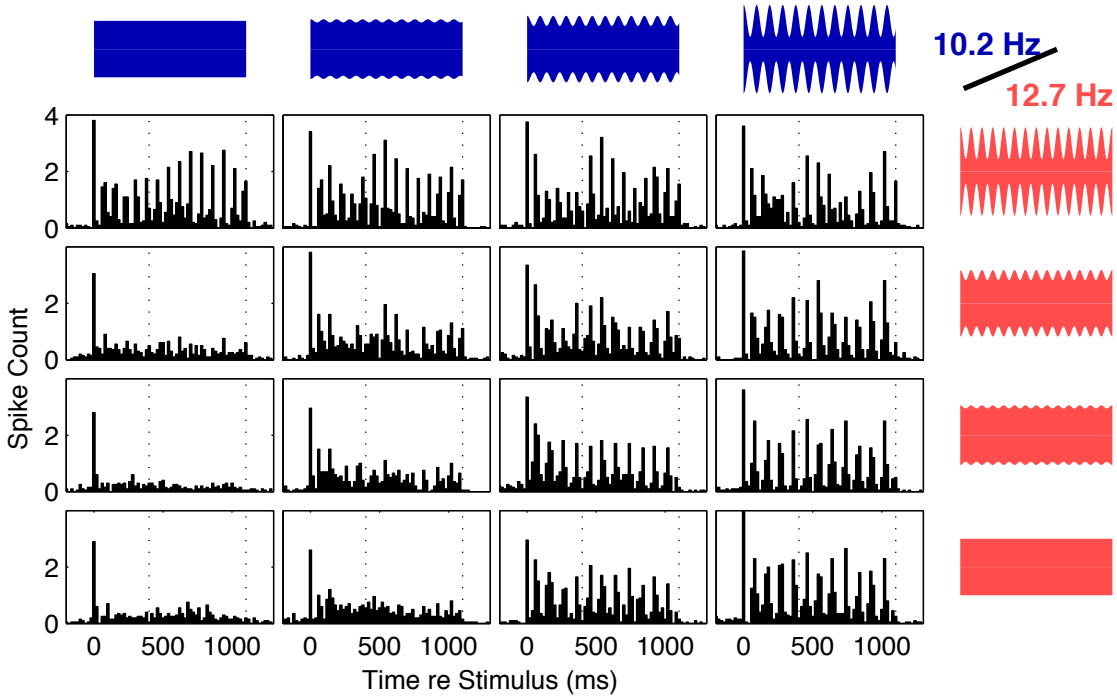

Figure 4.5: **Multi-unit cluster response to two interleaved, modulated stimuli.** Diagrams at the top of each column indicate the modulation frequency and depth of Stimulus A (blue) in each column, and diagrams at the right indicate the modulation frequency and depth of Stimulus B (red) in each row. Each panel shows the response to the corresponding combination of stimulus parameters. Stimuli were presented at a pulse rate of 254 pps, modulation frequency of 10.6 Hz and interleaving delay of 1966 μs. These panels represent a subset of the modulation-depth combinations presented to this unit. Dotted lines indicate the time range used in subsequent analysis.

In the presence of two amplitude-modulated signals with different modulation frequencies, cortical neurons responded with tonic modulated firing that varied with the modulation depth of each stimulus. Figure 4.5 shows sample stimulus waveforms and cortical responses from one cortical unit in response to 254-pps pulse trains modulated at 10.6 and 12.7 Hz. As in Experiment 1, phase-locking is evident to each stimulus waveform when the competing stimulus is an unmodulated 0-dB masker. Modulation detection thresholds were not necessarily the same for the two stimuli

— this unit phase-locked at a shallower modulation depth to Stimulus A than to Stimulus B. The simultaneous presentation of Stimuli A and B at modulation depths above their respective modulation-detection thresholds evoked more complex patterns of firing.

Beat Frequencies

The arithmetic summation of two sine waves of unequal frequency produces a waxing and waning of amplitude referred to as a "beat". Similarly, beats were evident in the cortical responses shown in Figure 4.5 as regular fluctuations in the magnitude of the phase-locked peaks. The peaks of the beat frequencies were particularly effective at eliciting phase locking. We examined cortical responses to pairs of modulation frequencies by computing PSTHs averaged across units, as described in the Methods; results are shown in Figs. 4.6, 4.7, and 4.8 for carrier rates of 254, 1017, and 4069 pps, respectively. For each unit, modulation depths were expressed relative to each units modulation threshold such that relative modulation depths >0 dB (A_{mod}, B_{mod}) would produce a phase locked response in combination with an unmodulated competing stimulus. Data were combined across units by categorization based on this relative modulation depth. The average responses to modulated Stimulus B in the presence of an unmodulated Stimulus A (A_0B_{mod}: Panels A and E) or vice versa ($A_{mod}B_0$: Panels D and H) showed phase locking to the corresponding modulated stimulus with no sign of modulation on the time scale of 1/2 second. In contrast, stimulus conditions in which both stimuli were modulated ($A_{mod}B_{mod}$: Panels B and F) elicited clear beating patterns of peaks and troughs, with periods equal to the that of difference in modulation frequencies: 2.1 or 3.0 Hz. As expected, there was no phase-locking evident in the response to two unmodulated pulse trains (A_0B_0; Panels C and G)

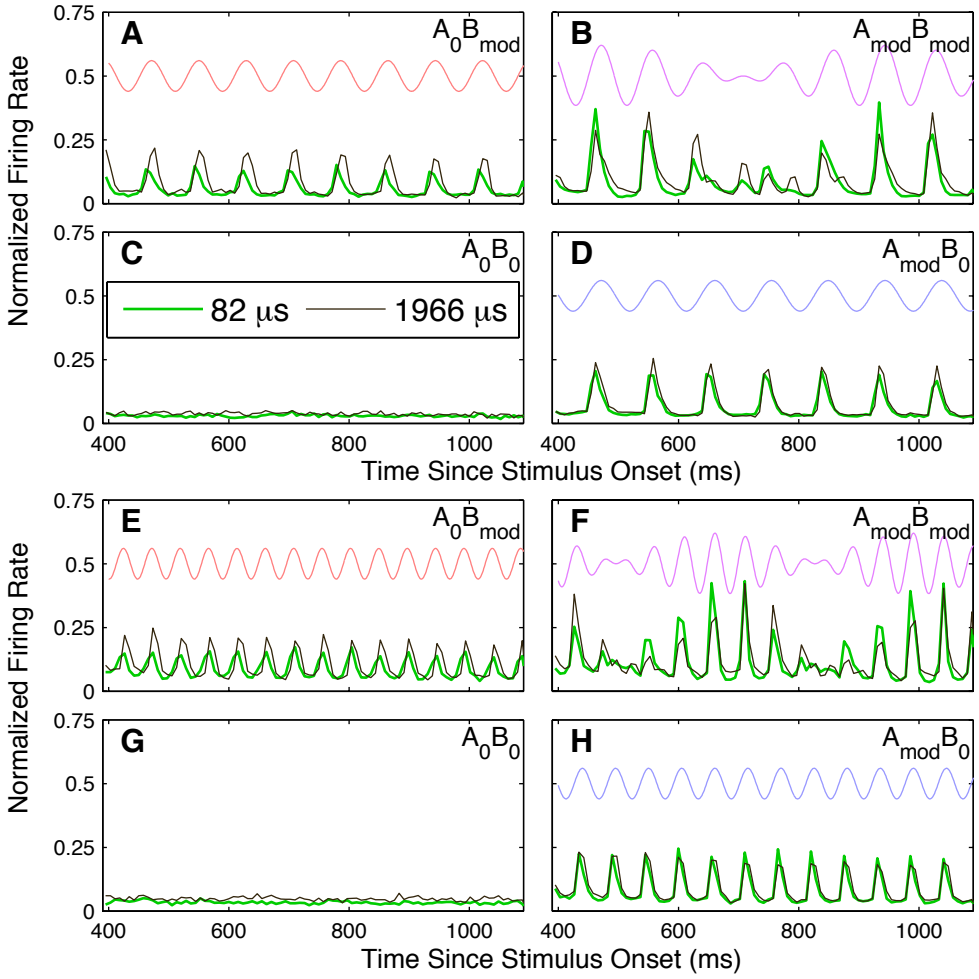

Figure 4.6: **Average Spike Responses to Four Stimulus Combinations, 254 pps.** The green and black lines trace out the average spike rate elicited by each stimulus condition combination for the 82-μs (green) and 1966-μs (black) interleaving delays. Upper panels (A-D) represent responses to 10.6/12.7-Hz modulation-frequency pair and lower panels, (E-H) 18.2/21.2-Hz modulation-frequency pair. Each panel represents a combination of modulated (above MDT) and unmodulated stimuli. A, E: B-Stimulus modulated and A-Stimulus unmodulated, red line traces summed stimulus waveform; B, F: Both stimuli modulated, purple line traces summed stimulus waveform; C,G: Both stimuli unmodulated; D, H: A-Stimulus modulated, B-Stimulus unmodulated, blue line traces summed stimulus waveform.

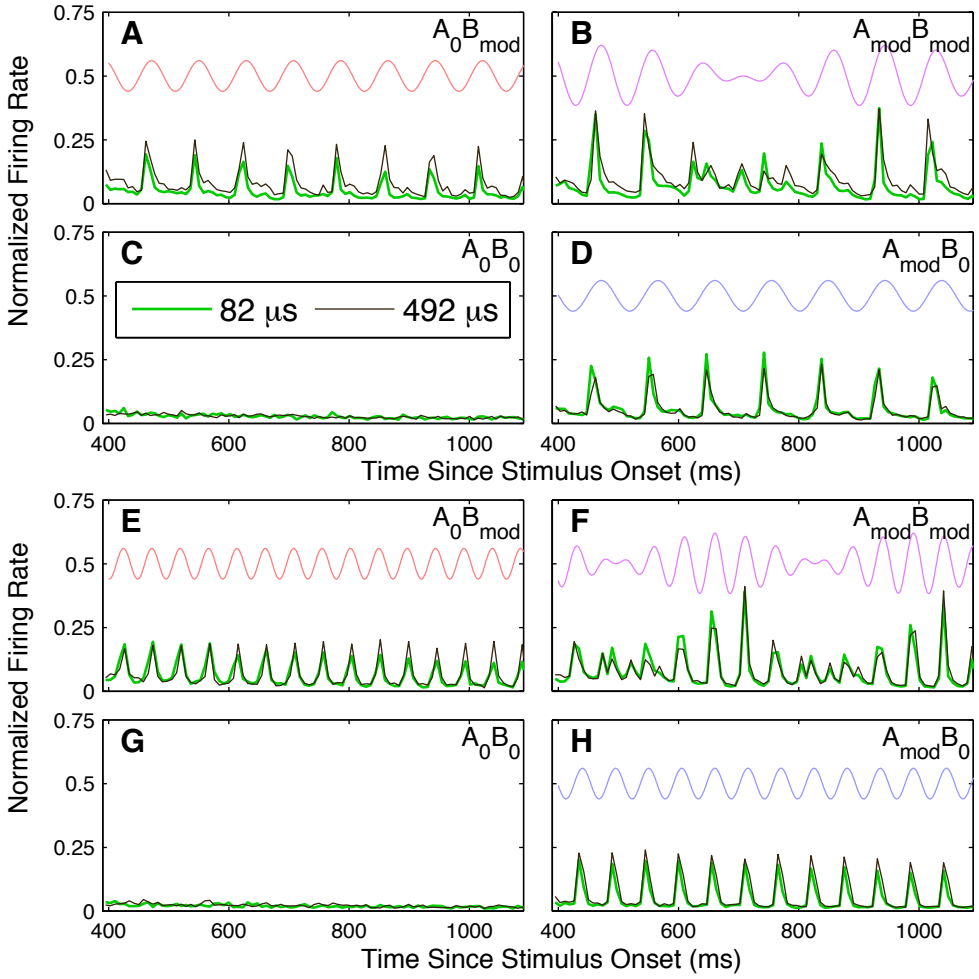

Figure 4.7: **Average Spike Responses to Four Stimulus Combinations, 1017 pps.** The green and black lines trace out the average spike rate elicited by each stimulus condition combination for the 82-μs (green) and 492-μs (black) interleaving delays. Upper panels (A-D) represent responses to 10.6/12.7-Hz modulation-frequency pair and lower panels, (E-H) 18.2/21.2-Hz modulation-frequency pair. Each panel represents a combination of modulated (above MDT) and unmodulated stimuli. A, E: B-Stimulus modulated and A-Stimulus unmodulated, red line traces summed stimulus waveform; B, F: Both stimuli modulated, purple line traces summed stimulus waveform; C,G: Both stimuli unmodulated; D, H: A-Stimulus modulated, B-Stimulus unmodulated, blue line traces summed stimulus waveform.

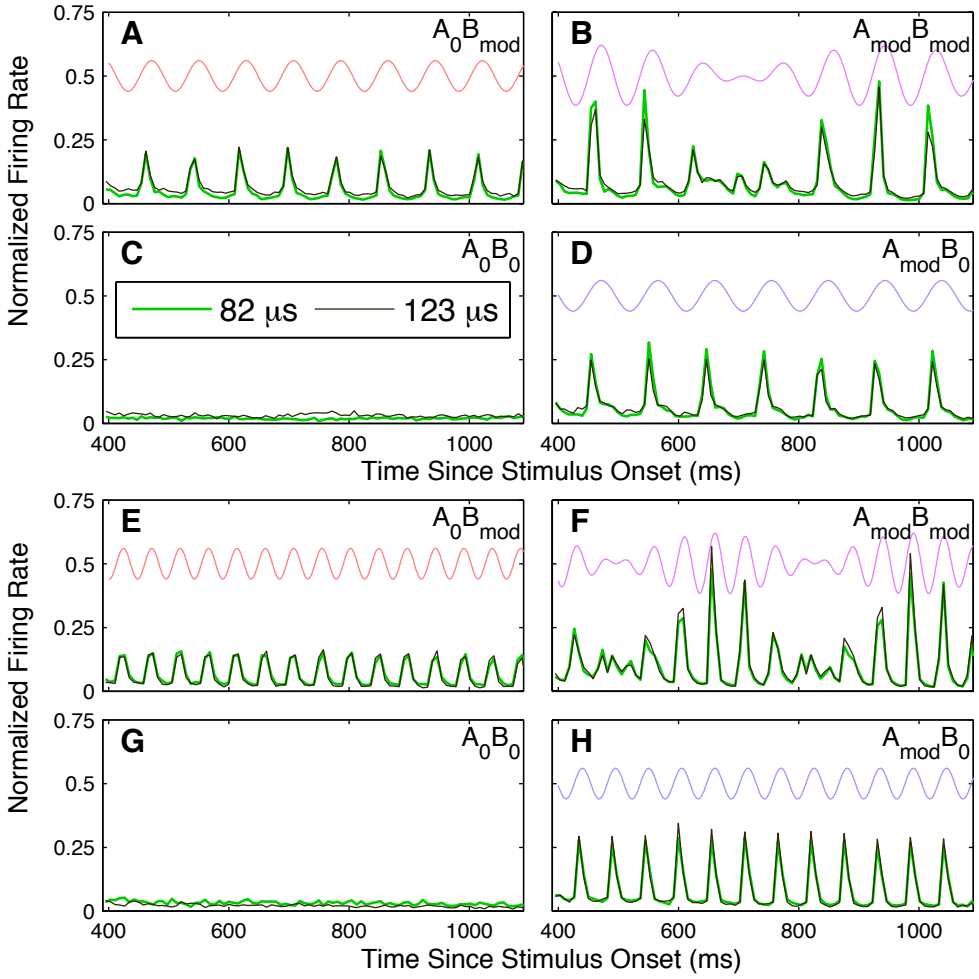

Figure 4.8: **Average Spike Responses to Four Stimulus Combinations, 4069 pps.** The green and black lines trace out the average spike rate elicited by each stimulus condition combination for the 82-μs (green) and 123-μs (black) interleaving delays. Upper panels (A-D) represent responses to 10.6/12.7-Hz modulation-frequency pair and lower panels, (E-H) 18.2/21.2-Hz modulation-frequency pair. Each panel represents a combination of modulated (above MDT) and unmodulated stimuli. A, E: B-Stimulus modulated and A-Stimulus unmodulated, red line traces summed stimulus waveform; B, F: Both stimuli modulated, purple line traces summed stimulus waveform; C,G: Both stimuli unmodulated; D, H: A-Stimulus modulated, B-Stimulus unmodulated, blue line traces summed stimulus waveform.

As in Experiment 1, we hypothesized that that higher pulse rates and shorter interleaving delays would produce stronger stimulus interactions in the auditory nerve, resulting in a pronounced summation of the two stimuli. On the other hand, longer interleaving delays at lower pulse rates might allow a cortical response that was selective to one stimulus, suppressing phase-locking to the other. Contrary to our expectations, the magnitude of the spiking response followed the envelope of the sum of the two stimuli regardless of pulse rate or interleaving delay. We considered the possibility that the averaging used to form these PSTHs could simply produce a response midway between two populations of neurons, each with a selective response to either A or B. However, this would not explain the fact that the phase-locking elicited at the beat peak was larger in magnitude than the response to either stimulus alone. Therefore we conclude that, even at the longest interleaving delays, the representation of the stimulus in the cortex followed the summed stimulus envelope.

There were a few effects of pulse-rate and interleaving-delay parameters on the average PSTHs, however. First, for 254- and 1017-pps conditions at the 82-μs interleaving delay, the magnitude of the phase-locked responses elicited by stimulus combination $A_{mod}B_0$ was greater than those evoked by A_0B_{mod}. This difference was reduced at the longer interleaving delays, and was not seen at all for 4069-pps stimuli. This effect of interleaving-delay likely arose from the alternation in inter-pulse intervals that occurred when the interleaving delay was much shorter than the period of the pulse rate, resulting in asymmetrical interactions between the leading and lagging stimuli. Second, at the 1966-μs interleaving delay, the peak responses to Stimulus-B occurred later than those elicited by an 82-μs delay for any pulse rate, which was simply a result of the basal pulse train being delayed by nearly 2 ms. Finally, in the 254 and 1017-pps $A_{mod}B_{mod}$ conditions, although the timing of the firing peaks

remained the same, more spikes were elicited later in the beat period for the longer interleaving delay. This contrast can be seen particularly well in Fig. 4.6F (compare, for instance, with Fig. 4.8F, where the two interleaving delays result in no difference). This phenomenon might arise from the variable lag between modulation peaks. At 0-phase, the two peaks were simultaneous, while at π-phase they were separated by 47 or 28 ms for 10.6/12.7 and 18.2/21.2 Hz respectively, with the Stimulus-B peaks leading in time from $0 - \pi$ and the Stimulus-A peaks leading from $\pi - 2\pi$. Phase locking in auditory cortex is generally observed only for modulation frequencies of <100 Hz in other words, intervals of 10 ms or greater. Thus, at long interleaving delays in which summation of activation does not occur in the cochlea, neurons may follow Stimulus B in the first half of the beat phase and Stimulus A in the second.

Fourier Transform Analysis

We quantified the representation of particular modulation frequencies in the responses of individual units by computing the Fourier transform of each units PSTH, normalized by the DC offset. Figure 4.9 represents the magnitude of the normalized Fourier components at modulation frequencies 10.6 Hz (Fig. 4.9A and C) and 12.7 Hz (Fig. 4.9B and D); upper and lower rows represent interleaving delays of 82 and 1966 μs. Horizontal and vertical axes represent modulation depths for the 10-6 and 12.7-Hz modulator.

The 10.6 Hz periodicity (Fig. 4.9A and C) of the response grew with the 10.6 Hz modulation depth of Stimulus A with relatively little influence of the depth of Stimulus B. Similarly, the 12.7 Hz periodicity of the response (Fig. 4.9C and F) grew with the modulation depth of Stimulus B largely independent of the depth of Stimulus A. We used singular value decomposition (SVD) to characterize the growth of each frequency response with increasing modulation depth. This procedure produced pairs

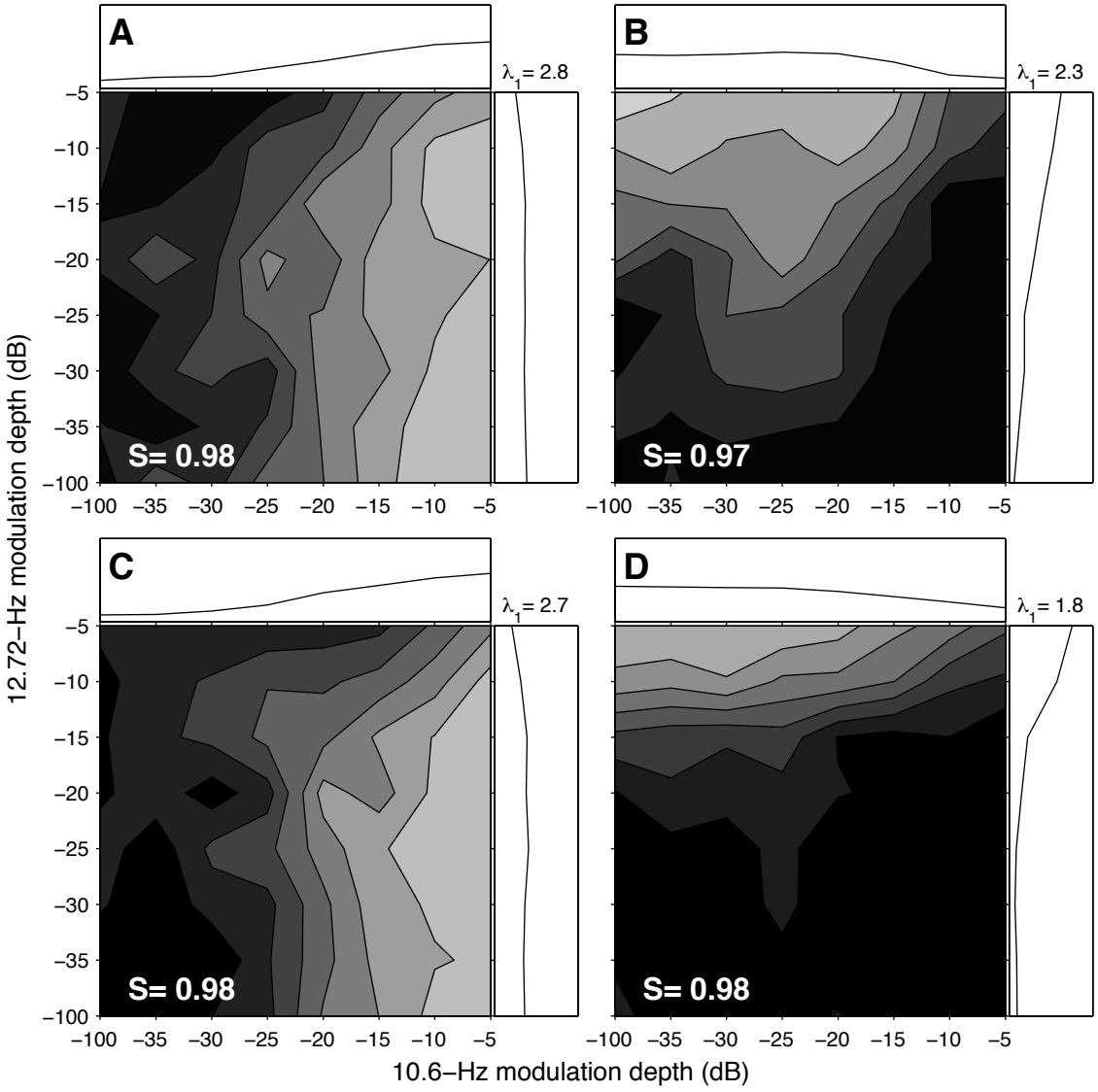

Figure 4.9: **Singular Value Decomposition Examples.** Each main panel contains a contour plot showing the normalized Fourier peak for a single frequency across all stimulus combinations. The left column (A, C) represents the magnitude of the Fourier peak at the A-frequency, 10.6 Hz and the right column (B, D) represents the magnitude of the Fourier peak at the B-frequency, 12.7 Hz. Stimuli were presented at 254 pps. The top row (A, B) contains the 82 μs interleaving delay and the bottom row (C, D) the 1966 μs interleaving delay. Surrounding each plot are the first vector components of the singular-value decomposition. The vector representing the dependence on 10.6-Hz modulation depth is located on top; the vector representing the dependence on 12.7-Hz modulation depth is located to the right. The eigenvalue for these components, λ_1, is noted in the top right, and the measure of separability S is located in the bottom left of each main panel. Data are shown for the same unit as Figure 5. The colormap range of Fourier peak magnitudes is 0-0.6 (out of 1) for all panels.

of vectors representing the dependence of the Fourier peak on the modulation depth of A and B, as well as an eigenvalue representing the overall magnitude of the response. The vectors are pictured to the top and right of each panel. The separability of each frequency response measured the power in the Fourier peak data that was captured by this pair of vectors. Generally a high separability was encountered across the entire sample population (S: mean 0.93, standard deviation 0.06 across all conditions for Stimulus A; mean 0.91, standard deviation 0.06 for Stimulus B). Comparisons across stimulus conditions indicated a higher separability in the case of the 4069-pps pulse rate than at lower rates ($p < 0.001$, Mann-Whitney rank-sum). There were no significant differences in separability between interleaving-delay conditions. The high separability indicated that the cross-product of these vectors provided a good approximation of the full dataset. The vectors obtained through SVD demonstrated that the Fourier strength of each component grew monotonically with an increase in the modulation depth of the driving stimulus, was larger for higher pulse rates ($p < 0.05$, all comparisons) and, at the 82 μs interleaving delay for 254- and 1017-pps stimuli, was larger for A than for B. As seen in Figure 9, for stimulus combinations at which there was a significant response to both stimuli, the Fourier-peak response to each stimulus decreased. However, this effect is to some extent inevitable because the normalized Fourier peak responses across all frequencies must add up to 1. Overall, these data show that the cortical response effectively represented both modulation frequencies, regardless of modulation frequency, pulse rate, or interleaving delay.

4.4 Discussion

The primary result of this study is that auditory cortex appears to respond to the summed envelope of stimuli presented to spatially separated electrodes. We

start by discussing psychophysical and physiological studies of amplitude-modulation detection in cochlear-implant listeners. Second, we compare the current results with prior studies of modulation masking. We then discuss channel interactions and stream segregation in cochlear-implant listeners and the implications of the current results for implant performance. Finally, we relate the observation of beat frequencies to previous studies.

4.4.1 Modulation Detection in Cochlear-Implant Listeners

Shannon (1992) first described the temporal modulation transfer functions of cochlear implant listeners using sinusoidal and pulsatile carriers and found modulation detection thresholds were similar to those measures in normal-hearing listeners at the highest current levels, some CI users were able to detect shallower modulations than are normal-hearing listeners. A normal low-pass pattern of modulation sensitivity appears to be important for speech recognition (Cazals et al., 1994). In general, performance in modulation-detection tasks is correlated with a number of important practical skills for cochlear-implant listeners, such as English-language phoneme recognition (Fu, 2002) and consonant, word, sentence and tone-recognition in Mandarin speakers (Luo et al., 2009). Electrode selection may also be guided by modulation-detection thresholds (Chatterjee and Yu, 2010; Pfingst et al., 2008).

Several studies in cochlear-implant listeners (Arora et al., 2011; Galvin and Fu, 2005; Pfingst et al., 2007) as well as physiological studies in anesthetized guinea pig (Middlebrooks, 2008b) have shown more sensitivity to amplitude modulation at lower pulse rates when modulated stimuli are presented in the middle of the dynamic range. However, McKay and Henshall (2010) suggested that an equivalent current-level comparison would be more appropriate for modulation-detection thresholds across pulse rates, and demonstrated this equivalence for modulation rates of 250- and 500-Hz,

which evoked a steady loudness percept. Support for this interpretation has also been shown for 10-Hz modulation, which evokes a fluctuating loudness percept, by preliminary data (Galvin and Fu, 2011) indicating that for cochlear-implant listeners, modulation detection thresholds are the same across pulse-rate for identical current levels. In the current study we showed an effect of pulse rate on unmasked modulation-detection thresholds, which varied across cortical sites according to their characteristic frequency. Neurons receiving projections from apical regions of the cochlea distant from the implant were most sensitive to modulations in unmasked 254-pps pulse trains, whereas higher frequency units showed no significant difference between modulation-detection thresholds across the pulse rates tested. It should be noted that current levels were chosen relative to threshold, and lower-rate pulse trains were presented at higher stimulus levels. Although activation by electric pulse trains is extremely broad across the cochlea, this observation may indicate that transmission of pulse-train amplitude modulation to the distant cochlear apex is more robust either for higher-level pulse trains or for lower-rate pulse trains or some combination of the two. Human listeners should be able to combine cues from across the cochlea.

This debate about the selection of stimulus level for comparisons of modulation detection arises because performance in modulation detection tasks is very sensitive to stimulus level, particularly in cochlear-implant listeners (Zhang and Zeng, 1997). Level-dependence is confounded with electric pulse rate, as higher pulse rates are perceived as louder, and dynamic ranges are compressed at lower pulse rates (Kreft et al., 2004). McKay et al. (2003) have proposed a loudness summation model that integrates the electric pulses received across a 2-7 ms window, regardless of the channel of presentation. Galvin and Fu (2011) tested this hypothesis in cochlear-implant listeners by comparing modulation detection thresholds obtained with stimulation by

several low-rate pulse trains interleaved across channels with modulation detection thresholds obtained for a carrier pulse train presented at the same overall stimulus rate, but on a single electrode, as well as for the low-rate pulse trains on each channel. They found that the modulation detection thresholds, which depend on the perception of loudness of the interleaved pulse trains, fell within the range established by the single-channel stimulation conditions but varied from listener to listener and channel to channel. In the present study we show that in the presence of unmodulated maskers at levels near threshold (−4-dB masker condition), modulation detection was unaffected or even enhanced, an effect that could arise due to a shift in the effective level of the overall stimulus. In the two-modulator case, neural responses fluctuated in magnitude according to the summed stimulus envelope. Notably, this effect was insensitive to interleaving delay in both experiments, consistent with the proposed model of loudness summation.

4.4.2 Modulation Masking

In the current study, we observed that unmodulated pulse trains presented at 0 dB relative to an amplitude-modulated signal had little effect on overall modulation detectability. Similar to the present results, unmodulated stimuli result in a small shift in the detectability of amplitude modulation: ∼5-dB elevation in modulation depth in normal-hearing listeners for a masker above the carrier frequency of the signal (Bacon et al., 1995), and 5.75 dB in cochlear-implant listeners (Richardson et al., 1998). The robustness of modulation detection may result from the increased sensitivity of temporal modulation transfer functions at higher stimulus levels. In Experiment 2 of the present study, we saw a reduced firing rate in response to modulation of the lagging stimulus in the presence of an unmodulated masker for an 82-μs interleaving delay at the lower pulse rates. As mentioned in the Results, this interaction likely arose in

the auditory nerve due to the asymmetry in interpulse interval: the longer interpulse interval allowed recovery from stimulation, synchronous activity to the leading pulse, resultant mass depolarization and a relatively small population of excitable neurons remaining to respond to the lagging stimulus. As demonstrated in the 4069-pps stimulation condition, this asymmetry does not arise when the inter-pulse intervals are short enough to maintain a state of stochastic recovery from depolarization. Such an effect is unlikely to present a significant challenge to cochlear implant users; in everyday stimulation modes, the long inter-pulse interval would be filled with pulse trains interleaved on other electrodes. However, for a low pulse rate, spatially-restricted activation, and a base-to-apex electrode stimulation order, the basal-most electrode could suppress responses in its neighbor.

The detection of acoustic amplitude modulation is more difficult when the masker is also amplitude-modulated, even if the carrier frequencies are separated by 2 octaves. Modulation masking has been demonstrated in normal-hearing subjects for various combinations of tones (Wakefield and Viemeister, 1985), SAM tones (Yost and Sheft, 1989), noise-modulated tones (Moore and Jorasz, 1996), multi-tone complexes (Sheft and Yost, 1997b), double-modulated tones (Moore et al., 1999) and even binaural beat modulations (Sheft and Yost, 1997a). In other words, any stimulus that evokes the perception of amplitude modulation impairs the detectability of similar modulation frequencies. Modulation masking is maximal when the masker modulation frequency matches the probe modulation frequency. Effects that satisfy this criterion are referred to as Modulation-Detection Interference (MDI). MDI has been observed in hearing-impaired (Grose and Hall, 1994) and cochlear-implant listeners as well (Richardson et al., 1998), indicating that this effect of envelope masking is central to the cochlea.

Chatterjee (2003) examined the detectability of a SAM pulse train in the presence of a Noise-Amplitude-Modulated (NAM) masking pulse train. For pulse rates of 500 pps and an interleaving delay of 1 ms, she found that for maskers presented through different channels than the signal, NAM maskers elevated modulation-detection thresholds more than did unmodulated maskers presented at the peak level of the noise, and masking increased with increasing noise modulation depth. Given the results from the present study, we expect that populations of cortical neurons would respond to a weighted sum of these interleaved stimuli. Whereas the sum of unmodulated and SAM pulse trains is a SAM pulse train at louder stimulus level and reduced AM depth, the salience of the sinusoidal amplitude modulation is reduced when added directly to noise. This interpretation is supported in Chatterjee's data: even though signal modulation frequencies of 20 and 50 Hz had different modulation-detection thresholds in quiet, and modulation-detection thresholds in the presence of an unmodulated masker differed between the two stimuli, the 20%-noise-masked modulation-detection thresholds were similar between these conditions, indicating that a particular modulation depth was necessary to achieve the perception of periodic amplitude-modulation.

In normal-hearing listeners, MDI is discussed in the context of tuning to the modulation frequency. The probe and masker stimuli are represented centrally by selective populations of neurons tuned to the respective carrier frequencies and interact through common modulation-sensitive channels. The current study indicates that competing stimuli with similar modulation frequencies are represented in an overlapping population of neurons even when cochlear stimulation is spatially and temporally distinct. We used monopolar stimulation, which provides broad activation of auditory cortex (Bierer and Middlebrooks, 2002). This non-selective activation,

especially at high stimulus levels, likely enhanced the common representation of the two stimuli, but a mechanism for integrating the responses at long interleaving delays would still be necessary to generate the observed enhancement of response when the stimulus peaks were coincident. It is possible, however, that a more restricted mode of stimulation such as bipolar or tripolar would lead to more distinct representations of each stimulus, particularly for the long interleaving delays.

4.4.3 Implications for Sound Source Segregation

Amplitude modulation may be used as a grouping cue for auditory object formation and stream segregation. For instance, the masking of a tonal signal by a frequency-matched narrowband noise that has been amplitude-modulated can be reduced by the addition of off-frequency stimuli whose amplitudes are co-modulated with the masker. This effect is known as co-modulation masking release and is dependent on the grouping of the masker with the flankers. If the flankers are perceptually isolated by grouping cues into a separate stream, then co-modulation release is not observed (Dau et al., 2009). Neural correlates of comodulation masking release have been observed in the ventral cochlear nucleus (Pressnitzer et al., 2001) dorsal cochlear nucleus of guinea pigs (Neuert et al., 2004) and in the auditory cortex of songbirds (Bee et al., 2007). The uniting feature of these results is that the representation of the target is enhanced by the modulation grouping cue, usually through suppression of the modulated masker.

In general, stream segregation can operate on a dimension along which stimuli are separable, such as frequency, onset timing, location, or timbre. However, many of these cues are degraded in cochlear implant listeners. Whereas CI-listeners are able to perform as well as normal-hearing listeners in a stream segregation task along a perceptually-discriminable dimension such as timbre (Hong and Turner, 2009), tasks

that require segregation across a domain such as frequency are more difficult (Hong and Turner, 2006). In the present study, we report that monopolar stimulation presented at two cochlear sites results in overlapping representations across a range of characteristic-frequency neurons in primary auditory cortex. We did not observe populations of neurons selective for a single stimulus. This may indicate that the lack of spectral cues dominate the cortical interactions between stimuli, although further testing with more selective stimulation modes would help to confirm this.

A related phenomenon, known as "modulated-unmodulated difference" or "listening in the gaps" refers to the perception of speech in the presence of a modulated energetic masker. For normal hearing listeners, the information "glimpsed" in the low-amplitude portions of the modulated stimulus is enough to improve speech recognition. This effect is enhanced by the manipulation of grouping cues such as location. However, cochlear-implant listeners do not benefit from the information present in these gaps (Nelson et al., 2003). In our stimuli, the troughs of the beat period provided more potential cues for stimulus segregation. Longer interleaving delays evoked cortical responses with a more robust representation of the individual peaks in the beat trough than did shorter interleaving delays. In addition, anesthetized guinea-pig cortex provides a minimum estimate of sensitivity, because neuronal selectivity increases during attention to a behavioral task (Lee and Middlebrooks, 2011). These results indicate that an appropriate choice of stimulus parameters has the potential to enhance separability of incoming channels of auditory information, but additional experiments would be necessary to confirm this speculation.

4.4.4 Beat Perception

A notable finding in the present results was the observation of strong fluctuations in the magnitude of the spiking response following the difference frequency of the

two modulation frequencies. In normal hearing listeners, such beats are perceived during presentations of a pair of tones differing in frequency. Responses to pure tones modulated with two-tone complexes were recorded in the cochlear nucleus of anesthetized chinchillas (Shofner et al., 1996). Amplitude fluctuations were evident in the PSTH envelope and peaks were present in the Fourier transform at the beat frequency, particularly in chopper neurons, which appeared to act as envelope extractors. The nonlinearities of the basilar membrane generate the distortions necessary for beat perception at the very beginning of auditory processing, and synchronized responses to beat frequencies have been observed in neurons tuned to low characteristic frequencies. However, this type of interaction is absent in individuals without functioning hair cells. Electric stimuli presented at short interleaving delays may create fluctuations in response amplitude within the auditory nerve due to temporal integration, but since these interactions are minimal for inter-pulse delays longer than $\sim$1 ms (Middlebrooks, 2004) this does not explain the present observation of beat frequencies at the 1966-μs interleaving delay.

There is some evidence for a more central generator of beat frequencies. Binaural beats occur when the envelope periodicity differs slightly between stimuli presented to the two ears (Licklider et al., 1950). The percept of fluctuating amplitude and oscillating azimuthal location is strongest for tone stimuli with frequencies below 1 kHz, but a fluctuating percept can also be obtained with higher-frequency carriers with periodic envelopes that differ slightly in modulation frequency (McFadden and Pasanen, 1975). Binaural beats clearly arise from central interactions, but the frequency dependence demonstrates that they require the specialized localization circuits of the superior olivary complex. Several monaural studies have demonstrated the effectiveness of masking an amplitude-modulated probe sound with a distant-

frequency carrier double-modulated with two modulation frequencies with difference frequency equal to that of the probe (Moore et al., 1999), despite the lack of acoustic energy at the probe frequency. In the inferior colliculus of awake chinchillas, (Biebel and Langner, 2002) found that low-frequency neurons with low-frequency CFs were activated by the presentation of high-frequency AM stimuli, and proposed that perception of modulations (such as beats) could be attributed to tuning of neurons to modulation frequency as well as carrier frequency. However, McAlpine (2004) has shown in anesthetized guinea pig that these responses likely arise through nonlinearities in the response of the basilar membrane. These cochlear distortions may explain the psychophysical results as well, suggestion a peripheral mechanism rather than a central one. However, such a mechanism cannot contribute to beating interactions in cochlear-implant stimulation. The current study therefore demonstrates beat interactions that are generated centrally to the auditory nerve.

4.5 Conclusions

We have shown that amplitude-modulated pulse trains interact at longer interleaving delays than do unmodulated pulse trains. From the present results it is clear that interleaved electric stimulation results in a superimposed representation of the stimuli in the auditory cortex. Low pulse rates and long interleaving delays provide a small benefit in stimulus segregation in auditory cortex. However, these interleaving delays are much longer than those used in conventional cochlear implant processors and their implementation would result in decrements in performance in other areas.

CHAPTER 5

Conclusions

In this dissertation I have examined several measures of temporal acuity and observed that temporal acuity depends on stimulus pulse rate, current level, and duration. I start with a discussion of the implications of the present results for auditory temporal processing and suggest future experiments. I then discuss the implications for cochlear implant listeners and describe future clinical research directions.

5.1 Implications for Mechanisms of Auditory Temporal Acuity

The first cochlear implantations resulting in open-set speech perception demonstrated that comprehensible auditory perceptions could be generated without the participation of the intricate machinery of the basilar membrane and hair cell complex (Clark et al., 1981). While these peripheral mechanisms must and do play a role in temporal sensitivity in acoustic hearing, the demonstration of forward masking (Lim et al., 1989), gap detection (Preece and Tyler, 1989) and amplitude modulation detection (Shannon, 1992) in electric hearing demonstrated that processes central to the cochlea were also necessary. Auditory stimulation in the absence of hair cells allows us to examine which auditory processes truly require basilar membrane and hair cell mechanisms. Recordings from auditory nerve fibers in response to electric stimulation demonstrate that the robust encoding of frequency-specific activation

seen in the intact auditory system is substantially altered with electric stimulation (Hartmann et al., 1984). However, the manner in which this input is transformed between cochlea and cortex is informative about the activity of the auditory pathway. In this fashion, I have demonstrated several principles of temporal coding in the central auditory system.

5.1.1 Relationship with Psychophysical Recovery from Masking

In Chapter 2, I showed that recovery from forward masking in primary auditory cortex could be described by the sum of two exponential recovery processes. Exponential fits have been used in several psychophysical measurements of recovery from forward masking (Chatterjee, 1999; Nelson and Donaldson, 2002). When quantifying psychophysical or physiological behavior on a restricted time scale, such a curve fit is appropriate. However, for neuronal processes at nearly every resolution, from ion channels to cortical circuits, the predominant recovery process depends on the duration of observation (Drew and Abbott, 2006). In the auditory system, for example, this behavior has been observed in models of the inner hair cell synapse (Zilany et al., 2009) and in recordings from single pyramidal neurons in a slice preparation of rat auditory cortex (La Camera et al., 2006). Power-law dynamics describe such processes over multiple time scales, and take the form:

$$X = At^k, k < 1. \tag{5.1}$$

Power-law behavior can be approximated by the sum of multiple exponential processes operating at different time scales. If I consider each exponential component to reflect an individual process, then I can combine data taken across multiple time scales into a single cohesive power-law model. Psychophysical recovery from forward

masking is well-fit by a power-law curve (Oxenham and Moore, 1994; Wojtczak and Oxenham, 2009). Psychophysical results reflect the perceptual output of the auditory pathway, presumably incorporating contributions of the sequential processing that has been observed along the auditory pathway (Frisina, 2001; Wang et al., 2006).

Our results from Chapter 2 quantify the contributions of two components of recovery from masking. I have attributed these components to processes in two separate auditory centers. Gilboa et al. (2005) offered a contrasting explanation, demonstrating that it is possible to create a model of a single neuron with ion channel ensembles that can reproduce history-dependent dynamics of activation, similar to what I observed for the single-exponential curve fit. The available data do not distinguish between these mechanisms. However, Shannon and Otto (1990) have demonstrated that the time course of recovery from forward masking is similar for listeners with cochlear implants and auditory brainstem implants, indicating that mechanisms of forward masking are present at retrocochlear levels. Therefore, I hypothesize that the exponential processes observed in Chapter 2 reflect a subset of the sum of recovery processes occurring throughout the auditory system, each at a different time scale. To address these mechanistic questions, a more thorough characterization of the time course of recovery would require the presentation of stimuli on several different time scales. A robust description of the source of each component of recovery would require paired recordings between sequential auditory centers. Based on the results from Chapter 3, such studies should be performed in awake animals to fully capture responses to short-duration stimuli.

Adaptation of auditory-nerve-fiber responses to an unmodulated electric pulse train increases with increasing rates of electric stimulation (Zhang et al., 2007). Presenting electric pulse trains at a rate of 4069 pps creates an input that is heavily

weighted toward the onset of the stimulus; reducing the rate to 254 pps creates an unusually sustained representation of the entire pulse train, including more prevalent OFF and TONIC responses in the awake animal. Repetition rate may have similar perceptual consequences in periodic acoustic stimuli. In normal-hearing human listeners, Brown and Stecker (2010) showed that the weighting of localization cues in trains of Gabor clicks (Gaussian-envelope tone pips) varied with the rate of the click train and that the perception of the location of a click trains was determined more by localization cues at stimulus onset for high-rate trains of 800 clicks per second (cps), whereas 100-200 cps click trains showed no temporal weighting of localization cues. The use of similar acoustic click-stimuli in a forward masking task could be used to confirm in normal hearing listeners or animals the results observed in the present study.

5.1.2 Predictions for Between-Channel Gap Detection

I have shown that the relative weighting of cues for stimulus onset, offset and duration are differentially activated by electric pulse rates from 254-4069 pps in awake animals. For within-channel gap detection stimuli, the present results indicate that onset responses are most informative about gap presence. Florentine et al. (1999) measured psychophysical within-channel gap-detection thresholds as a function of narrowband noise frequency and concluded that onset responses to the trailing marker were likely to be important for gap detection, based on comparisons with a loudness model. However, if the present results are extrapolated to a wider range of gap-detection stimuli, the relative importance of features denoting the gap may vary. Between-channel gap-detection tasks, in which the leading and trailing markers differ in frequency, spectrum, location, or some other perceptual dimension, elicit thresholds of 10-30 ms for late gaps and 20-70 ms for early gaps (leading marker duration < 50

ms). Gap-detection thresholds follow a similar temporal pattern regardless of the perceptual dimension along which the leading and trailing maskers differed (Phillips et al., 1997, 1998). This indicates that between-channel gap detection is limited by a central locus receiving converging inputs from multiple perceptual channels. Cortical responses to between- and within- channel gap detection stimuli measured with EEG (Lister et al., 2007) demonstrated that only gaps longer than the gap detection threshold activated the T-complex, and did so for both channel conditions. The T-complex is believed to represent activation of secondary auditory cortex (Wolpaw and Penry, 1975). Secondary auditory cortex should have access to the variety of responses encoding all of the features of the leading and trailing markers. Note that the neural response to the onset of the trailing marker in a between-channel stimulus would be even more robust than those elicited by a within-channel gap stimulus, since the amount of forward masking decreases as the difference in frequency between masker and probe increases (Harris and Dallos, 1979). Therefore, it appears that listeners are unable to make use of the full sensitivity of the onset cue in the between-channel condition.

Cues other than stimulus onset may become more relevant for between-channel gap-detection tasks. Lead-OFF and TONIC cues provide information about the duration of the trailing marker that may be more relevant in the between-channel condition. Some models of gap detection construct a decision metric based on the difference in firing rate during the leading and trailing markers and the firing rate during the silent gap (Hanekom, 2001; Heinz et al., 1996). In Chapter 3, I have described TONIC responses to cochlear-implant pulse trains that could form the basis of such judgements within the auditory cortex. In a non-behaving guinea pig, TONIC-derived gap-detection thresholds were 30 ms or longer. Also, I observed Lead-

OFF responses with latencies of 10-30 ms, which were preferentially evoked by the longer leading markers of late gaps. ON and OFF responses in a single neuron often have receptive fields tuned to different frequencies (Qin et al., 2007). In a subset of the cortical population, a between-channel stimulus may evoke a Lead-OFF and Trail-ON response in the same neuron. The OFF-ON interval would provide more information than the cross-channel ON-ON interval for the gap-no-gap comparison. Although the latency of these responses may differ between guinea pig and human, it is conceivable that between-channel gap-detection thresholds depend on different responses for each region of the parameter space. The observed psychophysical results may arise in the following fashion: for pre- and post-gap-markers separated in frequency, Trail-ON cues are present but less salient and therefore insufficient for gap detection. For late gaps, Lead-OFF cues are present for gaps with durations exceeding 10-30 ms, and render these gaps more detectible. For early gaps, Lead-OFF cues are absent, but TONIC cues are available for gap durations of 30 ms and greater.

Testing these hypotheses would involve recording from primary and secondary auditory cortices. The procedure would require multiple, simultaneous recording probe placements within primary auditory cortex to capture the activity across the cortical tonotopic axis. In addition, the "central" mechanisms of between-channel gap detection may occur at longer latencies (100-160 ms) in higher-level cortical areas (Lister et al., 2007). Therefore, experimental design of a physiological study of between-channel should also incorporate recordings from areas other than primary auditory cortex, and would require pilot studies to identify the most likely candidates for the neural basis of between-channel gap detection.

5.1.3 Central Mechanisms of Stimulus Summation

In acoustic stimulation, sound waves drive the motion of the basilar membrane, which is then transduced by hair cells. Attempts to identify central processing mechanisms of simultaneous stimulus interactions may be confounded with actual physical activation driven by the non-linearities of the basilar membrane (McAlpine, 2004). In order to guarantee central interactions, psychophysicists often study binaural interactions (Phillips et al., 1998; Sheft and Yost, 1997a). However, such stimuli activate specialized localization mechanisms that may not be applicable to monaural stimulus processing. Electric pulse trains allow us to simultaneously combine two stimuli yet ensure that they do not interact at the level of the auditory nerve. In Chapter 4, I demonstrated that even stimuli presented with a full 2-ms interleaving delay summed at the level of auditory cortex. The experiments presented here were not designed to discriminate the mechanisms of stimulus interaction and feature extraction. However, they demonstrate that simultaneous stimuli presented to an overlapping population of neurons result in summation in the auditory cortex. This observation of temporal integration is consistent with models of loudness (McKay and Henshall, 2010) and of amplitude modulation detection (Sheft and Yost, 1990). Future experiments could reveal the effect of stimulus level and of spread of activation on the properties of this summation.

5.2 Implications for Cochlear-Implant Listeners

The present studies of cortical responses to cochlear-implant stimulation demonstrate that psychophysical results in human listeners can be reproduced in the guinea pig auditory cortex. These results differ in sensitivity from measurements at the auditory periphery, and indicate that the performance of cochlear-implant listeners

depends on central processing of auditory stimuli. These cortical responses raise questions for future research, shed light on past findings in cochlear implants, and have implications for future cochlear-implant design and testing strategies.

5.2.1 Stimulus Segregation in Cochlear Implants

Cochlear-implant listeners using interleaved pulsatile strategies are limited to approximately 8 channels of transmitted auditory information (Fishman et al., 1997) due to channel interactions. Results from Chapter 4 indicate that, even for interleaving delays which produce no threshold shifts (Middlebrooks, 2004), responses to a pair of supra-threshold stimuli display significant interactions between the two. The tendency for the cortex to reflect the sum of two simultaneous, interleaved stimuli may be exacerbated by the increase in spread of activation at higher stimulus levels. The spread of current from cochlear implant channels (3-20 dB/mm spatial-tuning curve slopes, depending on stimulus mode) is much broader than with acoustic stimulation (100 dB/mm), and increases with increasing stimulus level (Kral et al., 1998). The greater the spectral similarity between two stimuli, the greater the tendency to fuse the two into one auditory object (Bregman et al., 2001; Gaudrain et al., 2007) and there is a corresponding reduction in the ability to use such grouping cues for stimulus segregation in vocoded speech, which reduces the available frequency resolution (Pierzycki and Seeber, 2010). The present results indicate that such channel interactions cannot be eliminated by long interleaving delays.

In normal-hearing listeners, comprehension of speech in the presence of a masker is improved by amplitude-modulation of the masker, perhaps because listeners are able to "listen in the gaps." However, this modulated-unmodulated difference is absent in cochlear-implant listeners; some CI listeners even show an increase in masking for the modulated masker (Nelson et al., 2003). The data presented in Chapter

4 are consistent with this observation: an unmodulated masker shifts the entire stimulus to a higher level, but the combination of speech and a modulated masker increases response variability without providing a perceptual dimension along which to separate the stimuli. Spectral smearing or poor spectral resolution also leads to difficulties in perceiving speech in noisy conditions, and more selective modes of activation may help with auditory stream segregation (Fu and Nogaki, 2005). In order for cochlear-implant listeners to make use of informational masking cues, stimulus strategies need to be defined which will provide selective activation both at the level of the cochlea and for more central auditory processing loci. Based on the results of Chapter 4, measurement of channel interactions should be performed at levels above stimulus threshold, and preferably with stimuli that are more temporally complex than unmodulated pulse trains.

5.2.2 Bilateral Cochlear Implants

The prevalence of bilateral cochlear implantation is rapidly increasing. Bilateral cochlear implant listeners benefit from a second implant, but this benefit is primarily from the better ear effect, in which listeners can isolate the target by listening only with the ear with a higher signal-to-noise ratio (Litovsky et al., 2006). Binaural cues such as interaural time differences (ITD) and interaural level differences (ILD) provide relatively little assistance for CI users in detecting speech in noisy backgrounds with multiple talkers (Loizou et al., 2008). The absence of fine structure cues contributes to the lack of binaural release from masking (Ihlefeld et al., 2010). In Chapter 4, I demonstrated that simultaneously-presented stimuli interact even for long interleaving delays, which requires a mechanism of summation central to the auditory nerve. It is possible that such a mechanism could affect bilateral stimulation as well, resulting in further reduction in segregation between sound sources.

Recently, Tyler et al. (2010) tested a bilateral stimulation strategy in which alternate frequency bands were presented to each ear, in an effort to increase the spectral segregation in each ear. Based on the present results, I would anticipate that the reduction in overlap between frequency channels, both within- and across-ear, would reduce the cross-channel summation and result in improved stimulus segregation. Out of 15 subjects, one achieved a binaural advantage with the interleaved strategy, and six others received varying amounts of benefit, particularly on speech-in-noise tasks. Only one subject performed worse with the interleaved strategy. Refinement of this strategy may offer benefits to bilateral cochlear-implant listeners, although complementary methods of transmitting the powerful grouping cues present in temporal fine structure will probably be necessary to restore true binaural processing to cochlear-implant listeners.

5.3 Summary

Modifications to cochlear-implant processing schemes are often intended to maximize the transmission of information within the cochlea. However, I have shown that subsequent central processing of the resultant auditory nerve activation plays an important role in the cortical representation of the stimulus. Such interactions will prove particularly important as the cochlear-implant research community moves beyond its successes and strives to improve perception in noisy backgrounds.

Bibliography

Alves-Pinto, A., Baudoux, S., Palmer, A., and Sumner, C. (2010). Forward masking estimated by signal detection theory analysis of neuronal responses in primary auditory cortex. *J Assoc Res Otolaryngol*, 11:477–494. 10.1007/s10162-010-0215-6. 74

Arora, K., Vandali, A. E., Dowell, R., and Dawson, P. (2011). Effects of stimulation rate on modulation detection and speech recognition by cochlear implant users. *Int J Audiol*, 50:123–132. 6, 77, 104

Bacon, S. P., Moore, B. C. J., Shailer, M. J., and Jorasz, U. (1995). Effects of combining maskers in modulation detection interference. *J Acoust Soc Am*, 97(3):1847–1853. 106

Battmer, R.-D., Dillier, N., Lai, W. K., Begall, K., Leypon, E. E., González, J. C. F., Manrique, M., Morera, C., Müller-Deile, J., Wesarg, T., Zarowski, A., Killian, M. J., von Wallenberg, E., and Smoorenburg, G. F. (2010). Speech perception performance as a function of stimulus pulse rate and processing strategy preference for the cochlear^{TM} nucleus® ci24re device: Relation to perceptual threshold and loudness comfort profiles. *Int J Audiol*, 49:657–666. 7, 46, 77

Bee, M. A., Buschermöhle, M., and Klump, G. M. (2007). Detecting modulated

signals in modulated noise: (ii) neural thresholds in the songbird forebrain. *Eur J Neurosci*, 26:1979–1994. 109

Biebel, U. W. and Langner, G. (2002). Evidence for interactions across frequency channels in the inferior colliculus of awake chinchilla. *Hear Res*, 169(1-2):151 – 168. 112

Bierer, J. A. (2007). Threshold and channel interaction in cochlear implant users: Evaluation of the tripolar electrode configuration. *J Acoust Soc Am*, 121:1642–1653. 5

Bierer, J. A. and Middlebrooks, J. C. (2002). Auditory cortical images of cochlear-implant stimuli: Dependence on electrode configuration. *J Neurophysiol*, 87(1):478–492. 108

Bregman, A. S., Ahad, P. A., and Van Loon, C. (2001). Stream segregation of narrow-band noise bursts. *Percept Psychophys*, 63(5):790–797. 120

Brown, A. D. and Stecker, G. C. (2010). Temporal weighting of interaural time and level differences in high-rate click trains. *J Acoust Soc Am*, 128:332–341. 116

Brown, C. J., Abbas, P. J., Borland, J., and Bertschy, M. R. (1996). Electrically evoked whole nerve action potentials in ineraid cochlear implant users: responses to different stimulating electrode configurations and comparison to psychophysical responses. *J Speech Hear Res*, 39:453–467. 40, 42

Busby, P. A. and Clark, G. M. (1999). Gap detection by early-deafened cochlear-implant subjects. *J Acoust Soc Am*, 105:1841–1852. 13, 36, 47

Cazals, Y., Pelizzone, M., Saudan, O., and Boëx, C. (1994). Low-pass filtering in

amplitude modulation detection associated with vowel and consonant identification in subjects with cochlear implants. *J Acoust Soc Am*, 96(4):2048–2054. 104

Chatterjee, M. (1999). Temporal mechanisms underlying recovery from forward masking in multielectrode-implant listeners. *J Acoust Soc Am*, 105:1853–1863. 38, 39, 114

Chatterjee, M. (2003). Modulation masking in cochlear implant listeners: envelope versus tonotopic components. *J Acoust Soc Am*, 113(4):2042–2053. 107

Chatterjee, M., Fu, Q. J., and Shannon, R. V. (1998). Within-channel gap detection using dissimilar markers in cochlear implant listeners. *J Acoust Soc Am*, 103:2515–2519. 37, 73

Chatterjee, M. and Yu, J. (2010). A relation between electrode discrimination and amplitude modulation detection by cochlear implant listeners. *J Acoust Soc Am*, 127(1):415–426. 104

Clark, G. M., Tong, Y. C., and Martin, L. F. A. (1981). A multiple-channel cochlear implant: An evaluation using open-set cid sentences. *Laryngoscope*, 91(4):628–634. 113

Dau, T., Ewert, S., and Oxenham, A. J. (2009). Auditory stream formation affects comodulation masking release retroactively. *J Acoust Soc Am*, 125(4):2182–2188. 109

Djourno, A., Eyries, C., and Vallancien, P. (1957). Preliminary attempts of electrical excitation of the auditory nerve in man, by permanently inserted micro-apparatus]. *Bull Acad Natl Med*, 141:481–483. 2

Drew, P. J. and Abbott, L. F. (2006). Models and properties of power-law adaptation in neural systems. *J Neurophysiol*, 96(2):826–833. 114

Eggermont, J. J. (1999a). The magnitude and phase of temporal modulation transfer functions in cat auditory cortex. *J Neurosci*, 19:2780–2788. 67

Eggermont, J. J. (1999b). Neural correlates of gap detection in three auditory cortical fields in the cat. *J Neurophysiol*, 81:2570–2581. 75

Eggermont, J. J. (2000). Neural responses in primary auditory cortex mimic psychophysical, across-frequency-channel, gap-detection thresholds. *J Neurophysiol*, 84:1452–1463. 37, 74

Elangovan, S. and Stuart, A. (2008). Natural boundaries in gap detection are related to categorical perception of stop consonants. *Ear Hear*, 29:761–774. 76

Elliot, T. M. and Theunissen, F. E. (2009). The modulation transfer function for speech intelligibility. *PLoS Comp Bio*, 5(3):e1000302. 44

Firszt, J. B., Holden, L. K., Skinner, M. W., Tobey, E. A., Peterson, A., Gaggl, W., Runge-Samuelson, C. L., and Wackym, P. A. (2004). Recognition of speech presented at soft to loud levels by adult cochlear implant recipients of three cochlear implant systems. *Ear Hear*, 25:375–387. 79

Fishman, K. E., Shannon, R. V., and Slattery, W. H. (1997). Speech recognition as a function of the number of electrodes used in the speak cochlear implant speech processor. *J Speech Lang Hear Res*, 40:1201–1215. 78, 120

Florentine, M., Buus, S., and Geng, W. (1999). Psychometric functions for gap detection in a yes-no procedure. *J Acoust Soc Am*, 106:3512–3520. 116

Frisina, R. D. (2001). Subcortical neural coding mechanisms for auditory temporal processing. *Hear Res*, 158:1–27. 8, 9, 115

Fu, Q. J. (2002). Temporal processing and speech recognition in cochlear implant users. *Neuroreport*, 13:1635–1639. 13, 44

Fu, Q. J. and Nogaki, G. (2005). Noise susceptibility of cochlear implant users: The role of spectral resolution and smearing. *J Assoc Res Otolaryngol*, 6:19–27. 10.1007/s10162-004-5024-3. 121

Galvin, J. J. and Fu, Q. J. (2011). Single- and multi-channel modulation detection by cochlear implant users. In *Abstracts of the* 34^{th} *Annual MidWinter Research Meeting.*, Baltimore, MD. Association for Research in Otolaryngology. 105

Galvin, J. J. r. and Fu, Q. J. (2005). Effects of stimulation rate, mode and level on modulation detection by cochlear implant users. *J Assoc Res Otolaryngol*, 6:269–279. 14, 77, 104

Garadat, S. N. and Pfingst, B. E. (2011). Relationship between gap detection thresholds and loudness in cochlear-implant users. *Hear Res*, 275(1-2):130–138. 67, 69

Garadat, S. N., Thompson, C. S., and Pfingst, B. E. (2010). Gap detection for pulsatile electrical stimulation: Effect of carrier rate and stimulus level. In *Abstracts of the* 33^{rd} *Annual MidWinter Research Meeting.*, Anaheim, CA. Association for Research in Otolaryngology. 73

Gaudrain, E., Grimault, N., Healy, E. W., and Béra, J.-C. (2007). Effect of spectral smearing on the perceptual segregation of vowel sequences. *Hear Res*, 231:32–41. 120

Gilboa, G., Chen, R., and Brenner, N. (2005). History-dependent multiple-time-scale dynamics in a single-neuron model. *J Neurosci*, 25(28):6479–6489. 115

Green, D. M. and Swets, J. A. (1966). *Signal detection theory and psychophysics.* John Wiley and Sons, New York, NY. 20, 53

Grose, J. H. and Buss, E. (2007). Within- and across-channel gap detection in cochlear implant listeners. *J Acoust Soc Am*, 122:3651–3658. 36, 73

Grose, J. H. and Hall, J. W. (1994). Modulation detection interference (mdi) in listeners with cochlear hearing loss. *J Speech Hear Res*, 37:680–687. 107

Guo, Y. and Burkard, R. (2002). Onset and offset responses from inferior colliculus and auditory cortex to paired noisebursts: inner hair cell loss. *Hear Res*, 171(1-2):158–166. 75

Hanekom, J. J. (2001). *Models and psychophysics of acoustic and electric hearing.* PhD thesis, University of Pretoria. 117

Harris, D. M. and Dallos, P. (1979). Forward masking of auditory nerve fiber responses. *J Neurophysiol*, 42(4):1083–1107. 117

Hartmann, R., Topp, G., and Klinke, R. (1984). Discharge patterns of cat primary auditory fibers with electrical stimulation of the cochlea. *Hear Res*, 13:47–62. 114

Heinrich, A., Alain, C., and Schneider, B. (2004). Within- and between-channel gap detection in the human auditory cortex. *Neuroreport*, 15:2051–2056. 37

Heinz, M. G., Goldstein, M. H., and Formby, C. C. (1996). Temporal gap detection thresholds in sinusoidal markers simulated with a multi-channel, multi-resolution model of the auditory periphery. *Aud Neurosci*, 3:35–56. 117

Holden, L. K., Skinner, M. W., Holden, T. A., and Demorest, M. E. (2002). Effects of stimulation rate with the nucleus 24 ace speech coding strategy. *Ear Hear*, 23:463–476. 46

Hong, R. S. and Turner, C. W. (2006). Pure-tone auditory stream segregation and speech perception in noise in cochlear implant recipients. *J Acoust Soc Am*, 120(1):360–374. 110

Hong, R. S. and Turner, C. W. (2009). Sequential stream segregation using temporal periodicity cues in cochlear implant recipients. *J Acoust Soc Am*, 126(1):291–299. 109

Ihlefeld, A., Deeks, J. M., Axon, P. R., and Carlyon, R. P. (2010). Simulations of cochlear-implant speech perception in modulated and unmodulated noise. *J Acoust Soc Am*, 128(2):870–880. 121

Johnson, M. D., Otto, K. J., Williams, J. C., and Kipke, D. R. (2004). Bias voltages at microelectrodes change neural interface properties in vivo. In *IEMBS*, pages 4103–4106. 26th Ann Int Conf IEEE. 50

Kirby, A. E. and Middlebrooks, J. C. (2010). Auditory temporal acuity probed with cochlear implant stimulation and cortical recording. *J Neurophysiol*, 103:531–542. 47, 71, 74, 75

Kral, A., Hartmann, R., Mortazavi, D., and Klinke, R. (1998). Spatial resolution of cochlear implants: the electrical field and excitation of auditory afferents. *Hear Res*, 121:11–28. 120

Kreft, H. A., Donaldson, G. S., and Nelson, D. A. (2004). Effects of pulse rate on

threshold and dynamic range in clarion cochlear-implant users. *J Acoust Soc Am*, 115:1885–1888. 7, 67, 69, 105

Kwon, B. and van den Honert, C. (2009). Spatial and temporal effects of interleaved masking in cochlear implants. *J Assoc Res Otolaryngol*, 10:447–457. 10.1007/s10162-009-0168-9. 7

La Camera, G., Rauch, A., Thurbon, D., Lüscher, H. R., Senn, W., and Fusi, S. (2006). Multiple time scales of temporal response in pyramidal and fast spiking cortical neurons. *J Neurophysiol*, 96:3448–3464. 114

Lee, C. C. and Middlebrooks, J. C. (2011). Auditory cortex spatial sensitivity sharpens during task performance. *Nat Neurosci*, 14:108–114. 8, 110

Licklider, J. C. R., Webster, J. C., and Hedlun, J. M. (1950). On the frequency limits of binaural beats. *J Acoust Soc Am*, 22(4):468–473. 111

Lim, H. H., Tong, Y. C., and Clark, G. M. (1989). Forward masking patterns produced by intracochlear electrical stimulation of one and two electrode pairs in the human cochlea. *J Acoust Soc Am*, 86(3):971–980. 113

Lister, J., Maxfield, M., and Pitt, G. (2007). Cortical evoked response to gaps in noise: within-channel and across-channel conditions. *Ear Hear*, 28:862–878. 37, 117, 118

Litovsky, R., Parkinson, A., Arcaroli, J., and Sammeth, C. (2006). Simultaneous bilateral cochlear implantation in adults: A multicenter clinical study. *Ear Hear*, 27(6):714–731. 121

Liu, Y., Qin, L., Zhang, X., Dong, C., and Sato, Y. (2010). Neural correlates of auditory temporal-interval discrimination in cats. *Behav Brain Res*, 215:28–38. 47

Loizou, P. C., Hu, Y., Litovsky, R., Yu, G., Peters, R., Lake, J., and Roland, P. (2008). Speech recognition by bilateral cochlear implant users in a cocktail-party setting. *J Acoust Soc Am*, 125(1):372–383. 121

Loizou, P. C., Poroy, O., and M, D. (2000). The effect of parametric variations of cochlear implant processors on speech understanding. *J Acoust Soc Am*, 108:790–802. 46

Lu, T., Liang, L., and Wang, X. (2001). Temporal and rate representations of time-varying signals in the auditory cortex of awake primates. *Nat Neurosci*, 4:1131–1138. 10

Luo, X., Fu, Q.-J., Wu, H.-P., and Hsu, C.-J. (2009). Concurrent-vowel and tone recognition by mandarin-speaking cochlear implant users. *Hear Res*, 256:75–84. 104

Macmillan, N. A. and Creelman, C. D. (2005). *Detection Theory: A User's Guide*. Lawrence Erlbaum Associates, Mahwah, NJ, 2 edition. 20, 53

McAlpine, D. (2004). Neural sensitivity to periodicity in the inferior colliculus: Evidence for the role of cochlear distortions. *J Neurophysiol*, 92(3):1295–1311. 112, 119

McFadden, D. and Pasanen, E. G. (1975). Binaural beats at high frequencies. *Science*, 190(4212):394–396. 111

McKay, C. and Henshall, K. (2010). Amplitude modulation and loudness in cochlear implantees. *J Assoc Res Otolaryngol*, 11:101–111. 10.1007/s10162-009-0188-5. 104, 119

McKay, C. M., Henshall, K. R., Farrell, R. J., and McDermott, H. J. (2003). A practical method of predicting the loudness of complex electrical stimuli. *J Acoust Soc Am*, 113(4):2054–2063. 105

Middlebrooks, J. C. (2004). Effects of cochlear-implant pulse rate and inter-channel timing on channel interactions and thresholds. *J Acoust Soc Am*, 116:452–468. 7, 20, 41, 49, 78, 81, 93, 111, 120

Middlebrooks, J. C. (2008a). Auditory cortex phase locking to amplitude-modulated cochlear implant pulse trains. *J Neurophysiol*, 100:76–91. 10, 16, 17, 43, 51, 67, 82, 84

Middlebrooks, J. C. (2008b). Cochlear-implant high pulse rate and narrow electrode configuration impair transmission of temporal information to the auditory cortex. *J Neurophysiol*, 100:92:107. 14, 16, 82, 89, 104

Middlebrooks, J. C. and Snyder, R. (2007). Auditory prosthesis with a penetrating nerve array. *J Assoc Res Otolaryngol*, 8:258–279. 10.1007/s10162-007-0070-2. 20, 53

Moore, B. (2008). The role of temporal fine structure processing in pitch perception, masking, and speech perception for normal-hearing and hearing-impaired people. *J Assoc Res Otolaryngol*, 9:399–406. 10.1007/s10162-008-0143-x. 8

Moore, B. C. J. and Jorasz, U. (1996). Modulation discrimination interference and comodulation masking release as a function of the number and spectral placement of narrow-band noise modulators. *J Acoust Soc Am*, 100:2373–2381. 107

Moore, B. C. J., Sek, A., and Glasberg, B. R. (1999). Modulation masking produced by beating modulators. *J Acoust Soc Am*, 106(2):908–918. 107, 112

Müller-Preuss, P. and Mitzdorf, U. (1984). Functional anatomy of the inferior colliculus and the auditory cortex: current source density analyses of click-evoked potentials. *Hear Res*, 16:133–142. 17, 51

Nadol, J. B. J. (1997). Patterns of neural degeneration in the human cochlea and auditory nerve: implications for cochlear implantation. *Otolaryngol Head Neck Surg.*, 117:220–228. 5

Nadol, J. B. J., Eddington, D. K., and Burgess, B. J. (2008). Foreign body or hypersensitivity granuloma of the inner ear after cochlear implantation: One possible cause of a soft failure? *Otol Neurotol*, 29:1076–1084. 6

Nelson, D. A. and Donaldson, G. S. (2001). Psychophysical recovery from single-pulse forward masking in electric hearing. *J Acoust Soc Am*, 109:2921–2933. 42

Nelson, D. A. and Donaldson, G. S. (2002). Psychophysical recovery from pulse-train forward masking in electric hearing. *J Acoust Soc Am*, 112:2932–2947. 38, 42, 114

Nelson, P. B., Jin, S.-H., Carney, A. E., and Nelson, D. A. (2003). Understanding speech in modulated interference: Cochlear implant users and normal-hearing listeners. *J Acoust Soc Am*, 113(2):961–968. 110, 120

Nelson, P. C., Smith, Z. M., and Young, E. D. (2009). Wide-dynamic-range forward suppression in marmoset inferior colliculus neurons is generated centrally and accounts for perceptual masking. *J Neurosci*, 29:2553–2562. 39, 74

Neuert, V., Verhey, J. L., and Winter, I. M. (2004). Responses of dorsal cochlear nucleus neurons to signals in the presence of modulated maskers. *J Neurosci*, 24(25):5789–5797. 109

Nunamaker, E. A., Purcell, E. K., and Kipke, D. R. (2007). In vivo stability and biocompatibility of implanted calcium alginate disks. *J Biomed Mater Res A*, 83:1128–1137. 49

Oxenham, A. J. and Moore, B. C. J. (1994). Modeling the additivity of nonsimultaneous masking. *Hear Res*, 80(1):105–118. 115

Oxenham, A. J. and Plack, C. J. (2000). Effects of masker frequency and duration in forward masking: further evidence for the influence of peripheral nonlinearity. *Hear Res*, 150:258–266. 39, 42

Pfingst, B. E., Burkholder-Juhasz, R. A., Xu, L., and Thompson, C. S. (2008). Across-site patterns of modulation detection in listeners with cochlear implants. *J Acoust Soc Am*, 123(2):1054–1062. 104

Pfingst, B. E., Xu, L., and Thompson, C. S. (2007). Effects of carrier pulse rate and stimulation site on modulation detection by subjects with cochlear implants. *J Acoust Soc Am*, 121:2236–2246. 14, 77, 104

Phillips, D. P. and Hall, S. E. (1990). Response timing constraints on the cortical representation of sound time structure. *J Acoust Soc Am*, 88:1403–1411. 43

Phillips, D. P., Hall, S. E., Harrington, I. A., and Taylor, T. L. (1998). "central" auditory gap detection: A spatial case. *J Acoust Soc Am*, 103:2064–2068. 65, 74, 117, 119

Phillips, D. P., Taylor, T. L., Hall, S. E., Carr, M. M., and Mossop, J. E. (1997). Detection of silent intervals between noises activating different perceptual channels: Some properties of "central" auditory gap detection. *J Acoust Soc Am*, 101:3694–3705. 44, 117

Pierzycki, R. H. and Seeber, B. U. (2010). Indications for temporal fine structure contribution to co-modulation masking release. *J Acoust Soc Am*, 128(6):3614–3624. 120

Plack, C. J. and Oxenham, A. J. (1998). Basilar-membrane nonlinearity and the growth of forward masking. *J Acoust Soc Am*, 103:1598–1608. 74

Plant, K., Holden, L. K., Skinner, M. W., Arcaroli, J., Whitford, L., Law, M.-A., and Nel, E. (2007). Clinical evaluation of higher stimulation rates in the nucleus research platform 8 system. *Ear Hear*, 28:381–393. 46

Plomp, R. (1964). Rate of decay of auditory sensation. *J Acoust Soc Am*, 36:277–282. 38

Preece, J. P. and Tyler, R. S. (1989). Temporal-gap detection by cochlear prosthesis users. *J Speech Hear Res*, 32:849–856. 13, 36, 42, 113

Pressnitzer, D., Meddis, R., Delahaye, R., and Winter, I. M. (2001). Physiological correlates of comodulation masking release in the mammalian ventral cochlear nucleus. *J Neurosci*, 21:6377–6386. 109

Qin, L., Chimoto, S., Sakai, M., Wang, J., and Sato, Y. (2007). Comparison between offset and onset responses of primary auditory cortex on-off neurons in awake cats. *J Neurophysiol*, 97:3421–3431. 76, 118

Recanzone, G. H., Engle, J. R., and Juarez-Salinas, D. L. (2011). Spatial and temporal processing of single auditory cortical neurons and populations of neurons in the macaque monkey. *Hear Res*, 271:115–122. 47

Richardson, L. M., Busby, P. A., and Clark, G. M. (1998). Modulation detection

interference in cochlear implant subjects. *J Acoust Soc Am*, 104(1):442–452. 106, 107

Roberts, B., Glasberg, B. R., and Moore, B. C. J. (2002). Primitive stream segregation of tone sequences without differences in fundamental frequency or passband. *J Acoust Soc Am*, 112:2074–2085. 8

Rubinstein, J. T., Wilson, B. S., Finley, C. C., and Abbas, P. J. (1999). Pseudospontaneous activity: stochastic independence of auditory nerve fibers with electrical stimulation. *Hear Res*, 127:108–118. 6, 13, 46

Rupp, A., Gutschalk, A., Uppenkamp, S., and Scherg, M. (2004). Middle latency auditory-evoked fields reflect psychoacoustic gap detection thresholds in human listeners. *J Neurophysiol*, 92:2239–2247. 47

Sagi, E., Kaiser, A. R., Meyer, T. A., and Svirsky, M. A. (2010). The effect of temporal gap identification on speech perception by users of cochlear implants. *J Speech Lang Hear Res*, 52:385–395. 76

Shannon, R. V. (1989). Detection of gaps in sinusoids and pulse trains by patients with cochlear implants. *J Acoust Soc Am*, 85:2587–2592. 13, 36, 42, 46, 73

Shannon, R. V. (1992). Temporal modulation transfer functions in patients with cochlear implants. *J Acoust Soc Am*, 91:2156–2164. 10, 104, 113

Shannon, R. V., Cruz, R. J., and Galvin, J. J. (2011). Effect of stimulation rate on cochlear implant users' phoneme, word and sentence recognition in quiet and in noise. *Audiol Neurotol*, 16:113–123. 46

Shannon, R. V., Galvin, J. J., and Baskent, D. (2002). Holes in hearing. *J Assoc Res Otolaryngol*, 3:185–199. 5

Shannon, R. V. and Otto, S. R. (1990). Psychophysical measures from electrical stimulation of the human cochlear nucleus. *Hear Res*, 47:159–168. 9, 39, 115

Shannon, R. V., Zeng, F.-G., Kamath, V., Wygonski, J., and Ekelid, M. (1995). Speech recognition with primarily temporal cues. *Science*, 270:303–4. 8

Sheft, S. and Yost, W. A. (1990). Temporal integration in amplitude modulation detection. *J Acoust Soc Am*, 88(2):796–805. 119

Sheft, S. and Yost, W. A. (1997a). Binaural modulation detection interference. *J Acoust Soc Am*, 102:1791–1798. 107, 119

Sheft, S. and Yost, W. A. (1997b). Modulation detection interference with two-component masker modulators. *J Acoust Soc Am*, 102:1106–1112. 107

Shofner, W. P., Sheft, S., and Guzman, S. J. (1996). Responses of ventral cochlear nucleus units in the chinchilla to amplitude modulation by low-frequency, two-tone complexes. *J Acoust Soc Am*, 99(6):3592–3605. 111

Sinex, D. G. and Chen, G. D. (2000). Neural responses to the onset of voicing are unrelated to other measures of temporal resolution. *J Acoust Soc Am*, 107:486–495. 43

Skinner, M. W., Arndt, P. W., and Staller, S. J. (2002). Nucleus 24 advanced encoder conversion study: performance versus preference. *Ear Hear*, 23:2S–17S. 5, 6

Skinner, M. W., Clark, G. M., Whitford, L. A., Seligman, P. M., Staller, S. J., Shipp, D. B., Shallop, J. D., Everingham, C., Menapace, C. M., Arndt, P. L., Antogenelli, T., Brimacome, J. A., Pijl, S., Daniels, P., George, C. R., McDermott, H. J., and Beiter, A. L. (1994). Evaluation of a new spectral peak coding strategy for the nucleus 22 channel cochlear implant system. *Am J Otol*, 15:15–27. 6, 7

Skinner, M. W., Fourakis, M. S., Holden, T. A., Holden, L. K., and Demorest, M. E. (1996). Identification of speech by cochlear implant recipients with the multipeak (mpeak) and spectral peak (speak) speech coding strategies. i. vowels. *Ear Hear*, 17:182–197. 5

Skinner, M. W., Holden, T. A., Whiting, B. R., Vole, A., Brundsen, B., Neely, J. G., Saxon, E. A., Hullar, T., and Finley, C. C. (2007). The position of advanced bionics electrodes arrays in the human cochlea. *Ann. Otol. Rhinol. Laryngol. Suppl.*, 197:2–24. 5

Snell, K. B. and Hu, H.-L. (1999). The effect of temporal placement on gap detectability. *J Acoust Soc Am*, 106:3571–3577. 74

Stickney, G. S., Zeng, F.-G., Litovsky, R., and Assmann, P. (2004). Cochlear implant speech recognition with speech maskers. *J Acoust Soc Am*, 116(2):1081–1091. 79

Tyler, R., Witt, S., Perreau, A., Parkinson, A., and Wilson, B. S. (2010). An attempt to improve bilateral cochlear implants by increasing the distance between electrodes and providing complementary information to the two ears. *J Am Acad Audiol*, 21:52–65. 122

van Tasell, D. J., Soli, S. D., Kirby, V. M., and Widin, G. P. (1987). Speech waveform envelope cues for consonant recognition. *J Acoust Soc Am*, 82:1152–1161. 8, 12

van Wierengen, A. and Wouters, J. (1999). Gap detection in single- and multiple-channel stimuli by laura cochlear implantees. *J Acoust Soc Am*, 106:1925–1939. 13, 36, 73

Verschuur, C. A. (2005). Effect of stimulation rate on speech perception in adult users of the med-el cis speech processing strategy. *Int J Audiol*, 44:58–63. 46

Viemeister, N. F. (1979). Temporal modulation transfer functions based upon modulation thresholds. *J Acoust Soc Am*, 66(5):1364–1380. 10

Wakefield, G. H. and Viemeister, N. F. (1985). Temporal interactions between pure tones and amplitude-modulated noise. *J Acoust Soc Am*, 77(4):1535–1542. 107

Wang, J., Fenga, Y., and Yin, S. (2006). The effect of gap-marker spectrum on gap-evoked auditory response from the inferior colliculus and auditory cortex of guinea pigs. *Int J Audiol*, 45:521–527. 37, 115

Wilson, B. S., Finley, C. C., Lawson, D. T., Wolford, R. D., Eddington, D. K., and Rabinowitz, W. M. (1991). Better speech recognition with cochlear implants. *Nature*, 352:236–238. 3, 6

Wojtczak, M. and Oxenham, A. J. (2009). Pitfalls in behavioral estimates of basilar-membrane compression in humans. *J Acoust Soc Am*, 125(1):270–281. 115

Wolpaw, J. R. and Penry, J. K. (1975). A temporal component of the auditory evoked response. *Electroencephalography and Clin Neurophysiol*, 39(6):609–620. 117

Xu, L. and Pfingst, B. E. (2007). Spectral and temporal cues for speech recognition: Implications for auditory prostheses. *Hear Res*, 242(1-2):132–140. 79

Yost, W. A. and Sheft, S. (1989). Across-critical-band processing of amplitude-modulated tones. *J Acoust Soc Am*, 85:848–857. 107

Zeng, F.-G., Kong, Y.-Y., Michalewski, H. J., and Starr, A. (2005). Perceptual consequences of disrupted auditory nerve activity. *J Neurophysiol*, 93(6):3050–3063. 9, 47

Zhang, C. and Zeng, F.-G. (1997). Loudness of dynamic stimuli in acoustic and electric hearinga). *J Acoust Soc Am*, 102(5):2925–2934. 105

Zhang, F., Miller, C. A., Robinson, B. K., Abbas, P. J., and Hu, N. (2007). Changes across time in spike rate and spike amplitude of auditory nerve fibers stimulated by electric pulse trains. *J Assoc Res Otolaryngol*, 8:356–372. 6, 39, 41, 46, 71, 77, 115

Zhang, W., Salvi, R. J., and Saunders, S. S. (1990). Neural correlates of gap detection in auditory nerve fibers of the chinchilla. *Hear Res*, 46:181–200. 74

Zilany, M. S. A., Bruce, I. C., Nelson, P. C., and Carney, L. H. (2009). A phenomenological model of the synapse between the inner hair cell and auditory nerve: Long-term adaptation with power-law dynamics. *J Acoust Soc Am*, 126(5):2390–2412. 114